Nº d'ordre : 10/2010-M/CH

REPUBLIQUE ALGERIENNE DEMOCRATIQUE ET POPULAIRE

MINISTERE DE L'ENSEIGNEMENT SUPERIEUR
ET DE LA RECHERCHE SCIENTIFIQUE

UNIVERSITE DES SCIENCES ET DE LA TECHNOLOGIE
HOUARI BOUMEDIENE

FACULTE DE CHIMIE

جامعة هواري بومدين
للعلوم والتكنولوجيا
U S T H B

MEMOIRE

Présenté pour l'obtention du diplôme de MAGISTER

En: CHIMIE

SPECIALITE : Chimie Physique et Théorique

Par: Wahiba KERBOUB

Measurements and Correlation of Liquid-Liquid Equilibria for Solutions Containing Water, Alcohols, Ethers and Fluorinated Hydrocarbons

Soutenu le 12 janvier 2010 devant le jury composé de:

Mr. M. MOUZALI	Professeur (USTHB)	Président
Me. Z. ATIK	Professeur (USTHB)	Directrice de thèse
Mr. M. H. GUERMOUCHE	Professeur (USTHB)	Examinateur
Mr. A. BOUDINA	Maître de conférences (USTHB)	Examinateur
Mme. M. BENDOVA	Docteur (ICPF), Prague	Invitée

Measurements and Correlation of Liquid-Liquid Equilibria for Solutions Containing Water, Alcohols, Ethers and Fluorinated Hydrocarbons

Wahiba KERBOUB

University of Sciences and Technology Houari Boumediene
Faculty of Chemistry
Crystallography-Thermodynamics Laboratory

CONTENTS

ABSTRACT

New data of solubility and liquid-liquid equilibrium (LLE) are mostly needed by scientists and in chemical processes, chemical and industrial units, and optimization of separation operations: to interpret, correlate, and to predict physic-chemical properties of specific mixtures of major industrial and technical importance.

This work reports new solubility and liquid-liquid equilibrium data, together with quantitative thermodynamic information with respect to molecular interactions, for the binary and ternary systems composed of water, oxygenated organic solvents, and halogenated compounds at different temperatures and at pressure of 0.1 MPa.

For technical procedure, two tests of binary systems and three tests of ternary systems were performed and were in good agreement with literature values.
The new experimental data were used to estimate the separation factors and the selectivity of the solvents (alcohols) for type I liquid-liquid equilibrium systems.

The binodal and liquid-liquid equilibrium data curves were well correlated using empirical equations (Hand, Othmer-Tobias). The experimental liquid-liquid equilibrium data of all systems were reduced by two thermodynamic models, NRTL and UNIQUAC, with mean standard deviation 1.2 %.

The critical solution points of type I systems were estimated and correlated by NRTL and UNIQUAC.
The effect of temperature and molecular structure on immiscibility gap of the systems were evaluated.

RESUME

Les résultats expérimentaux de solubilité et d'équilibre de phases liquide-liquide sont nécessaires pour les scientifiques dans les processus chimiques, les unités industrielles et l'optimisation des opérations de séparation ainsi que leurs interprétation, corrélation, et prédiction des propriétés physico-chimiques des mélanges spécifiques de grande importance industrielle et technique.

Ce travail reporte de nouvelles données de solubilité et d'équilibre liquide-liquide, ainsi que des informations thermodynamiques quantitatives vis à vis des interactions moléculaires, pour des systèmes binaires et ternaires contenant de l'eau, des solvants organiques oxygénés et des composés halogénés, à différentes températures et à une pression de 0.1MPa.

Des mesures effectuées sur des systèmes étalons nous ont permis de confirmer que les résultats obtenus étaient en bon accord avec les données de la littérature.
Les nouvelles données expérimentales ont été utilisées pour estimer les points critiques, les facteurs de séparation, et la sélectivité des solvants pour les systèmes ternaires de type I.

Les courbes binodales et les données d'équilibre liquide-liquide ont été bien corrélées par des équations empiriques (Hand, Othmer-Tobias). Les données expérimentales d'équilibre liquide-liquide des systèmes étudiés ont été traitées par deux modèles thermodynamiques, NRTL et UNIQUAC, avec un écart type moyen de 1.2% en fractions molaires.
Le point critique pour les systèmes d'équilibre liquide-liquide de type I a été estimé et corrélé par NRTL et UNIQUAC.
Les effets de la température et de la structure moléculaire des constituants sur l'intervalle d'immiscibilité des systèmes ont été évalués.

ACKNOWLEDGEMENTS

I owe deep gratitude and thanks to my Supervisor Prof. Dr. Z. ATIK for her scientific guidance and unfailing assistance throughout this work. Her persistence and willingness had given me confidence and competence to carry out my work in a very structured scientific environment.

I wish to express my warm thanks to my parents, brothers and sisters for their unfailing encouragements and full support.

I am grateful to all my colleagues for providing me their friendship and pleasant times while working on my thesis. I also thank Mr. R. REBAI for his help with chromatographic techniques.

Finally, my sincere acknowledgements to the President and the Examinaters of the Thesis Jury for their scientific cooperation with us and helpful assistance.

W. KERBOUB

7 December 2009

GLOSSARY

List of Symbols

a	activity
A, B	Hand constants
A_1, B_2	Othmer-Tobias constants
C	number of components
d	distribution coefficient
F	degree of freedom, objective, function
G	Gibbs function
H	enthalpy
M	molar mass
n_D	refractive index
p	pressure
Q^0, Q	chromatograph constants
R	universal gas constant
S	entropy, selectivity
s	surface area
T	thermodynamic temperature
V	volume
w	weight
x	mole fraction

Abbreviations

Calc.	Calculated
Expt.	Experimental
GLC	Gas-Liquid Chromatograph
LLE	Liquid-Liquid Equilibrium
mix	mixing
min	minute
MeOH	Methanol
p.p.	plait point
RMSD	root-mean square deviation
TFE	2,2,2-trifluoroethanol

Greek

Δ	total change
$\Delta\lambda_{ij}$, Δu_{ij}	binary interaction parameters
δ	uncertainty
φ	phase
γ	activity coefficient
μ	chemical potential
ρ	density

Subscripts

A, B, C	components
i, j	components
m	molar

Superscripts

cs	critical solution
E	excess property
r	real
id	ideal
α, β, φ	phase

List of Tables

Tables in Text

ANNEXE A: Experimental Results

List of Figures

Figures in Text

ANNEXE A: Experimental Results

CHAPTER 1

INTRODUCTION

The chemical industry is ever more focusing on producing and developing chemicals and materials that meet hard environmental demand. In general, the difficulties associated with the development and implementations of the industrial processes are availability of thermodynamic property data for various types of mixtures and solution to assist in the data prediction and unit simulation.[1] The knowledge of thermodynamic phase behaviour of multi-component systems is important in many scientific and technical fields.

New data on solubility and liquid-liquid equilibrium are mostly needed by scientist and chemical engineering to interpret, correlate, and to predict properties of specific mixtures of major industrial and technical importance.

Phase equilibrium data of binary and ternary systems are commonly studied and are important in industrial applications; the precise liquid-liquid equilibrium data are needed in design of many chemical processes separation operations industry.[2] The liquid extraction is one of the main separation techniques of materials. Liquid extraction is used in the pharmaceutical and food industry, in which the separation factor and mutual solubility of materials play important role in the extraction process.[3-11]

Alcohols are used on gasoline additives to provide antiknock quality and to help reduce harmful combustion emissions. The use of methanol in gasoline blends can raise phase separation problems.[12-15] The use of natural gas as a vehicular fuel is environmentally advantageous. Nonetheless, the storage and transportation of natural gas for such application

need careful attention. The use of methanol as an energy-storage medium and as a fuel receives attention due to its availability, low cost, clean burning characteristics. Methanol also plays a critical role in the production of biodiesel.[16-18]
The hydroxyl group of alcohols makes them polar substances promoting their solubility in water. At the same time the carbon chain of the alcohols resists to some extent their solubility in water. Methanol, ethanol, and propanols, are fully miscible in water because the hydroxyl group predominates while butanols are moderately miscible due to a larger molecular chain.

Liquid-liquid extraction provides an important alternative to distillation for the recovery of ethanol from dilute aqueous solution using an immiscible solvent.[19]

Propanols are used as solvents in the pharmaceutical industry, a cleaning agent in the production of many electronic devices, and for resins and cellulose esters. They are formed naturally in small amounts during many fermentation processes. Propanols are a major constituent of fusel oil when producing bio ethanol.[20] Butanol (or butan-1-ol) is considered as a potential biofuel in cars, and is used as a blended additive to diesel fuel to reduce harmful emissions.

Hexane is a chemical made from crude oil, and it is found in many petroleum and gasoline products, and is widely used as a cleaning agent in many industries.

Cyclohexane is nonpolar solvent, colourless and highly flammable material. It is insoluble in water.[2] Cyclohexane, and its derivatives, is widely used as solvent in laboratory analysis, oil extractant, paint and varnish remover, and dry cleaning materials. It is also used in chemical industries as a raw material for production of nylon, pharmaceuticals, dyes, plasticizers, herbicides, and insecticides.

Organic solvents containing fluorine atom(s) have been used in the field of the cleaning technology of electronic industry.[21] Fluorinated hydrocarbons are non-flammable and non-explosive solvents which have low toxicity and short environmental lifetime, and are excellent substitutes of chlorinated solvents. 2,2,2-Trifluoroethanol is considered as a novel and clean energetic fluid source. 2,2,2-Trifluoroethanol forms technical mixture solvents which are taking an important branch in chemical engineering research and unit development; as organic working fluids for thermal engines and heat pumps for terrestrial and space

applications,[22-24] and a future-car fuel. Regrettably, 2,2,2-trifluoroethanol is an expensive chemical substance.[25]

Numerous fluorinated-hydrocarbon substances are partially miscible with hydrocarbons of comparable molar structure and they are poor solvents for most solid solutes, and have low boiling temperatures. Where the substitution of hydrogen atoms by fluorine atoms in hydrocarbon play a major role in the physico-chemical properties in the corresponding fluorohydrocarbon substances. The strong polarity of C—F bond attributed to fluorine atom, yields low solubility parameters chemical substances.[26]

Fluorinated alcohols, such as 2,2,2-trifluoroethanol, are taking more importance in the medicinal and pharmaceutical industries, as well as their high efficiency as engine fuels. The pure solvent and the solvent mixtures of 2,2,2-trifluoroethanol demonstrate chemical and thermal stability, and they find a wide range of technical applications. Solutions containing 2,2,2-trifluoroethanol, methanol, and cyclohexane are good reacting media.[24]

Iodoethane is used for the addition of ethyl groups to delicate substances such as pharmaceuticals, and for silver catalysts activation. Recovery of the expensive iodoethane requires separation from product streams and therefore knowledge of thermodynamic properties and phase equilibrium data are required.[27,28]
Iodoethane is easily oxidized to iodine by atmospheric oxygen, and it also undergoes photodecomposition that causes free iodine to form, resulting in pale-rose-colored samples. Therefore, solubility and tie-line measurements were realized in the absence of day light.

This work reports new solubility and liquid-liquid equilibrium data, together with quantitative thermodynamic information with respect to molecular interactions. For the binary systems of (hydrocarbon + methanol or 2,2,2-trifluoroethanol) at various temperatures, for the ternary systems of (hydrocarbon + alcohol + 2,2,2-trifluoroethanol) at four temperatures; where hydrocarbon = hexane or cyclohexane; alcohol = methanol or butan-1-ol, and the system of (water + alcohol + iodoethane) at 298.15 K; where alcohol = methanol; ethanol; propan-1-ol.

For multi-component systems, the solubility data of mixtures were obtained by titration method, and were correlated by empirical equations. For the liquid-liquid equilibrium, the

tie-line mole fractions of the constituents of the mixtures were obtained by gas chromatography.[29-33]

The liquid-liquid equilibrium data of the studied mixtures were correlated using empirical equations of Hand,[34] and Othmer-Tobias.[35] In addition, the liquid-liquid equilibrium experimental data of binary and ternary systems of this work were reduced and correlated by the thermodynamic models of The Non Random Two Liquid (NRTL)[36] and UNIversal QUAsi Chemical (UNIQUAC)[37] with mean standard deviation smaller then 1.2% in phase mole fractions.

In this work, we studied liquid-liquid equilibrium phase diagrams of type I and type II. The observed liquid-liquid equilibrium data for type I phase diagrams were used to estimate the separation factor and the selectivity of few technical solvents (alcohols).[38,39]

CHAPTER 2

FUNDAMENTALS OF PHASE EQUILIBRIUM THERMODYNAMICS OF MIXTURES

2.1 Introduction to Thermodynamics of Liquid Mixtures

The change in the Gibbs molar energy function dG_m^{φ} of the multi-component multi-phase mixtures is given by:[40]

$$dG_m^{\varphi} = -\sum_{\varphi} S_m^{\varphi} dT^{\varphi} + \sum_{\varphi} V_m^{\varphi} dP^{\varphi} + \sum_{\varphi}\sum_{i} \mu_i^{\varphi} dx_i^{\varphi}, \qquad (2.1)$$

where the summation is over all components *i* and all phases φ, $S_{m,i}^{\varphi}$, $V_{m,i}^{\varphi}$, and x_i^{φ} are, molar entropy , molar volume, mole fraction of component *i* in phase φ in the mixtures, respectively. For a pure substance *i* in phase φ, the chemical potential is related to the temperature and pressure by the differential equation:

$$\mu_i^{\varphi} = G_m^{\varphi} - x_i^{\varphi} \left(\partial G_m / \partial x_i\right)_{T,P}^{\varphi} \qquad (2.2a)$$

For which the change in the chemical potential μ_i^{φ} (*T*, *p*) is:

$$d\mu_i^{\varphi} = -S_{m,i}^{\varphi} dT + V_{m,i}^{\varphi} dp \qquad (2.2b)$$

The Gibbs-Duhem equation for a phase φ is:

$$S_m^{\varphi} dT - V_m^{\varphi} dp + \sum_i x_i^{\varphi} d\mu_i^{\varphi} = 0 \qquad (2.3)$$

The degree of freedom *F* of a multi-component multi-phase system is determined by Gibbs phase rule:

$$F = C - \varphi + 2 \geq 0, \qquad (2.4)$$

where C, φ are the number of components and number of phases in the mixture, respectively. The degree of freedom F is the least number of intensive variables used to fully and precisely characterize the system.

For two phase ternary system: $F = 3$; so, the three independent variables such as temperature T, pressure p, and mole fraction x_i are needed for a precise study of the mixture at the equilibrium conditions:

$$\mu_i^{\alpha} = \mu_i^{\beta}, \tag{2.5a}$$

$$T^{\alpha} = T^{\beta} = T, \tag{2.5b}$$

$$p^{\alpha} = p^{\beta} = p. \tag{2.5c}$$

For a ternary system at constant temperature, $F' = 2$, so only two mole fractions x_1 and x_2 are needed to well identify the system since $x_3 = 1 - (x_1 + x_2)$

Figure (2.1), presents x_A, x_B mole fractions of coexisting phases. The plot of mole fraction of coexisting phases gives the binodal curve.

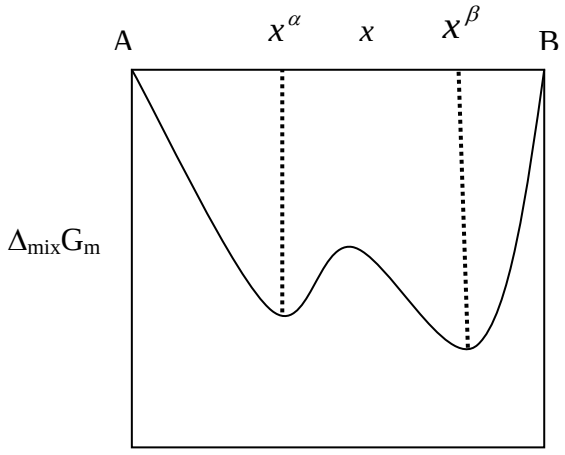

Figure (2.1): Scheme of Gibbs energy of mixing for an immiscible binary mixture

The activity a_i of a component i in a real mixture is related to the mole fraction x_i as:

$$a_i = x_i \gamma_i, \tag{2.6}$$

where γ_i is the activity coefficient of component i.

For an ideal mixture: $\gamma_i = 1.0$, so $a_i = x_i$.

The molar Gibbs function of mixing of a real mixture $\Delta_{mix}G_m^r$ is given by:

$$\Delta_{mix}G_m^r = RT\sum_{i=1}^{N} x_i \ln a_i \tag{2.7}$$

Similarly to equation (2.2a), the chemical potential of mixing of component i in phase φ is expressed by:

$$\mu_{mix,i}^{\varphi} = \left(\frac{\partial \Delta_{mix} G_m}{\partial x_i} \right)_{T,p}^{\varphi} \tag{2.8}$$

In the phase φ, the change in the chemical potential of mixing with respect to the mole fraction of component *i*; x_i is:

$$\left(\frac{\partial \mu_{mix,i}}{\partial x_i} \right)_{T,p}^{\varphi} = \left(\frac{\partial^2 \Delta_{mix} G_m}{\partial x_i^2} \right)_{T,p}^{\varphi} \tag{2.9}$$

Equation (2.9) is used to predict the phase stability of the mixture.

2.2 Excess Thermodynamic Functions of Mixtures

An excess molar function X_m^E is a thermodynamic function that describes the deviation of a real mixture from the ideal behaviour at the same conditions of (*T*, *p*, *x*):

$$X_m^E(T, p, x) = \Delta_{mix} X_m^r(T, p, x) - \Delta_{mix} X_m^{id}(T, p, x) \tag{2.10}$$

The excess molar Gibbs function G_m^E is defined by:

$$G_m^E(T, p, x) = \Delta_{mix} G_m^r(T, p, x) - \Delta_{mix} G_m^{id}(T, p, x), \tag{2.10a}$$

with:

$$\Delta_{mix} G_m^r = RT \sum_i^N x_i \ln x_i + RT \sum_i^N x_i \ln \gamma_i, \tag{2.11}$$

and we get:

$$G_m^E = RT \sum_i^N x_i \ln \gamma_i, \tag{2.12}$$

with the activity coefficient γ_i of component *i*:

$$\left(\frac{\partial G_m^E}{\partial x_i} \right)_{T,p,x_j \neq x_i} = RT \ln \gamma_i \tag{2.13}$$

Excess Gibbs function G_m^E is difficult thermodynamic quantity to measure. However, the studies of phase equilibrium of multi-component multi-phase systems apply directly its determination, as shown in equations (2.12) and (2.13).

2.3 Partial Miscibility in Liquid Mixtures

Many liquids are only partially miscible for heterogeneous liquid mixtures. The relation between excess Gibbs energy and mutual solubilities outlined in the following:

The natural mass transfer of component *i* between phases α and β implies.

$$d\mu_i^{\varphi} < 0, \text{ and}: \left(\frac{\partial \mu_{mix,i}}{\partial x_i}\right)_{T,p}^{\varphi} > 0 \tag{2.14}$$

The condition of material stability in homogenous mixture is expressed by the inequality:

$$\left(\frac{\partial^2 \Delta_{mix} G_m}{\partial x_i^2}\right)_{T,p} > 0 \tag{2.15}$$

and the instability of the mixture fulfils:

$$\left(\frac{\partial^2 \Delta_{mix} G_m}{\partial x_i^2}\right)_{T,p} < 0 \tag{2.16}$$

The passage from two phase region (α + β) to one phase region (α or β) corresponds to a unique state known as the critical state (*cs*) or the plait point (p.p.). The critical state is characterized by a unique variable values (T^{cs}, p, x_i). At the critical point, an infinitesimal change in the equilibrium variables provokes the appearance or the disappearance of a particular phase in the mixture (ex. homogenous phase splits to two conjugate phases α and β, or vis versa).

In a liquid mixture with a miscibility gap (α + β), the critical point is the physical state where the system change, its immiscibility gap to a total miscibility with a single-phased state.

The critical state of a heterogeneous mixture is established at a unique temperature; which is the critical solution temperature T^{cs} and a unique mole fraction x^{cs}.

For temperatures below the critical point, $T < T^{cs}$, a partial miscible binary mixture shows three mole fraction regions:

- homogenous region:

  $0 \le x \le x^{\alpha}: \left(\frac{\partial^2 \Delta_{mix} G_m}{\partial x^2}\right)_{T,p} > 0$, phase α is stable,

  $x^{\beta} \le x \le 1: \left(\frac{\partial^2 \Delta_{mix} G_m}{\partial x^2}\right)_{T,p} > 0$, phase β is stable

- heterogeneous region (α + β):

$$x^{\alpha} \le x \le x^{\beta} : \left(\frac{\partial^2 \Delta_{mix} G_m}{\partial x^2} \right)_{T,p} < 0 \text{ , two stable phases coexist; } (\alpha + \beta)$$

For temperatures above the critical point, $T > T^{cs}$, a complete miscibility overcomes the mixtures throughout all mole fractions, $0 \le x \le 1.0$:

$$\left(\frac{\partial^2 \Delta_{mix} G_m}{\partial x^2} \right)_{T,p} > 0 \qquad (2.17)$$

2.4 Liquid-Liquid Equilibrium in Binary Systems

Spinodal and Binodal Curves

Phase diagrams representing the effect of temperature on phase mole fraction, (T, x_i^{φ}) of liquid-liquid equilibrium of binary systems are of two types: the spinodal, and the binodal diagrams.

- spinodal curve: represents the passage from conditions where single-phase mixture is metastable to conditions where it becomes unstable and undergoes phase separation to two conjugate phases by spinodal decomposition.
- binodal curve: represents the passage from miscibility of the mixture to conditions where single-phase mixture is metastable or unstable.

Figure (2.2) illustrates the different phase regions in a partial miscible binary mixture.

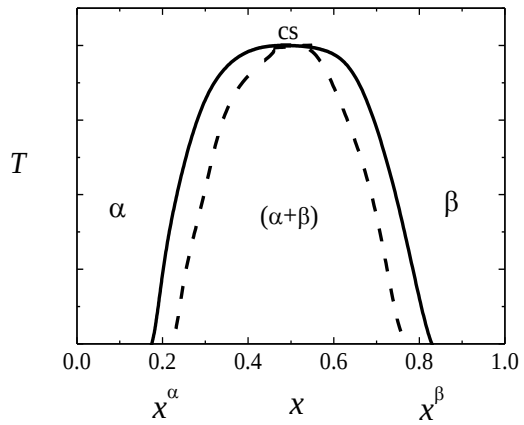

Figure (2.2): Scheme of $(T, x)_p$ for an immiscible binary mixture: …, spinodal; —, binodal

The critical point justifies the thermodynamic equations:

$$x^{\alpha} = x^{\beta} = x^{cs} \qquad (2.18)$$

$$\left(\frac{\partial^2 \Delta_{mix} G_m}{\partial x^2}\right)_{T^{cs},p} = 0, \tag{2.19}$$

$$\left(\frac{\partial^3 \Delta_{mix} G_m}{\partial x^3}\right)_{T^{cs},p} = 0, \tag{2.20}$$

and:
$$\left(\frac{\partial^4 \Delta_{mix} G_m}{\partial x^4}\right)_{T^{cs},p} > 0. \tag{2.21}$$

where T^{cs}, denotes critical solution (plait point) temperature, is the extreme temperature where the heterogeneous mixtures converges to a homogeneous one. Generally, at temperatures above the critical solution temperature; T > T^{cs}, the mixture is homogeneous over the whole mole fraction range with: $\left(\frac{\partial^2 \Delta_{mix} G_m}{\partial x^2}\right)_{T,p} > 0.$

The liquid-liquid phase equilibrium of a multi-component mixture is expressed in term of its phase-component activity a_i^{φ} :

$$a_i^{\alpha} = a_i^{\beta} \tag{2.22}$$

Applying equations (2.6) and (2.22), the liquid-liquid equilibrium condition is described by:
$$\gamma_i^{\alpha} x_i^{\alpha} = \gamma_i^{\beta} x_i^{\beta}, \tag{2.23}$$

where x_i^{φ} and γ_i^{φ} are the equilibrium mole fractions and the activity coefficient of component *i* in phase φ, respectively.

The liquid-liquid equilibrium state for binary mixtures is represented by:

$$\left\{\left(1-x^{\alpha}\right)A + x^{\alpha}B\right\}^{\alpha} \leftrightarrow \left\{\left(1-x^{\beta}\right)A + x^{\beta}B\right\}^{\beta} \tag{2.24}$$

The distribution of the amount of substance of a particular mixture M in the conjugate phases is represented by tie lines, such as line LMN in Figure (2.3).

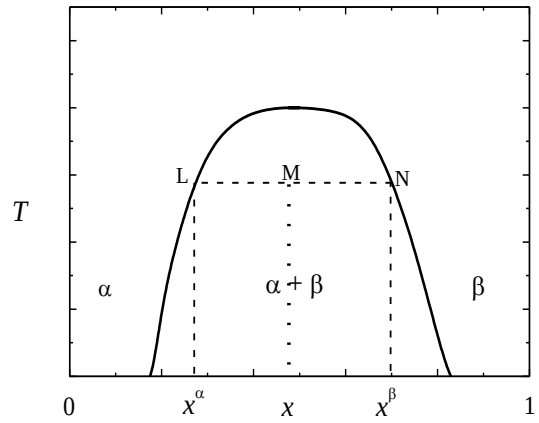

Figure (2.3): Distribution of substance in liquid-liquid equilibrium in a binary mixture

When thermal and chemical equilibrium is established at temperature *T*, the distribution of amount of substance of components *A* and *B* in mixture between phase α and β are:

$$n_A = n_A^{\alpha} + n_A^{\beta}$$

$$n_B = n_B^{\alpha} + n_B^{\beta} \qquad (2.25)$$

But, the amount of substance in phases α and β are:

$$n^{\alpha} = n_A^{\alpha} + n_B^{\alpha}$$

$$n^{\beta} = n_A^{\beta} + n_B^{\beta} \qquad (2.26)$$

On the other hand, the total amount of substance in the system is:

$$n = n^{\alpha} + n^{\beta}$$

$$n = n_A + n_B \qquad (2.27)$$

Applying equations (2.25 to 2.27), the mole fractions and amount of substance of each phase are related by the following relations:

$$\left(\frac{n^{\alpha}}{n^{\beta}}\right) = \frac{MN}{ML} \qquad (2.28a)$$

Finally, we get:

$$\left(\frac{n^{\alpha}}{n^{\beta}}\right) = \frac{\left(x^{\beta} - x\right)}{\left(x - x^{\alpha}\right)} \qquad (2.28b)$$

Equation (2.28) has important applications in liquid extraction processes applied in chemical engineering and chemical industries.

2.5 Liquid-Liquid Equilibrium in Ternary Systems

A ternary system in two phase equilibrium at (*T*, *p*, constant) is univariant; $F' = 1$. The mole fractions in a phase φ satisfies: $\sum x_i^{\varphi} = 1$. Therefore, a two phase ternary system can be represented by one variable; $x_2 = f(x_1)$.

The mole fractions of ternary mixture are represented by the Gibbs triangle, where each side of the triangle represents a binary mixture of mole fraction $(x_A + x_B = 1)$: where as the ternary mole fraction of the mixture is represented by a single point on the triangle mole-fraction plane; with $(x_A + x_B + x_C = 1)$.

Figure (2.4) show a triangular diagram.

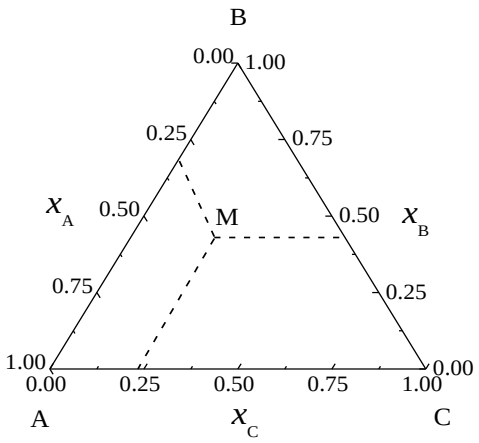

Figure (2.4): Representation of a mixture M (x_A, x_B, x_C) in a triangular diagram.

The ternary liquid-liquid equilibrium phase diagrams of mixture (*A* + *B* + *C*) are of two types:
Type I: in which only one binary mixture is immiscible and dominates the system as shown in Figure (2.5a).

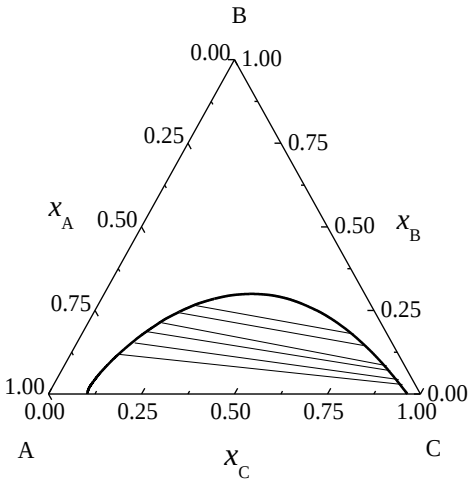

Figure (2.5a): Type I of a ternary liquid-liquid phase diagram.

Type II: in which two binary immiscible mixtures ($A + B$) and ($A + C$) dominate the system, and it is represented in Figure (2.5b).

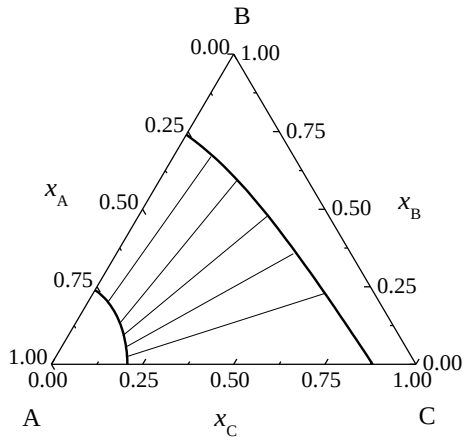

Figure (2.5b): Type II of a ternary liquid-liquid phase diagram.

Applying equation (2.23) for a ternary mixture we get:

$$\left(\gamma_1 x_1\right)^{\alpha} = \left(\gamma_1 x_1\right)^{\beta} \tag{2.29a}$$

$$\left(\gamma_2 x_2\right)^{\alpha} = \left(\gamma_2 x_2\right)^{\beta} \tag{2.29b}$$

$$\left(\gamma_3 x_3\right)^{\alpha} = \left(\gamma_3 x_3\right)^{\beta} \tag{2.29c}$$

In addition to equations (2.29) the material balances in liquid-liquid equilibrium of a binary mixture fulfil:

$$n^{\alpha} + n^{\beta} = n \tag{2.30}$$

$$x_1^{\alpha} n^{\alpha} + x_1^{\beta} n^{\beta} = x_1 \tag{2.31}$$

$$x_2^{\alpha} n^{\alpha} + x_2^{\beta} n^{\beta} = x_2 \tag{2.32}$$

Where x_i is the overall mole fraction of component *i* and n is the number of moles.

The distribution coefficient d_i of a solute *i* between two coexistent phases ($\alpha + \beta$) is defined by:

$$d_i = \frac{x_i^{\alpha}}{x_i^{\beta}} \tag{2.33}$$

The selectivity *S* (separation factor), is related to the distribution coefficient of a solvent *j* for solute *i* distributed between phases ($\alpha + \beta$) in a multi component mixture.

$$S_{ji} = \frac{d_j}{d_i} = \left(\frac{x_j^{\alpha} / x_j^{\beta}}{x_i^{\alpha} / x_i^{\beta}} \right) \tag{2.34}$$

2.6 Solubility Data Correlation

The experimental binodal curve for the ternary phase equilibrium is correlated by the empirical equation:[41-43]

$$x_2 = a + b x_3^{0.5} + c x_3 + d x_3^2 + e x_3^3, \tag{2.35}$$

where x_i is the mole fraction of component *i* in the ternary mixture.

2.7 Liquid-Liquid Equilibrium Data Correlation

Using Empirical Equations

In this work, the reliability of experimentally measured liquid-liquid equilibrium data is ascertained by applying two empirical equations:

Equation of Hand:[34]

$$\ln\left(\frac{x_2^{\beta}}{x_3^{\beta}} \right) = A + B \ln\left(\frac{x_2^{\alpha}}{x_1^{\alpha}} \right), \tag{2.36}$$

Equation of Othmer-Tobias: [35]

$$\ln\left(\frac{1 - x_3^{\beta}}{x_3^{\beta}} \right) = A_1 + B_1 \ln\left(\frac{1 - x_1^{\alpha}}{x_1^{\alpha}} \right), \tag{2.37}$$

where x_i^{φ} is the mole fraction of component *i* in phase φ.

Using Thermodynamic Models

Adequate equilibrium models nowadays are commonly used to correlate liquid-liquid equilibrium data in multi-component mixtures, where the most successful ones are the Non Random Two Liquid (NRTL) and the UNIversal QUAsi Chemical (UNIQUAC).

In the NRTL and the UNIQUAC models, the interaction parameters between each pair of mixture components are obtained by reduction and optimization of the observed liquid-liquid equilibrium data by statistical regression methods. The two model equations are presented in the following:

The NRTL Model:[36]

The equations describing the NRTL model are:

$$\ln \gamma_i = \frac{\sum_j \tau_{ji} G_{ji} x_j}{G_{ki} x_k} + \sum_j^N \frac{x_j G_{ij}}{G_{kj} x_k} \left[\tau_{ij} - \frac{\sum_k x_k \tau_{kj} G_{kj}}{\sum_k G_{kj} x_k} \right] \tag{2.38}$$

The interaction parameter τ_{ij} :

$$\tau_{ij} = \frac{\Delta\lambda_{ij}}{RT} \tag{2.39a}$$

$$\ln\ G_{ij} = -\alpha_{ij}\tau_{ij}, \tag{2.39b}$$

where $\Delta\lambda_{ij}$ denotes a binary interaction parameters, it is a characteristics exchange energies between the interacting molecules *i* and *j*; the nonrandomness parameter, α_{ij}, in the NRTL equation was fixed to 0.200.

The UNIQUAC Model:[37]

The equations of the UNIQUAC model are given below:

The activity coefficient for component *i* is given by:

$$\ln \gamma_i = \ln \gamma_i^C + \ln \gamma_i^R \tag{2.40}$$

γ_i^c represents the combinatory term, which describes the size effect of molecules in the mixture:

$$\ln \gamma_i^c = \ln \frac{\phi_i}{x_i} + \frac{z}{2} q_i \ln \frac{\theta_i}{\phi_i} + l_i - \frac{\phi_i}{x_i} \sum_{j=1}^m x_j l_j\ , \tag{2.41}$$

where γ_i^R represents the residual term, which describes the energetic effect of molecules *i* in the mixture:

$$\ln \gamma_i^R = -q_i \ln\left(\sum_{j=1}^m \theta_j \tau_{ij} \right) + q_i - q_i \sum_{j=1}^m \left(\frac{\theta_j \tau_{ij}}{\sum \theta_k \tau_{kj}} \right) \tag{2.42}$$

The volume fraction ϕ_i and the area fraction θ_i are given by:

$$\phi_i = \frac{r_i x_i}{\sum_{j=1}^{m} r_j x_j} \tag{2.43a}$$

$$\theta_i = \frac{q_i x_i}{\sum_{j=1}^{m} q_j x_j} \tag{2.43b}$$

and:

$$\tau_{ij} = \exp\left(\frac{-\Delta u_{ij}}{RT}\right) \tag{2.43c}$$

$$l_j = \frac{z}{2}(r_j - q_j) - (r_j - 1), \tag{2.43d}$$

where Δu_{ij}, denotes a binary interaction parameters, it is a characteristics exchange energies between the interacting molecules *i* and *j*; z, coordination number; *r*, *q*, are size and surface area parameters, respectively.

For two models the binary interaction parameters for our binary and ternary systems were obtained by minimizing the objective function *F*.

The root-mean square deviation (RMSD), or the standard deviation $\sigma(x_i^{\varphi})$, of the data fitting is a measure of the agreement between the observed and the calculated values. The objective function *F* and the standard deviation $\sigma(x_i^{\varphi})$ is calculated as:[44-52]

for binary mixtures:

$$F = \sum_{l}^{M}\sum_{i}^{2}\sum_{\varphi}^{2}\left(x_{i,\exp t}^{\varphi} - x_{i,calc}^{\varphi}\right)^2 \tag{2.44}$$

$$\sigma\left(\Delta x_i^{\varphi}\right) = \left[\sum_{l}^{M}\sum_{\varphi}^{2}\frac{\left(x_{i,\exp t}^{\varphi} - x_{i,calc}^{\varphi}\right)^2}{(2M-4)}\right]^{0.5} \tag{2.45}$$

for ternary mixtures:

$$F = \sum_{l}^{M}\sum_{i}^{3}\sum_{\varphi}^{2}\left(x_{i,\exp t}^{\varphi} - x_{i,calc}^{\varphi}\right)^2 \tag{2.46}$$

$$\sigma\left(\Delta x_i^{\varphi}\right) = \left[\sum_{l}^{M}\sum_{i}^{3}\sum_{\varphi}^{2}\frac{\left(x_{i,\exp t}^{\varphi} - x_{i,calc}^{\varphi}\right)^2}{6M}\right]^{0.5}, \tag{2.47}$$

where $x_{i,\exp t}^{\varphi}$ and $x_{i,calc}^{\varphi}$ are the experimental and calculated mole fractions and the subscripts *i*, φ and *l* represent the component, the phase and the tie line, respectively.

CHAPTER 3

EXPERIMENTAL TECHNIQUES

3.1 Chemical Substances

The pure chemicals used in this work are: methanol, ethanol, 1-propanol, 1-butanol, 2,2,2-trifluoroethanol, iodoethane hexane, and heptane were obtained from Fluka AG, 2-propanol from Riedel deHaën and cyclohexane from Panreac. The chemicals were stored over molecular sieves having a pore diameter 3A from Fluka.

The purities of the chemicals were checked by gas-liquid chromatography (Perkin Elmer Model Clarus 500) and were found to be better than 99.5 % in mole fraction.

Densities of the pure chemicals were measured at the temperature 298.15 K with an Anton Paar vibrating tube densimeter (model DMA5000).

The refractive indices of pure components were measured at the temperature 298.15 K using an Abbe-type refractometer (Phywe, No.990646). The density measurements were accurate to $(\rho \pm 0.0005)$ g.cm^{-3}, and the refractive indices to $(n \pm 0.0005)$ and all agreed well with the literature values.[53]

The purities, experimental densities, and refractive indices of pure components at 298.15 K are reported in table (3.1) with the corresponding literature values.

Table (3.1): Component purity (w %), density ρ, refractive index n_D, and the van der Waals parameters (r, q) at 298.15 K

Component	Symbol	Purity	ρ /g.cm^{-3}		n_D		UNIQUAC[40]	
		w %	Expt.	Lit.[53]	Expt.	Lit.[53]	r	q
Methanol	CH_3OH	99.7	0.7864	0.7864	1.3304	1.3303	1.4311	1.4320
Ethanol	C_2H_5OH	99.9	0.7849	0.7852	1.3595	1.3594	2.1055	1.9720
1-Propanol	C_3H_7OH	99.5	0.7996	0.7996	1.3836	1.3837	2.7799	2.5130
2-Propanol	C_3H_7OH	99.5	0.7815	0.7813	1.3755	1.3752	2.7791	1.9720
1-Butanol	C_4H_9OH	99.5	0.8056	0.8058	1.3748	1.3752	3.9240	3.6680
Heptane	C_7H_{16}	99.5	0.6811	0.6795	1.3854	1.3851	4.5000	3.8600
Hexane	C_6H_{14}	99.5	0.6550	0.6548	1.4241	1.4235	4.4998	3.8560
Cyclohexane	C_6H_{12}	99.8	0.7774	0.7739	1.3723	1.3723	4.0464	3.2400
Iodoethane	C_2H_5I	99.7	1.9248	1.9244	1.5099	1.5101	2.8395	2.8300
2,2,2–Trifluoroethanol	CF_3CH_2OH	99.2	1.3822	1.3818[21]	1.2932	1.2907[21]	2.6100	2.5040

3.2 Experimental Techniques

Mixtures of known mole fraction were prepared by mass using an OHAUS balance (model: Explorer) with a precision of ± 0.1 mg. The uncertainty in the mole fractions of the prepared mixtures was estimated to be ± 0.0003.

The solubility measurements (binodal curve) of ternary mixtures were performed by the titration[30,54] method in an equilibrium glass cell equipped with a magnetic bar and connected to a thermo cryostat[55-59] (LAUDA, model: RC6CP-Edition 2000, δT = ± 0.01 K). The cell temperature is measured with a digital thermistor-thermometer (Cole-Parmer Instrument, model: 8502-16, thermistor: YSI-400) with precision better than ± 0.05 K.

For a run, a mixture of known mixture was introduced into the glass cell;[30,60] the temperature of the cell was controlled by a water jacket and maintained with a precision of within ± 0.01 K. The mixture was stirred vigorously for least 30 min;[30,61] the titrating component was progressively added until total clearance of the mixture.

The scheme of the measuring cell is shown in Figure (3.1).

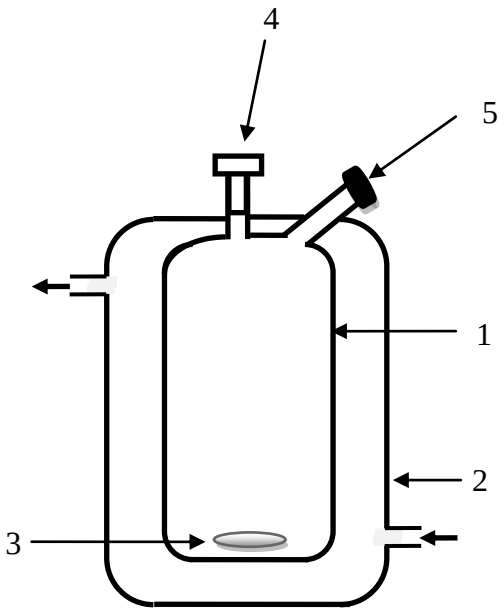

Figure (3.1): Scheme of the equilibrium cell for liquid-liquid equilibrium measurements: 1. cell body, 2. thermostated jacket, 3. magnetic bar, 4. stopper, 5. symptom pore.

For tie-line data, the prepared feed mixtures of known mole fraction were stirred vigorously for 4 h in glass flasks,[62-69] and then where placed in thermocryostat for three days or more to attain complete phase equilibrium. Samples from the two equilibrated liquid phases were

taken by syringes equipped with 15 cm long needles and were then stored in well stopped bottles.

3.3 Chromatographic Analysis

The mole fractions of samples of pure components as well as mixtures were obtained using Gas-Liquid Chromatography (G.L.C.) analysis[70-72] by applying the internal standard calibration method.[73-78] The gas chromatograph was from Perkin-Elmer (model: Clarus 500). The chromatograph was equipped with two detectors: Flame Ionization Detector (F.I.D.) which was used with a capillary column, and Thermal Conductivity Detector (T.C.D.) which was used with packed columns. Two filters were attached to the carrier-gas line to protect the chromatograph detector TCD from any traces of water and oxygen in the carrier gas (Supelco Park Bellefonte, PA 16823 (814) 359-3441; Moisture Trap Model 23987).

The aqueous solutions were analysed by the help of a Porapak packed column, 0.6m, Q80/100 Mesh, and TCD. The chromatographic conditions were: temperatures: injector = 513.15 K; column = 423.15 K; detector = 473.15 K; nitrogen flow rate = 20 $ml.min^{-1}$. The mean retention times of pure components were: water = 0.993 min; ethanol = 4.523 min; methanol = 1.723 min; 1-propanol = 12.325 min; 2-propanol = 10.123 min; iodoethane = 17.953 min.

For the binary and ternary mixtures containing cyclohexane and 2,2,2-trifluoroethanol the two liquid phase samples were analysed by packed column, Carbopak (B 80/100 Mesh, 5 % Carboix 20M) and TCD. The GLC conditions were: temperatures: injector = 513.15 K; column = 393.15 K; detector = 473.15 K; nitrogen flow rate = 20 $ml.min^{-1}$. The pure component retention times were: methanol = 1.135 min; ethanol = 4.523 min; 2-propanol = 2.164 min; cyclohexane = 3.528 min; 2,2,2-trifluoroethanol = 5.032 min; heptane = 13.936 min.

For the binary and ternary mixtures containing hexane and 2,2,2-trifluoroethanol the two liquid phase samples were analysed by capillary column, (SPB-624, 30 m long, 0.25 mm i.d.,1.4 μm film thickness and FID. The GLC conditions for the hexane mixtures were: injection split mode = 1/60, temperatures: injector = 493.2 K; column = (308.2 K→ 473.2 K, heating rate: 4 $K.min^{-1}$); detector = 523.2 K; nitrogen flow rate = 14.3 $ml.min^{-1}$. The mean retention times of pure components were: methanol = 3.170 min; 2-propanol = 5.213 min; hexane = 6.694 min; 2,2,2-trifluoroethanol = 7.186 min; heptane = 10.854 min.

The chromatographic-technical procedures were checked by binary and ternary test systems. The internal standard used was 2-propanol, and heptane was added to homogenize the standard mixtures which were partially miscible.

The chromatograph calibration equation is:

$$\frac{s_i}{s_{st}} = Q + Q^0 \frac{n_i}{n_{st}}, \qquad (3.1)$$

Where s_i and s_{st} are the percentage peak area of the compound and of the internal standard, respectively, n_i and n_{std} are the number of moles of the measured compound and of the internal standard in the calibration mixture respectively, Q and Q^0 are the chromatograph constants.

For technical procedure, two tests for binary systems were performed, liquid-liquid equilibrium data measurement for: (cyclohexane/ hexane + methanol).

And three test for ternary systems were performed, type I phase diagram: solubility and liquid-liquid equilibrium data measurement for: (water + ethanol + solvent), solvent = toluene or cyclohexane at 298.15 K; type II phase diagram: liquid-liquid equilibrium for (methanol + hexane + cyclohexane) at 293.15 K.

The experimental data obtained for these five test systems showed good agreement with literature values.[47,79-85]

3.4 Experimental Uncertainty Analysis

The mole fraction x_i in multi component system is defined by:

$$x_i = \frac{\left(\frac{m_i}{M_i}\right)}{\sum_1^N \left(\frac{m_i}{M_i}\right)}, \qquad (3.2)$$

Therefore, the uncertainty in mole fraction δx_i is:

$$(\delta x_i)^2 = \sum_{i=1}^{N} \left[\left\{ \frac{1}{M_i} \sum_{i=1}^{N} \left(\frac{m_i}{M_i^2} \right) \frac{m_i}{M_i^2} \right\} / \left\{ \sum_{i=1}^{N} \left(\frac{m_i}{M_i} \right) \right\}^4 (\delta m_i)^2 \right], \qquad (3.3)$$

where N, is the number of components; M_i, the molar mass; and m_i, experimental mass.

CHAPTER 4

EXPERIMENTAL RESULTS

4.1 The Studied Systems

This work reports new solubility and liquid-liquid equilibrium data for binary and ternary mixtures containing water, methanol, ethanol, 1-propanol, 1-butanol, toluene, hexane, cyclohexane, iodoethane, 2,2,2-trifluoroethanol, at temperatures T = (278.15 → 318.15) K and atmospheric pressure.

The studied systems are:

Test (Reference) systems:

Binary systems:

T = (278.15 → 318.15) K

hexane (1) + methanol (2),

cyclohexane (1) + methanol (2).

Ternary systems: type I:

T = 298.15 K

water (1) + ethanol (2) + toluene (3),

water (1) + ethanol (2) + cyclohexane (3).

Ternary systems: type II:

methanol (1) + hexane (2) + cyclohexane (3).

New systems:

Binary systems:

T = (278.15 → 318.15) K

hexane (1) + 2,2,2-trifluoroethanol (2),

cyclohexane (1) + 2,2,2-trifluoroethanol (2).

Ternary systems: Type I:

T = 298.15 K

water (1) + methanol (2) + iodoethane (3),

water (1) + ethanol (2) + iodoethane (3),

water (1) + 1-propanol (2) + iodoethane (3).

T = (288.15, 298.15, 308.15) K:

cyclohexane (1) +1- butanol (2) + 2,2,2-trifluoroethanol (3).

Ternary systems: Type II:

T = (288.15, 293.15, 298.15, 308.15) K:

hexane (1) + methanol (2) + 2,2,2-trifluoroethanol (3).

T = (283.15, 293.15, 303.15, 313.15) K:

cyclohexane (1) + methanol (2) + 2,2,2-trifluoroethanol (3).

4.2 Reduction and Correlation of Experimental Data

The experimental solubility and liquid–liquid equilibrium data of binary and ternary systems at the measured temperatures for the studied systems are given in appendix A.

The solubility data were correlated by equation (2.35). The liquid-liquid equilibrium data were correlated by: Hand, equation (2.36), and Othmer-Tobias, equation (2.37).

The distribution coefficient of component i; d_i, was estimated from liquid-liquid equilibrium data using equation (2.33). The selectivity s_{ji} of the solvent j to extract the solute i from its liquid solution was obtained by equation (2.34).

The experimental liquid-liquid equilibrium data were reduced by two thermodynamic models: the Non-Random Two Liquid and the Universal QUAsi Chemical NRTL, UNIQUAC using equations (2.38) and (2.40), respectively. For the NRTL equation, the non-randomness parameter of mixing α_{ij} was set equal to 0.200 for all the studied systems, with least square deviation in data correlation.

The UNIQUAC structural parameters (*r* and *q*) of the pure chemicals are given in table (3.1). The binary interaction parameters between components *i* and *j* in the solution $\Delta\lambda_{ij}$ and Δu_{ij} for the binary and ternary mixtures were obtained by minimizing the objective function *F* using, For the binary systems, using equation (2.44), for the ternary systems, using equation (2.46). The Root-Mean-Square deviation (RMSD); or the standard deviation $\sigma\left(\Delta x_i^{\varphi}\right)$, of the liquid-liquid equilibrium data fitting is evaluated by the help of the following equations:
For the binary systems, using equation (2.45), for the ternary systems, using equation (2.47).

For instance, the standard deviation in phase mole fractions $\sigma\left(\Delta x_i^{\varphi}\right)$ of data points for hexane + methanol + 2,2,2-trifluoroethanol at 298.15 K by NRTL and UNIQUAC models is:

NRTL: $\sigma\left(\Delta x_i^{\varphi}\right) = 0.014,$

UNIQUAC: $\sigma\left(\Delta x_i^{\varphi}\right) = 0.015.$

In the present chapter, we give a representative summary of our new experimental and correlated data for:

- binary system: cyclohexane + 2,2,2-trifluoroethanol from (278.15 to 318.15) K,
- ternary system-type (I): cyclohexane + 1-butanol + 2,2,2-trifluoroethanol at 298.15 K,
- ternary system-type (II): cyclohexane + methanol + 2,2,2-trifluoroethanol at 293.15 K.

For the above three systems, the observed and correlated liquid-liquid equilibrium values are shown in Tables (4.1) to (4.4) and Figures (4.1) to (4.3). The binary interaction parameters from NRTL and UNIQUAC are shown in Tables (4.5) to (4.7).

The deviations for predicting the liquid-liquid equilibrium data for the system (cyclohexane + methanol + 2,2,2-trifluoroethanol) at 303.15 K is shown in Figure (4.4).

Table (4.1): Experimental liquid-liquid equilibrium data for cyclohexane (1) + 2,2,2-trifluoroethanol (2) at 0.1 MPa

	feed mixture		cyclohexane-rich phase		trifluoroethanol-rich phase	
T/K	x_1	x_2	x_1^{α}	x_2^{α}	x_1^{β}	x_2^{β}
283.15	0.501	0.499	0.925	0.075	0.045	0.955
288.15	0.500	0.500	0.899	0.101	0.054	0.946
293.15	0.500	0.500	0.880	0.120	0.069	0.931
298.15	0.499	0.502	0.865	0.135	0.088	0.912
303.15	0.496	0.504	0.850	0.150	0.106	0.894
308.15	0.503	0.498	0.837	0.163	0.111	0.889
313.15	0.498	0.502	0.812	0.188	0.119	0.881
316.15	0.502	0.498	0.786	0.214	0.144	0.856
318.15	0.499	0.502	0.767	0.253	0.167	0.833

Table (4.2): Experimental solubilities for cyclohexane (1) + 1-butanol (2) + 2,2,2-trifluoroethanol (3) at 298.15 K and 0.1 MPa

x_1	x_2	x_3	x_1	x_2	x_3
0.091	0.070	0.839	0.396	0.252	0.352
0.098	0.098	0.804	0.462	0.241	0.307
0.103	0.114	0.783	0.562	0.200	0.247
0.125	0.159	0.716	0.492	0.224	0.284
0.162	0.188	0.650	0.600	0.180	0.220
0.200	0.219	0.581	0.634	0.160	0.205
0.253	0.238	0.508	0.662	0.142	0.196
0.272	0.246	0.483	0.679	0.125	0.186
0.303	0.249	0.448	0.750	0.085	0.165
0.356	0.254	0.394	0.792	0.055	0.153

Binodal eq.: $x_2 = -2.043 + 9.399\,x_3^{0.5} - 11.185\,x_3 + 6.123\,x_3^2 - 2.409\,x_3^3$; $R^2 = 0.999$

Table (4.3): Experimental liquid-liquid equilibrium data for cyclohexane (1) + 1-butanol (2) + 2,2,2-trifluoroethanol (2) at 298.15 K and 0.1 MPa

feed mixture		cyclohexane-rich phase		TFE-rich phase	
x_1	x_2	x_1^{α}	x_2^{α}	x_1^{β}	x_2^{β}
0.472	0.197	0.650	0.151	0.328	0.251
0.461	0.185	0.693	0.122	0.267	0.239
0.462	0.163	0.727	0.095	0.227	0.220
0.494	0.121	0.773	0.064	0.179	0.182
0.497	0.095	0.812	0.041	0.122	0.156
0.501	0.074	0.832	0.026	0.110	0.130
0.523	0.036	0.847	0.014	0.088	0.064
x^{cs}		0.534	0.205	0.534	0.205

Hand eq.: $\ln\left(x_2^{\beta}/x_3^{\beta}\right) = A + B\ln\left(x_2^{\alpha}/x_1^{\alpha}\right)$; y = 0.361 + 0.626 x; R^2 = 0.994

Othmer-Tobias eq.: $\ln\left\{\left(1-x_3^{\beta}\right)/x_3^{\beta}\right\} = A + B.\ln\left\{\left(1-x_1^{\alpha}\right)/x_1^{\alpha}\right\}$; y = 1.247 + 1.496 x; R^2 = 0.998

Table (4.4): Experimental liquid-liquid equilibrium data for cyclohexane (1) + methanol (2) + 2,2,2-trifluoroethanol (3) at 293.15 K and 0.1 MPa

feed mixture		cyclohexane-rich phase		(TFE-MeOH)-rich phase	
x_1	x_2	x_1^{α}	x_2^{α}	x_1^{β}	x_2^{β}
0.493	0.036	0.864	0.009	0.099	0.157
0.490	0.433	0.865	0.010	0.098	0.052
0.495	0.070	0.860	0.011	0.101	0.202
0.498	0.102	0.861	0.019	0.104	0.253
0.491	0.132	0.860	0.033	0.117	0.337
0.489	0.177	0.858	0.045	0.103	0.432
0.488	0.230	0.857	0.057	0.104	0.461
0.485	0.260	0.856	0.079	0.107	0.578
0.474	0.322	0.854	0.095	0.103	0.636
0.482	0.362	0.860	0.106	0.104	0.698
0.492	0.396	0.851	0.119	0.106	0.744

Table (4.5): Interaction parameters, $\Delta\lambda_{ij} = a_{ij} + b_{ij}T$, for NRTL and UNIQUAC equations for cyclohexane (1) + 2,2,2-trifluoroethanol (2) at 0.1 MPa

	NRTL			UNIQUAC	
Component i , j	α_{ij}	a_{ij}/K	b_{ij}	a_{ij}/K	b_{ij}
1.2	0.2	1126.75	-2.54	352.93	-0.51
2.1	0.2	1493.01	-2.98	483.02	-1.24

Table (4.6): Binary interaction parameters from NRTL and UNIQUAC for cyclohexane (1) + 1-butanol (2) + 2,2,2-trifluoroethanol (3) at 0.1 MPa

	NRTL (α_{ij} = 0.2)		UNIQUAC	
Component *i-j*	$\Delta\lambda_{ij}$ /K	$\Delta\lambda_{ji}$ /K	Δu_{ij} /K	Δu_{ji} /K
		T = 288.15 K		
1, 2	-376.2	-52.2	-230.8	-79.2
1, 3	316.0	794.3	144.5	199.8
2, 3	-436.2	-641.1	-130.0	-455.0
		T = 298.15 K		
1, 2	417.3	-124.6	202.0	-32.6
1, 3	286.2	736.9	141.6	138.4
2, 3	-182.6	-185.2	254.0	-203.1
		T = 308.15 K		
1, 2	-945.0	2317.8	-733.2	134.4
1, 3	314.3	572.3	149.1	93.7
2, 3	-789.1	-204.4	-201.0	-695.7

Table (4.7): Binary interaction parameters from NRTL and UNIQUAC for cyclohexane (1) + methanol (2) + 2,2,2-trifluoroethanol (3) at 0.1 MPa

	NRTL (α_{ij} = 0,2)		UNIQUAC	
Component *i* -*j*	$\Delta\lambda_{ij}$ /K	$\Delta\lambda_{ji}$ /K	Δu_{ij} /K	Δu_{ji} /K
	T = 283.15 K			
1, 2	401.7	-55.3	470.3	-75.3
1, 3	878.2	398.3	215.0	166.4
2, 3	424.4	548.8	670.2	21.8
	T = 293.15 K			
1, 2	1082.2	-573.6	91.3	-36.5
1, 3	671.0	327.2	194.5	105.7
2, 3	435.0	327.2	21.1	623.2
	T = 303.15 K			
1, 2	89.07	46.38	293.01	-81.69
1, 3	509.56	298.25	100.26	193.24
2, 3	379.91	515.25	6.92	613.42
	T = 313.15 K			
1, 2	371.8	-256.7	208.5	-74.2
1, 3	692.8	244.3	117.5	168.0
2, 3	408.8	387.1	0.8	595.1

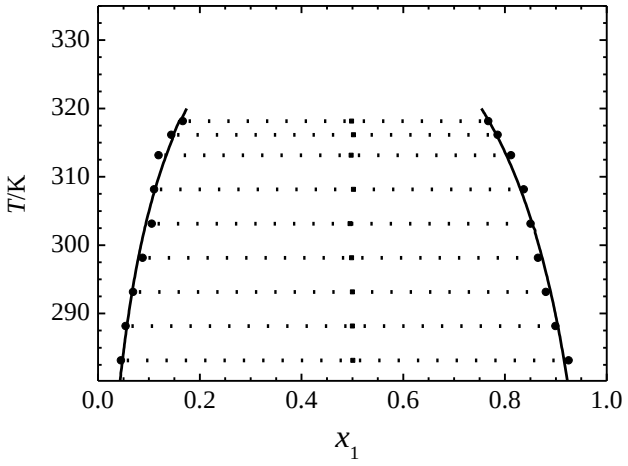

Figure (4.1): Liquid-liquid equilibrium phase diagram for cyclohexane (1) + 2,2,2-trifluoroethanol (2): ■, feed mixture; ●, LLE; …, tie line.

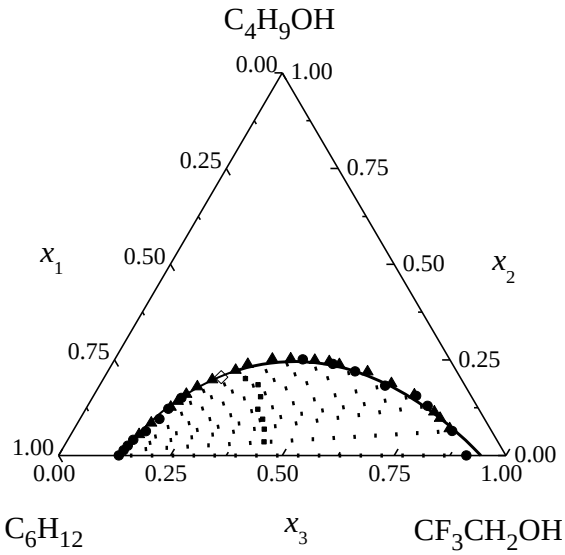

Figure (4.2): Solubility and liquid-liquid equilibrium data for cyclohexane (1) + 1-butanol (2) + 2,2,2-trifluoroethanol (3) at 298.15 K: ▲, solubility; ■, feed mixture; ●, LLE; ◊, plait point; ..., tie line; —, NRTL.

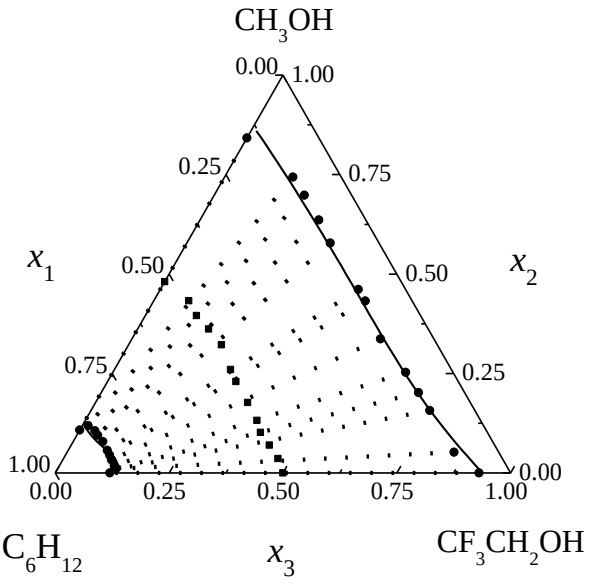

Figure (4.3): Liquid-liquid equilibrium data for cyclohexane (1) + methanol (2) + 2,2,2-trifluoroethanol (3) at 293.15 K: ■, feed mixture; ●, LLE; ..., tie line.

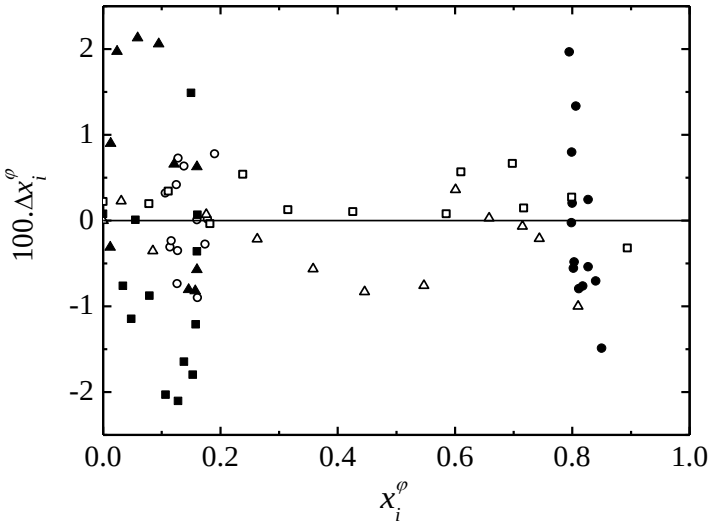

Figure (4.4): Deviations for predicting liquid-liquid equilibrium data for cyclohexane (1) + methanol (2) + 2,2,2-trifluoroethanol (3) at 303.15 K using UNIQUAC eq. solid symbols, (methanol + trifluoroethanol)-rich phase; open symbols, cyclohexane-rich phase: ■, □, cyclohexane; ▲, Δ, methanol; ●,○, 2,2,2-trifluoroethanol

a) For the experimental and correlated solubility data, of the studied systems, these are listed in appendix A; Tables (A_0.3) to (A_0.6) and (A.2.1) to (A.3.6), and shown in Figures (A_0.3) to (A_0.6), (A.1.1) to (A.2.6).

b) For liquid-liquid equilibrium data, the experimental and correlated results are plotted in Tables (A_0.1), (A_0.2), (A_0.7), (A.1.1), (A.1.2) and (A.4.1) to (A.5.4) and shown in Figures (A_0.1), (A_0.2), (A_0.9), (A.1.1), (A.1.2) and (A.4.1) to (A.5.4).

- The Hand and Othmer-Tobias correlation are shown in Figures (A_0.7), (A.2.7) and (A.3.7).

- The distribution coefficients d_1, d_2 and selectivity S are reported in Tables (A.2.7) and (A.3.7) and shown in Figures (A_0.8), (A.2.8) and (A.3.8).

- The deviations for predicting the liquid-liquid equilibrium data using NRTL and UNIQUAC models are shown in Tables (A.2.8), (A.3.8), (A.4.6), (A.5.6), and shown in Figures (A.1.3), (A.2.9), (A.3.9), (A.4.5), (A.5.5).

- The binary interaction parameters from NRTL and UNIQUAC models for each system at each temperature T are given in Tables (A.1.3), (A.2.9), (A.3.9), (A.4.7), and (A.5.7).

CHAPTER 5

DISCUSSION

This study was aimed to evaluate the efficiency of alcohols as drying agents for hydrocarbons in aqueous and non-aqueous mixtures.

The binodal and liquid-liquid equilibrium curves were well correlated using empirical equations (Hand, Othmer-Tobias) and thermodynamic models (UNIQUAC and NRTL); with standard deviations less then 0.2 % in phase mole fractions, and only small deviations from observed data were found. The average value of $\sigma(x_i^{\varphi})$ for all systems by the two models (NRTL and UNIQUAC) was estimated to be 1.2 %. Whereas the $\sigma(x_i^{\varphi})$ values for correlated phase mole fractions were smaller than 2.2 % for both liquid phases.

The liquid-liquid equilibrium of the binary systems of (cyclohexane + 2,2,2-trifluoroethanol) and (hexane + 2,2,2-trifluoroethanol) have been measured in the temperature range (278.15 to 313.15) K and well predicted by means of the NRTL and UNIQUAC models.

The predicted critical solution point by the NRTL equation for the former system is $T^{cs} = 335.1$ K, $x_{TFE}^{cs} = 0.548$, while being equal to $T^{cs} = 315.6$ K, $x_{TFE}^{cs} = 0.562$ for the latter.

In our study we found that the immiscibility region of the system hydrocarbon (1) + 2,2,2-trifluoroethanol (2) decreases significantly with increasing of the hydrocarbon molecular structure, as correlated in Figure (5.1). However, the distribution coefficient of hydrocarbon in 2,2,2-trifluoroethanol is less effected by its molecular structure, as seen in Figure (5.2).

For ternary mixtures, liquid-liquid equilibrium representing one pair of partially miscible components, or type I phase diagrams,[15,86-88] have been studied at temperatures of 288.15 K,

298.15 K, and 308.15 K for two ternary systems containing water, cyclohaxane, methanol ethanol, 1-butanol, 2,2,2-trifluoroethanol, and iodoethane.

Liquid-liquid equilibrium representing two pairs [89] of partially miscible components, known as type II phase diagrams, have been extensively studied at four temperatures in the range $288.15 \leq T/\mathrm{K} \leq 308.15$ for the ternary systems containing hexane, cyclohaxane, methanol and 2,2,2-trifluoroethanol.

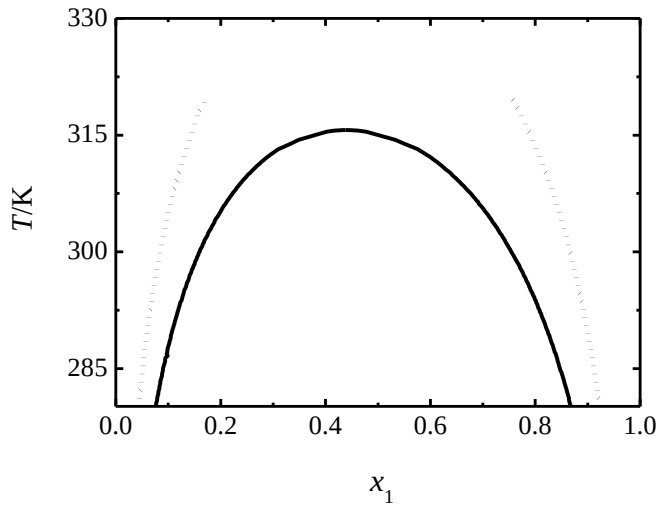

Figure (5.1): The structure effect correlation on liquid-liquid equilibrium for hydrocarbon (1) + 2,2,2-trifluoroethanol (2) by NRTL: —, hexane; · · ·, cyclohexane.

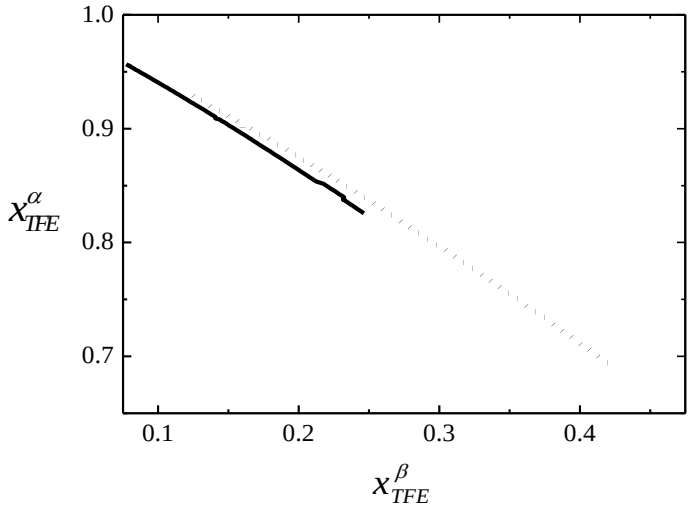

Figure (5.2): The structure effect correlation on distribution for hydrocarbon (1) + 2,2,2-trifluoroethanol (2) by NRTL: —, hexane; · · ·, cyclohexane.

The binary interaction parameters from the thermodynamic models obtained from liquid-liquid equilibrium data, can be used to some extent in predicting vapour-liquid equilibrium (VLE) data. This is shown for the binary system (cyclohexane + 2,2,2-trifluoroethanol).

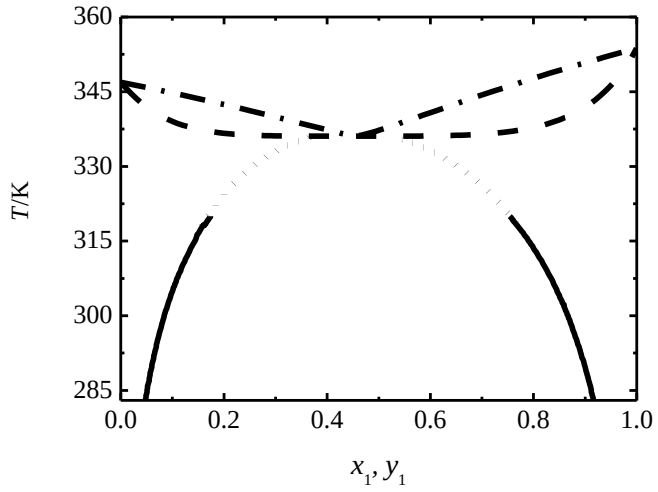

Figure (5.3). Calculated phase diagrams by UNIQUAC for cyclohexane (1) + 2,2,2-trifluoroethanol (2): ─, LLE; **…**, LLE extrapolated line; VLE: **- - -,** (T, x_1); **- · -,** (T, y_1).

For type I phase diagram, the plait point mole fractions ($x_1^{cs}, x_2^{cs}, x_3^{cs}$) of the ternary mixtures were estimated by the method of Othmer-Tobias, and correlated by NRTL and UNIQUAC models. The mean values of their deviations $\Delta x_i^{cs} = (x_{ical}^{cs} - x_{i\,\mathrm{exp}}^{cs})$ are:

For water (1) + alcohol (2) + iodoethane (3):

NRTL: $\Delta x_1^{cs} = 0.064$, $\Delta x_2^{cs} = 0.042$,

UNIQUAC: $\Delta x_1^{cs} = 0.010$, $\Delta x_2^{cs} = 0.006$.

For cyclohexane (1) + 1-butanol + 2,2,2-trifluoroethanol (3):

NRTL: $\Delta x_1^{cs} = 0.027$, $\Delta x_2^{cs} = 0.016$,

UNIQUAC: $\Delta x_1^{cs} = 0.021$, $\Delta x_2^{cs} = 0.012$.

The ternary liquid-liquid equilibrium of the azeotrope methanol (1) + iodoethane (2) presents very high selectivity of water for methanol, where: 16 < S < 1190. Accordingly, the extraction

of methanol, at moderate temperatures, by water as solvent from the azeotropic binary system[28]: T = 313.2 K: p_{az} = 57.7 kPa, $x_{1,az}$ = 0.485, is definitely potential by means of water to yield pure iodoethane

The immiscibility region of the system water + alcohol + iodoethane decreases significantly with increasing of the alcohol molecular chain, as illustrated in Figure (5.4). Yet, 1-propanol was being more selective for iodoethane from its highly diluted solutions, as represented in Figure (5.5).

Moreover, the hygroscopic methanol and the photodecomposition of iodoethane have to be taken into account to assess an inner phase behavior of the system of water + methanol + iodoethane

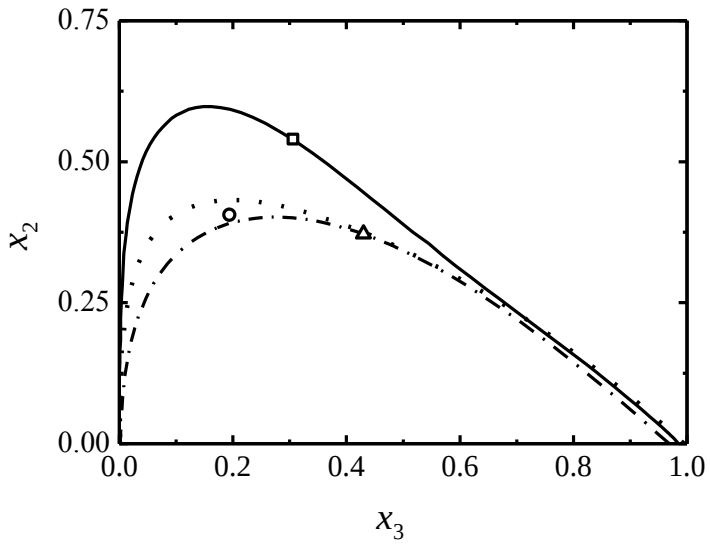

Figure (5.4): Alcohol structure effect on liquid-liquid equilibrium for water (1) + alcohol (2) + iodoethane (3) by NRTL correlation at 298.15 K: ── , □, methanol; · · ·, Δ, ethanol; ─ · ─ , ○, 1-propanol.

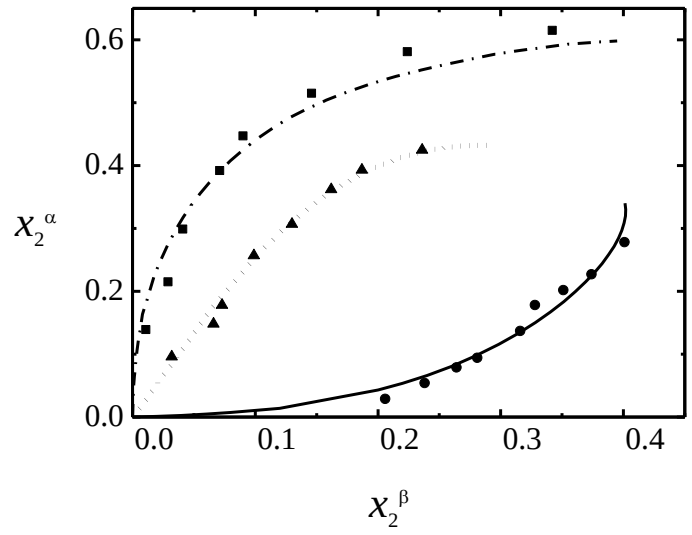

Figure (5.5): Correlated effect of alcohol-molecular chain at 298.15 K on the aqueous and organic phases for water (1) + alcohol (2) + iodoethane (3) by NRTL: ── , ■, methanol; · · ·, ▲, ethanol; ─ · ─ , ●, 1-propanol.

For the system (cyclohexane + 1-butanol + 2,2,2-trifluoroethanol), the immiscibility gap decreases with increasing temperature.

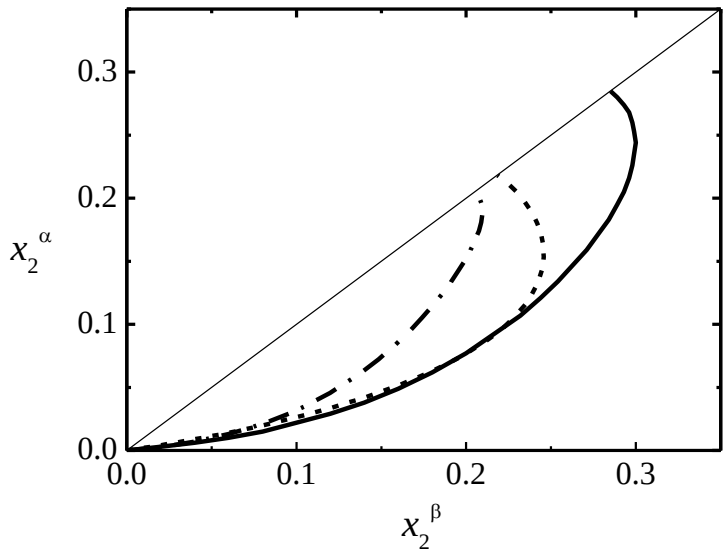

Figure (5.6): NRTL correlation of the temperature effect on the distribution of 1-butanol for cyclohexane (1) + 1-butanol (2) + 2,2,2-trifluoroethanol (3) ── , ■, 288.15 K; · · ·, 298.15 K; ─ · ─ , 308.15 K.

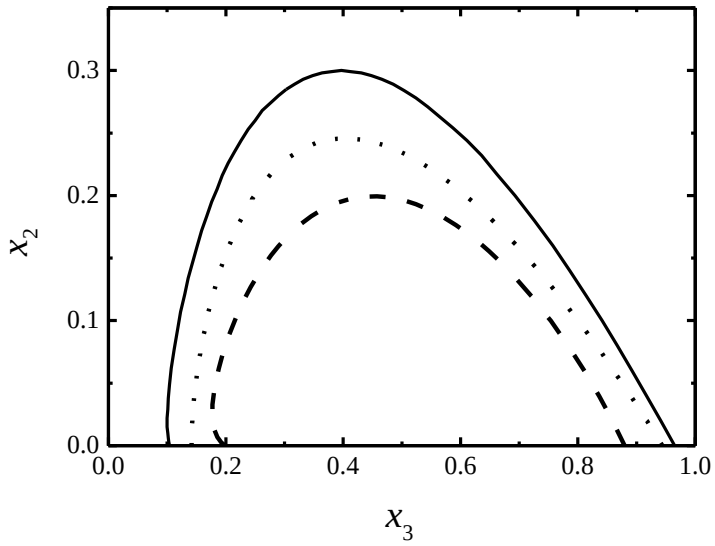

Figure (5.7): The UNIQUAC correlation of the temperature effect on the distribution of 1-butanol for cyclohexane (1) + 1-butanol (2) + 2,2,2-trifluoroethanol (3): ⎯, 288.15 K; · · ·, 298.15 K; - - - , 308.15 K.

For type II phase diagrams, it is found that the apolar molecules of hexane or cyclohexane with the temperature increase weaken the macrocluster stability of the self- and cross-associations formed by hydrogen bonding which are existing in pure and mixed 2,2,2-trifluoroethanol in the presence of the hydroxyl group of the methanol molecules.

Consequently, the effect of temperature on the miscibility of the system (cyclohexane + methanol + 2,2,2-trifluoroethanol) is slightly more significant on the cyclohexane or hexane-rich phase than on (2,2,2-trifluoroethanol + methanol)-rich phase. This is seen in Figures (5.8) and (5.9).

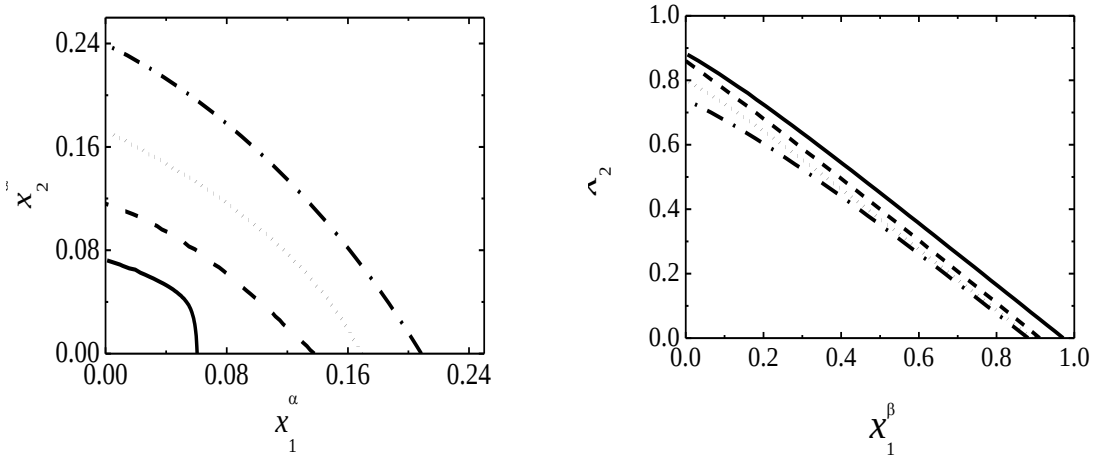

Figure (5.8): The effect of temperature on the liquid-liquid equilibrium for 2,2,2-trifluoroethanol (1) + methanol (2) + cyclohexane (3) from UNIQUAC eq.: ──, 283.15 K; - - -, 293.15 K; ...., 303.15 K; ─ · ─, 313.15 K.

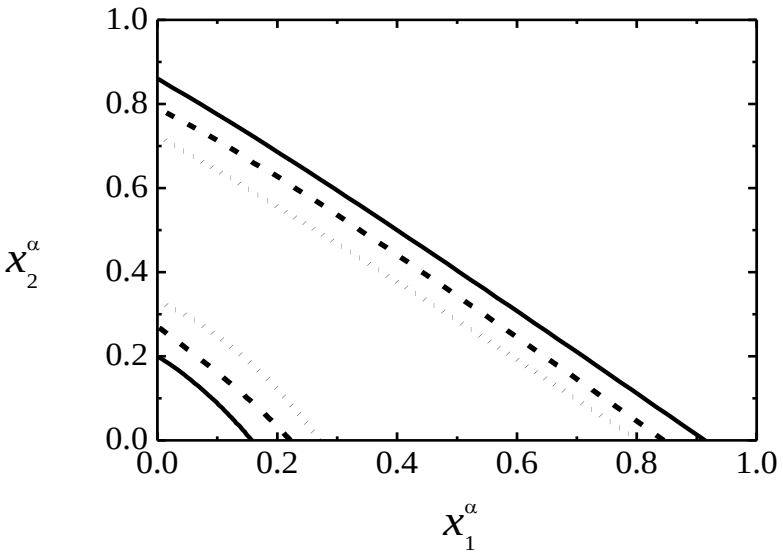

Figure (5.9): The effect of temperature on the liquid-liquid equilibrium for (hexane (1) + methanol (2) + 2,2,2-trifluoroethanol (3)) from UNIQUAC eq.: —, 288.15 K; - - -, 298.15 K; ...., 303.15 K.

The dependence of the immiscibility gap on the molecular structure is outlined for the system hexane or cyclohexane + (methanol + 2,2,2-trifluoroethanol), where it decreases in the order from cyclohexane to hexane as seen in the plot shown in Figure (5.10).

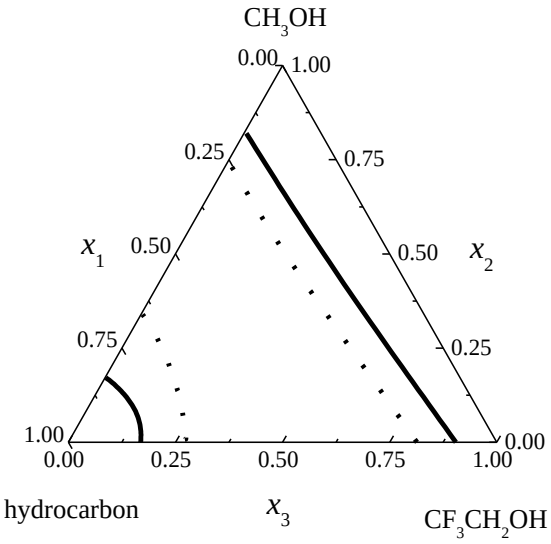

Figure (5.10): Comparison of correlated liquid-liquid equilibrium data for hexane, or cyclohexane (1) + methanol (2) + 2,2,2-trifluoroethanol (3) at 303.15 K, by NRTL model: ****....****, hexane; **—**, cyclohexane.

Figure (5.11) indicates a slight decrease with increasing temperature of the immiscibility region of the system (cyclohexane + methanol + 2,2,2-trifluoroethanol).

The effect of temperature on the immiscibility of the system (hexane + methanol + 2,2,2-trifluoroethanol) is slightly larger as shown in Figure (5.12).

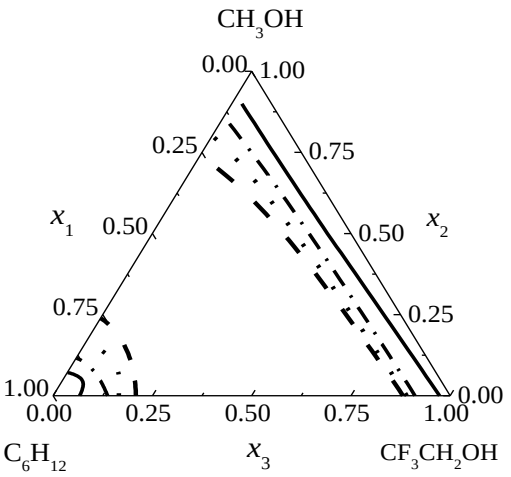

Figure (5.11): Correlated liquid-liquid equilibrium data for cyclohexane (1) + methanol (2) + 2,2,2 trifluoroethanol (3) by UNIQUAC model: —, 283.15 K; ─ · ─, 293.15 K; **….** 303.15 K; – – –, 313.15 K.

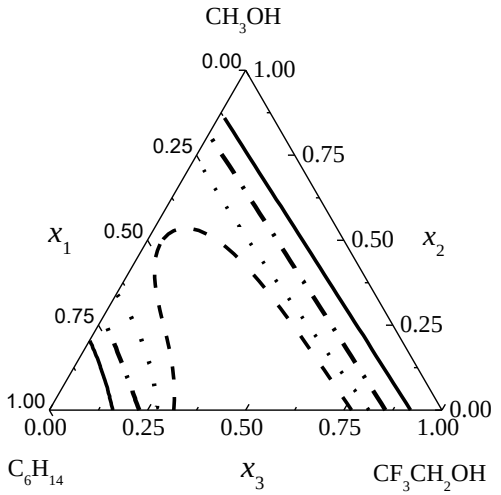

Figure (5.12): Correlated liquid-liquid equilibrium data for hexane (1) + methanol (2) + 2,2,2 trifluoroethanol (3) by UNIQUAC model: —, 288.15 K; ─ · ─., 298.15 K; **….** 303.15 K; – – –, 308.15 K.

CONCLUSION

This work reports new solubility and liquid-liquid equilibrium data of the two binary systems of hydrocarbons + 2,2,2-trifluoroethanol; where hydrocarbons = hexane or cyclohexane, and fourteen ternary systems of water, C_1-C_4-alcohols, hexane, cyclohexane, 2,2,2-trifluoroethanol and iodoethane at different temperatures and pressure 0.1 MPa.

Solubility data were obtained by titration method, whereas mole fractions of the tie-lines end were obtained by gas chromatography.

The immiscibility region of all systems decreases slightly with increasing temperature. The increase of alcohol-molecular chain reduces the immiscibility gap significantly in the presence of water.

The observed liquid-liquid equilibrium data were very well reduced by empirical equations of Hand and Othmer-Tobias, and thermodynamic models of NRTL and UNIQUAC, and only small deviations from observed data were found.
The effect of temperature on the immiscibility gap of our systems was reasonably small.

This study confirms the efficiency of alcohols as extracting agents for hydrocarbons from 2,2,2-trifluoroethanol mixtures and iodoethane from aqueous mixtures.

REFERENCES

Cited Publications

1. H. Ghanadzadeh, A. Ghanadzadeh,

   (Liquid + liquid) phase behavior for systems containing (aromatic + TBA + methylcyclohexane).

   J. Chem. Thermodyn. 36 (2004), 161-165.

2. D. Ozmen, U. Dramur, B.Tatli,

   Liquid-liquid equilibria of propionic acid – water - solvent (n-hexane, cyclohexane, cyclohexanol and cyclohexyl acetate) ternaries at 298.15 K.

   Braz. J. Chem. Eng. 21 (2004) 647-657.

3. H. Ghanadzadah , A. Ghanadzadah, M. Alitavol,

   LLE of ternary mixtures of water / acetone / 2-ethyl -1-hexanol at different temperatures.

   Fluid Phase Equilibria 219 (2004) 165-169.

4. A. B. Pereiro, A. Rodríguez,

   Ternary (liquid +liquid equilibria) of the azeotrope (ethyl acetate + 2-propanol) with different ionic liquids at T = 298.15 K.

   J. Chem. Thermodyn. 39 (2007) 1608-1613.

5. L. M. Casas, B. Orge, C. Diaz, J. Tojo,

   Liquid-liquid equilibria for mixtures of {methyl acetate + methanol + n-alkane (C_{10}-C_{12})}at several temperatures and 1 atm.

   J. Chem. Thermodyn. 36 (2004) 237-243

6. A. Landauer, R. N. Lichtenthaler, J. M. Praunitz,

   Mutual solubilities of alkanes and methyl cellosolve.

   J. Chem. Eng. Data 25 (1980) 152-153.

7. G. Maurer,

   Modeling the liquid liquid equilibria for the recovery of carboxylic acids from aqueous solutions.

   Fluid Phase Equilibr. 241 (2006) 86-95.

8. H. Ghanadzadeh, A. Ghanadzadeh, R. Sariri,

(Liquid + liquid) equilibria for (water + acetic acid + 2-ethyl-1-hexanol): experimental data and prediction.

J. Chem. Thermodyn. 36 (2004) 1001-1006.

9. M. M. Nia, E. Nekoei, F.S. M. Doulabi,

Ternary (liquid + liquid) equilibria for mixtures of (methanol + aniline + n- octane or n-dodecane) at T = 298.15 K.

J. Chem. Thermodyn. 40 (2008) 330-333.

10. A. Senol, G. Alptekin, A. A. Sayar,

(Liquid + liquid) equilibria of some (water + tetrahydrofuran + solvent) ternaries at the temperature (293.2 ± 0.1) K and pressure (101.3 ± 0.7) kPa.

J. Chem. Thermodyn. 27(1995) 525-529.

11. S. I. Kirbaslar, S. Sahin, M. Bilgin,

(Liquid + liquid) equilibria of (water + butyric acid + esters) ternary systems.

J. Chem. Thermodyn. 39 (2007) 1279-1285.

12. A. Arce, O. Rodriguez, A. Soto,

Liquid-liquid equilibria for butyl tert-butyl ether + (methanol or ethanol) + water at several temperatures.

Fluid Phase Equilibr. 224 (2004) 185-192.

13. B. M. G. de Doz, C. M. Bonatti, N. Barnes, H. N. Sólimo,

(Liquid + liquid) equilibria of ternary and quaternary systems including 2,2,4-trimethyl pentane, benzene, methanol, and water at T = 303.15 K.

J. Chem. Thermodyn. 33 (2001) 1663-1677.

14. B. M. G. de Doz, C. M. Bonatti, N. H. Sólimo,

(Liquid+liquid) equilibria of ternary and quaternary systems with two hydrocarbons, an alcohol, and water at 303.15 K. systems containing cyclohexane, benzen, methanol, and water.

J. Chem. Thermodyn. 35 (2003) 825-837.

15. I. C. Hwang, S. J. Park, J. S. Choi,

Liquid-liquid equilibria for the binary system of di-isopropyl ether (DIPE) + water in between 288.15 and 323.15 K and the ternary systems of DIPE + water + C_1-C_4 alcohols at 298.15 K.

Fluid Phase Equilibr. 269 (2008) 1-5.

16. B. M. G. de Doz, C. M. Bonatti, N. H.. Solimo,

Liquid-liquid equilibria of ternary and quaternary systems with two hydrocarbons, an alcohol, and water at 303.15 K systems containing 2,2,4-trimethyl pentane, toluene, methanol, and water or 2,2,4-trimethylpentane, toluene, ethanol, and water.

Fluid Phase Equilibr. 205 (2003) 53-67.

17. A. Arce, H. Rodriguez, O. Rodrıguez, A. Soto,
(Liquid + liquid) equilibrium of (dibutyl ether + methanol + water) at different temperatures.
J. Chem. Thermodyn. 37 (2005) 1007–1012.

18. M. G. de Doz, C. M. Bonatti, N. H. Solimo,
Liquid-liquid equilibria of water + ethanol + reformate.
Fluid Phase Equilibr. 230 (2005) 45-50.

19. E. Ince, S. I. Kirbaslar,
(Liquid+liquid) equilibria of (water+ethanol+dimethyl glutarate) at several temperatures.
J. Chem. Thermodyn. 35 (2003) 1671-1679.

20. G. B. Hong, M. J. Lee , H. M. Lin,
Liquid-liquid equilibria of ternary mixtures of water+2-propanol with ethyl acetate , isopropyl acetate, or ethyl caproate.
Fluid Phase Equilibr. 202 (2002) 239-252.

21. T. Minamihonok, H. Ogawa, H. Nomura, S. Murakami,
Thermodynamic properties of binary mixtures of 2,2,2-trifluoroethanol with water or alkanols at T = 298.15 K.
Thermochimica Acta 459 (2007) 80-86.

22. M. Sassi, Z. Atik,
Exess molar volumes of binary mixtures of 2,2,2-trifluoroethanol with water, or acetone, or 1,4-difluorobenzene, or 4-fluorotoluene, or α,α,α-trifluorotoluene or 1-alcohols at a temperature of 298.15 K and pressure of 101 kPa.
J. Chem. Thermodyn. 35 (2003) 1161-1169.

23. Z. Atik, K. Lourdani,
Volumetric properties of binary and ternary mixtures of disopropyl ether, α,α,α-trifluorotoluene, 2,2,2-trifluoroethanol, and ethanol at a temperature 298.15 K and pressure 101 KPa.
J. Chem. Thermodyn. 39 (2007) 576-582.

24. Z. Atik, A. Kritli,
Liquid-liquid equilibrium for 2,2,2-trifluoroethanol + ethanol + cyclohexane from (288.15 to 308.15) K.
J. Chem. Eng. Data. 53 (2008) 1146–1150.

25. Z. Atik,
Experimental vapor-liquid equilibria of binary mixtures of 2,2,2-trifluoroethanol with benzene or toluene.

J. Chem. Eng. Data. 52 (2007) 1086–1088.

26. J. S. Rowlinson,

Liquids and liquid mixtures.

2nd ed., Butterworth, (1969) 156-167.

27. Z. Atik,

Experimental and predicted volumetric and refractive index properties of ternary mixtures of iodoethane with toluene and alcohols at temperature 298.15 K and pressure 101 kPa.

J. Chem. Thermodyn. 38 (2006) 201-208.

28. H. I. Paul, Z. Atik, H. Knapp,

Measurements of vapor-liquid equilibrium, h^E and v^E for binary and ternary mixtures of methanol, ethyl iodide and toluene.

Chem. Eng. and Processing, 31 (1992) 77-85.

29. S. L. Mistry, A. Kaul, J. C. Merchuk, J. A. Asenjo,

Mathematical modelling and computer simulation of aqueous two-phase continous protein extraction.

J. Chromatogr. A741 (1996) 151-163.

30. Z. Atik, M. Chaou,

Temperature effect on liquid-liquid phase equilibria of aqueous solutions of fluorobenzene in ethanol at pressure p= 101.2 kPa.

J. Solution Chem. 36 (2006) 387-394.

31. K. Rehak, M. Bendova, J. Matous, J. P. Novak,

Liquid-liquid equilibrium study in the systems containing phthalate esters + water + 1-alkanol.

CHISA 2000, Prague.

32. J. L. Zurita, N. G. B. de Arreguez, H N. Solimo,

Equilibrium diagrams of water + succinic acid + (n-butanol or + benzyl alcohol or + tributyl phosphate) ternary systems at 303.15 K.

AFINIDAD L II 460 (1995) 419-424.

33. B. M. G. de Doz, A. M. Gases, H. N. Solimo,

(Liquid + liquid) equilibria of (water + linalool + limonene) ternary system at T = (298.15,308.15 and 318.15) K

J. Chem. Thermodyn. 40 (2008) 1575-1579.

34. D. Hand, B. Dineric,

The distribution of a consolute liquid between two immiscible liquids.

J. Phys. Chem. 34 (1930) 1961-2000.

35. D. F. Othmer, P. E.Tobias

Tie line correlation.

Ind. Eng. Chem. 34 (1942) 693-696.

36. H. Renon, J. M. Prausnitz.

AIChE J. 14 (1968) 135-142.

37. D. S. Abram, J. M. Prausnitz,

AIChE J. 21 (1975) 116-128.

38. J. de la Torre, A. chafer, A. Berna, R. Mufioz,

Liquid-liquid equilibria of the system dimethyl carbonate + methanol + water at different temperatures.

Fluid Phase Equilibr. 247(2006) 40-46.

39. T. M. Letcher, G. G. Redhi,

Phase equilibria for liquid mixtures of (benzonitrile + carboxylic acid + water) at 298.15 K.

J. Chem. Thermodyn. 33 (2001) 1555-1565.

40. B. E. Poling, J. M. Prausnitz, J. P. O'Connell,

The properties of gases and liquids.

5th ed ; McGraw-Hill: New York, 2000.

41. S. L. Mistry, A. Kaul, J. C. Merchuk, J. A. Asenjo,

Mathematical modelling and computer simulation of aqueous two-phase continous protein extraction.

J. Chromatogr. A 741 (1996) 151-163.

42. M. E. Toboada,

Liquid-liquid and solid-liquid equilibrium of the 1-propanol + lithium sulfatat + water system at 25,35, and 45°c.

Fluid Phase Equilibr. 204 (2003) 155-165.

43. Z. Atik, M. Chaou,

Solubilities and phase equilibria for ternary solutions of α,α,α-trifluorotoluene, water, and 2-propanol at three temperatures and pressure of 101.2 kPa.

J. Chem. Eng. Data. 52 (2007) 932-935.

44. T. M. Litcher, N. Deenadayalu,

Liquid-liquid equilibria for mixtures of 1-methyl-3-octyl-imidazolium chloride+benzene+an alkane at T = 298.2 K and 1atm.

J. Chem. Thermodyn. 35 (2003) 67-76.

45. U. Domanska, M. Marciniak,

Experimental (solid + liquid) or (liquid + liquid) phase equilibria of (amine + nitrile) binary mixtures.

J. Chem. Thermodyn. 39 (2007) 247-253.

46. X. Xu, P. P. Madeira, E. A. Macedo,

Representation of liquid-liquid equilibria for polymer-salt aqueous two-phase systems.

J. Chem. Eng. Science 59 (2004) 1153-1159.

47. H. Matsuda, K. Kurihara, K. Ochi, K. Kojima,

Prediction of liquid-liquid equilibria at high pressure for binary systems using EOS-G^E models: methanol + hydrocarbon systems.

Fluid Phase Equilibr. 203 (2002) 269-284.

48. S. I. Kirbaslar, M. Bilgin, D. Batr,

(Liquid + liquid) equilibria of (water + butyric acid + cyclohexyl acetate) ternary system.

J. Chem. Thermodyn. 37 (2005) 175-180.

49. S.I. Kirbaslar,

(Liquid + liquid) equilibria of the (water+butyric acid+dodecanol) ternary system.

J. Chem. Thermodyn. 38 (2006) 696-700.

50. S. I. Kırbaslar, S. Sahin, M. Bilgin,

(Liquid + liquid) equilibria of (water + propionic acid + diethyl succinate or diethyl glutarate or diethyl adipate) ternary systems.

J. Chem. Thermodyn. 39 (2007) 1463-1469.

51. S. B. Hung, H. M. Lin, C. Ching Yu, H. P. Huang, M. J. Lee,

Liquid-liquid equilibria of aqueous mixtures containing selected dibasic esters and/or methanol.

Fluid Phase Equilibr. 248 (2006) 174-180.

52. J. M. Resa, J. M. Goenaga,

(liquid-liquid) equilibrium diagrams of ethanol + water + (ethyl acetate or 1-pentanol) at several temperatures.

J. Chem. Eng. Data 51 (2006) 1300-1305.

53. J. A. Riddich, W. B. Bunger, T. K. Sakano,

Physical properties and methods of purification. Organic solvents, John Willey.

New York, (1986) vol. II.

54. Z. Atik, M. Chaou,

Solubilities and liquid-liquid equilibria of (water + ethanol + α,α,α-trifluorotoluene) at temperatures T = (288.15, 298.15, and 308.15) K and pressure p = 101.2 kPa.

J. Chem. Thermodyn. 39 (2007) 583–587.

55. A. Senol,
Liquid liquid equilibria for ternary systems of (water+carboxylic acid+ 1-octanol) at 293.15 K: modeling phase equilibria using a solvatochromic approach.
Fluid Phase Equilibr. 227 (2005) 87-96.
56. E. Ince, I. Kirbaslar,
Liquid-liquid equilibria of the water-acetic acid-butyl acetate system.
Braz. J. Chem. Eng. 19 (2002) 1-14.
57. K. Rehak, J. Matous, J. P. Novak. M. Bendova,
(Liquid + liquid) equilibrium for (dimethyl phthalate + water), (diethyl phthalate + water), and (dibutyl phthalate + water).
J. Chem. Thermodyn. 32 (2000) 393-400.
58. C. D. Chu, Y. H. Qi, W. Hao,
(liquid + liquid) equilibria of {heptane + xylene + *N*-formylmorpholine} ternary system.
J. Chem. Thermodyn. 39 (2007) 1571-1577.
59. Horacio N. Solimo, José L. Zurita,
Influence of temperature on the liquid-to-liquid extraction of ethanol from (water + ethanol + 1,2-dichloroethane).
Can. J. Chem. 70 (1992) 2310-2311.
60. Y.Y. Wu, J. W. Zhu, K. Chen, B. Wu , Y. L. Shen,
Liquid–liquid equilibria of water + 2,3-butanediol + ethyl acetate at several temperatures.
Fluid Phase Equilibr. 266 (2008) 42-46.
61. P. H. Ho, R. G. Burnette, M. H. Lietzike,
Miscibility relationships in sytems containing various hydrocarbons, n-butylcarbitol, and aqueous solution of sodium salicylate.
J. Chem. Eng. Data 25 (1980) 41-45.
62. H. Li, K. Tamura,
Ternary liquid-liquid for (water + terpene + 1-propanol or 1-butanol) systems at the temperature 298.15 K.
Fluid Phase Equilibr. 263 (2008) 223-230.
63. A. Chafer, M. C. Burguet, J. B. Monton, E. Liadosa,
Liquid-liquid equilibria of the systems dipropyl ether + n-propanol + water and dipropyl ether + n-propanol + ethylene glycol at different temperatures.
Fluid Phase Equilibr. 262 (2007) 76-81.
64. Y. Y. Wu, J. W. Zhu, K. Chen, B. Wu, J. Fang, Y. L. Shen,

Liquid-liquid equilibria for water + 2,3- butanediol + 1-butanol at *T* = 298.15 K, *T* = 308.15 K and *T* = 318.15 K.

Fluid Phase Equilibr. 265 (2008) 1-6.

65. S. I. Kırbaslar, E. Ince, S. Sahin, U. Dramur,

(Liquid + liquid) equilibria of (water + propionic acid + dibasic esters) ternary systems.

J. Chem. Thermodyn. 39 (2007) 1493–1499.

66. A. N. Darwich,

Liquid-liquid equilibrium for the system n-heptane + o-xylene + triethylene glycol from 293.1 to 323.1 K.

J. Chem. Eng. and Processing 41 (2001) 737-741.

67. F. J. Lozano,

Ternary equilibrium for the system wate/methyl isobutyl ketone/2-ethyl-2-(hydroxymethyl)-1,3-propanediol.

J. Chem. Eng. Data 26 (1981) 131-133.

68. H. Ghanadzadeh, A. Ghanadzadeh, K. Bahrpaima, S. L. S. Saadat,

(Liquid + liquid) equilibria for (water + propionic acid + 2-ethyl-1-hexanol): experimental data and correlation.

J. Chem. Thermodyn. 40 (2008) 879-884

69. S. I. Kirbaslar, E. Ince, S. Yuksel,

(Liquid + liquid) equilibria of the (water+acetic acid+dibutyl phthalate) system.

J. Chem. Thermodyn. 37 (2005) 1256-1260.

70. S. Cehreli, D. Ozmen, B. Tatli,

(Liquid + liquid) equilibria of (water + propionic acid + diethyl phthalate) at several temperatures.

J. Chem. Thermodyn. 37 (2005) 1144–1150.

71. D. Ozmen,

Determination and correlation of liquid-liquid equilibria for the (water + carboxylic acid + dimethyl maleate) ternary systems at *T* = 298.2 K.

Fluid Phase Equilibr. 269 (2008) 12-18.

72. D. Ozmen, S. Çehreli, U. Dramur,

(Liquid + liquid) equilibria of (water + propionic acid + dimethyl phthalate) at several temperatures

J. Chem. Thermodyn. 37 (2005) 837-842.

73. A. Arce, A. Marchiaro, O. Rodriguez, A. Soto,

Liquid–liquid equilibria of limonene + linalool + diethylene glycol system at different temperatures.
J. Chem. Eng. Data 89 (2002) 223–227.

74. A. Arce, J. M. Ageitos ,O. Rodrigues, A. Soto,
(Liquid-liquid) equilibria of (tert-amyl ethyl ether+ethanol+water) at several temperatures.
J. Chem. Thermodyn. 33 (2001) 139-146.

75. A. Chafer, J de la Torre, J. B. Monton, E. Ladosa,
Liquid-liquid equilibria of the systems isobutyl acetate + isobutyl alcohol + water and isobutyl acetate + isobutyl alcohol + glycerol at different temperatures.
Fluid Phase Equilibr. 265 (2008) 122-128.

76. A. Arce, A. Marchiaro, A. Soto,
Propandiols for separation of citrus oil: liquid-liquid equilibria of limonene + linalool + linalool + (1,2-propandiol or 1,3 propandiol).
Fluid Phase Equilibr. 211 (2003) 129-140.

77. R. Stephenson, J. Stuart,
Mutual binary solubilities: water-alcohols and water-esters.
J. Chem. Eng. Data 31 (1986) 56-70.

78. S. B. Bottini,
Liquid-liquid equilibria for the system toluene-isooctane-diethylele glycol methyl ether.
J. Chem. Eng. Data 31 (1986) 84-86.

79. H. Matsuda, K. Ochi, K. Kojima,
Determination and correlation of LLE and SLE data for the methanol + cyclohexane, aniline + heptane, and phenol + hexane system.
J. Chem. Eng. Data 48 (2003) 184-189.

80. V. Gomis, A. Font, M. D. Saquete,
Homogeneity of the water + ethanol + toluene azeotrope at 101.3 kPa
Fluid Phase Equilibr. 266 (2008) 8-13

81. T. M. Letcher, P. M. Siswana,
Liquid-liquid equilibria for mixtures of an alkanol + water + a methyl substituted benzene at 25°C.
Fluid Phase Equilibr. 74 (1992) 203-217.

82. F. R. Bevia, D. P. Rico, V. G. Yagues,

Determination of quaternary liquid-liquid equilibrium data using either measurements of a single physical property of the analysis of only one of the components. Application to the quaternary system: water-ethanol-chloroform-toluene at 25°C.

Fluid Phase Equilibra 23 (1985) 269-292.

83. T. Moriyoshi, Y. Uosaki, K. Takahashi, T. Yamakawa,

(Liquid + liquid) equilibria of (water + ethanol + cyclohexane) at the temperature 298.15 K and 323.15 K.

J.Chem.Thermodyn. 23 (1991) 37-42.

84. D. Plackov, I. Stern,

Liquid-liquid equilibria for ternary systems of cyclohexane-water and C_1 to C_3 alcohols : data and predictions.

Fluid phase equilibr. 71 (1992) 189-209.

85. G. Hradetzky, D. A. Lempe,

Phase equilibria in binary and higher systems methanol + hydrocarbon(s). Experimental determination of liquid-liquid equilibrium data and their representation using the NRTL equation.

Fluid Phase Equilibr. 69 (1991) 285-301.

86. J. T. Chen, M. C. Chen,

Salting effect on the liquid-liquid equilibria for the ternary system water +*N*-methyl-2-pyrrolidone + 1-pentanol.

Fluid Phase Equilibr. 266 (2008) 1-7.

87. L. Alonso, A. Arce, M. Francisco, A. Soto,

(Liquid + liquid) equilibria of [C8mim][NTf2] ionic liquid with a sulfur-component and hydrocarbons.

J. Chem. Thermodyn. 40 (2008) 265-270

88. H. Uslua, A. Gökb, S. I. Kirbaslar,

Phase equilibria of (water + levunilic acid + alcohol) ternary systems.

Fluid Phase Equilibria 273 (2008) 21-26.

89. M. Bendova, K. Rehak, J. Matous, J. P. Novak,

Liquid-liquid equilibrium in ternary systems N,N-dimethyl formamide + 2-methyl pentane + Methanol and N,N-dimethyl formamide + methylcyclohexane + Methanol.

Fluid Phase Equilibr. 239 (2006) 16-25.

90. Z. Atik. W. Kerboub,

Liquid-liquid equilibrium of (cyclohexane + 2,2,2-trifluoroethanol) and (cyclohexane + methanol) from (278.15 to 318.15) K.

J. Chem. Eng. Data 53 (2008)1669-1671.

91. Z. Atik. W. Kerboub,

Effect of temperature on phase equilibrium of the mixed-solvent system of (2,2,2-trifluoroethanol + methanol + cyclohexane).

J. Chem. Eng. Data 54 (2009) 282-285.

92. W. Kerboub, Z. Atik,

Phase diagram of (hexane + methanol + 2,2,2-trifluoroethanol) at three temperatures: Measurement and Correlation.

J. Chem. Thermodyn. 41 (2009) 549–552.

93. W. Kerboub, Z. Atik,

The solubility and liquid-liquid equilibrium of aqueous systems of iodoethane with alcohols at temperature 298.15 K and 101 kPa.

J. Chem. Eng. Data 54 (2009) 2132–2136.

ANNEXE A

EXPERIMENTAL RESULTS

Experimental and Correlated Solubility and Liquid-Liquid Equilibrium Data of Binary and Ternary Mixtures of Water, 2,2,2-Trifluoroethanol, Alcohols, Iodoethane, and Hydrocarbons at Various Temperatures and Pressure 0.1 MPa

Table (A_0.1): Experimental liquid-liquid equilibrium data for hexane (1) + methanol (2) at 0.1 MPa

	feed mixture		hexane-rich phase		methanol-rich phase	
T/K	x_1	x_2	x_1^{α}	x_2^{α}	x_1^{β}	x_2^{β}
278.15	0.490	0.510	0.910	0.091	0.133	0.867
283.15	0.497	0.503	0.871	0.129	0.146	0.854
288.15	0.492	0.508	0.828	0.172	0.155	0.845
293.15	0.496	0.504	0.789	0.211	0.174	0.826
298.15	0.505	0.495	0.741	0.259	0.214	0.786
303.15	0.511	0.489	0.676	0.324	0.276	0.724
305.15	0.499	0.501	0.626	0.374	0.312	0.688
306.15	0.495	0.505	0.582	0.418	0.370	0.631

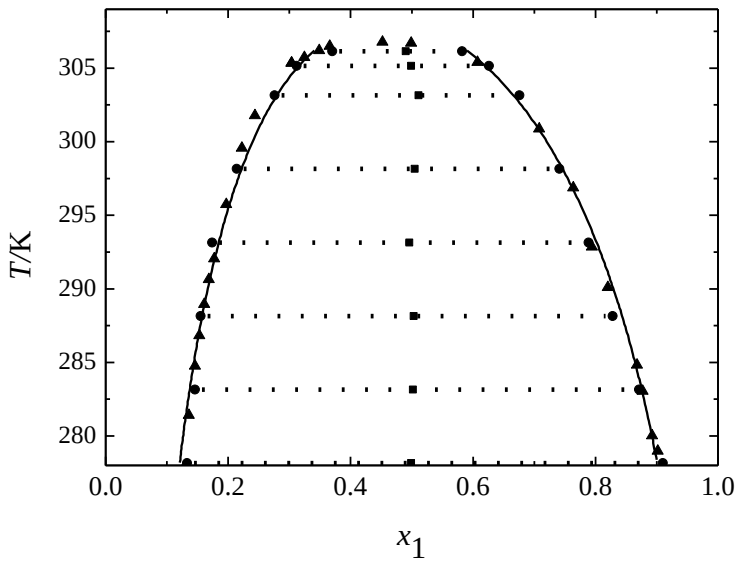

Figure (A_0.1): Liquid-liquid equilibrium for hexane (1) + methanol (2): ■, feed mixture; ●, LLE; ▲, from ref. [47]; …, tie line; ~~, NRTL.

Table (A_0.2): Experimental liquid-liquid equilibrium data for cyclohexane (1) + methanol (2) at 0.1 MPa

T/K	feed mixture		cyclohexane-rich phase		methanol-rich phase	
	x_1	x_2	x_1^{α}	x_2^{α}	x_1^{β}	x_2^{β}
278.15	0.502	0.498	0.942	0.058	0.104	0.896
283.15	0.520	0.480	0.939	0.061	0.125	0.875
288.15	0.510	0.490	0.922	0.078	0.135	0.865
293.15	0.519	0.481	0.892	0.108	0.158	0.842
298.15	0.496	0.504	0.876	0.124	0.177	0.837
303.15	0.530	0.470	0.841	0.160	0.190	0.810
308.15	0.516	0.484	0.812	0.210	0.218	0.796
313.15	0.523	0.477	0.758	0.242	0.261	0.739
316.15	0.520	0.480	0.702	0.298	0.301	0.699

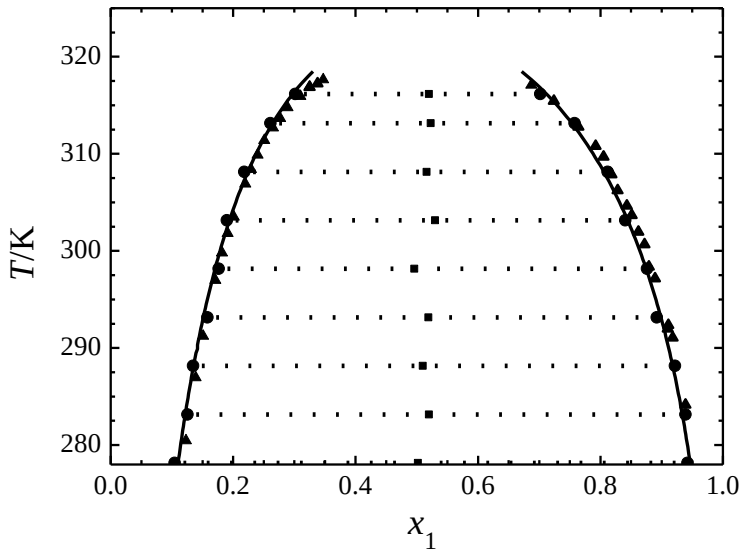

Figure (A_0.2): Liquid-liquid equilibrium for cyclohexane (1) + methanol (2): ■, feed mixture; ●, LLE; ▲, from ref. [79]; ..., tie line; —, NRTL

Table (A_0.3): Experimental solubility data for water (1) + ethanol (2) + toluene (3) at 298.15 K and 0.1 MPa

x_1	x_2	x_3	x_1	x_2	x_3
0.613	0.346	0.022	0.297	0.458	0.244
0.587	0.379	0.034	0.274	0.450	0.276
0.554	0.400	0.046	0.255	0.442	0.303
0.515	0.425	0.061	0.241	0.434	0.325
0.482	0.441	0.077	0.220	0.418	0.362
0.456	0.454	0.090	0.189	0.388	0.424
0.437	0.460	0.103	0.149	0.349	0.502
0.435	0.460	0.105	0.119	0.310	0.570
0.400	0.469	0.131	0.095	0.289	0.617
0.360	0.474	0.166	0.077	0.254	0.669
0.331	0.469	0.201	0.055	0.225	0.720
0.300	0.458	0.243	0.034	0.171	0.795

Binodal eq.: $x_2 = -0.081 + 3.282\,x_3^{0.5} - 5.230\,x_3 + 3.721\,x_3^2 - 1.709\,x_3^3$; $R^2 = 0.985$

Table (A_0.4): Experimental liquid-liquid equilibrium data for water (1) + ethanol (2) + toluene (3) at 298.15 K and 0.1 MPa

feed mixture		water-rich phase		toluene-rich phase	
x_1	x_2	x_1^{α}	x_2^{α}	x_1^{β}	x_2^{β}
0.582	0.072	0.523	0.425	0.065	0.242
0.534	0.152	0.604	0.363	0.025	0.179
0.469	0.263	0.656	0.325	0.016	0.105
0.502	0.209	0.704	0.280	0.010	0.084
0.432	0.310	0.771	0.214	0.005	0.042
0.405	0.370	0.875	0.112	0.002	0.012
x^{cs}		0.285	0.466	0.285	0.466

Hand eq.: $\ln\left(x_2^{\beta} / x_3^{\beta}\right) = A + B\ln\left(x_2^{\alpha} / x_1^{\alpha}\right)$; y = -0.631 + 1.873 x, $R^2 = 0.988$

Othmer-Tobias eq.: $\ln\left\{\left(1 - x_3^{\beta}\right)/x_3^{\beta}\right\} = A + B.\ln\left\{\left(1 - x_1^{\alpha}\right)/x_1^{\alpha}\right\}$; y = -0.616 + 1.909 x, $R^2 = 0.994$

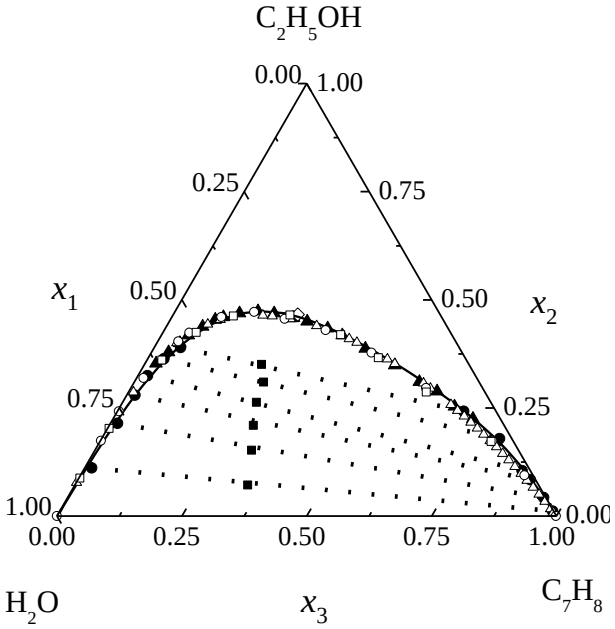

Figure (A_0.3): Solubility and liquid-liquid equilibrium data for water (1) + ethanol (2) + toluene (3) at 298.15 K: ▲, solubility; ∇, from ref. [80]; ○, from ref. [81]; □, from ref. [82]; ■, feed mixture; ●, LLE; ◊, p.p.; …, tie line; —, NRTL.

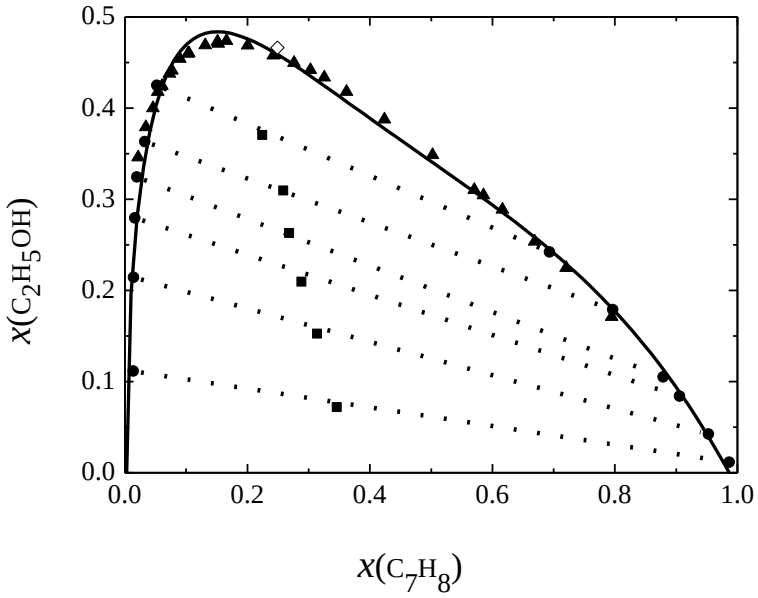

Figure (A_0.4): Solubility and liquid-liquid data for water (1) + ethanol (2) + toluene (3) at 298.15 K: ▲, solubility; ■, feed mixture; ●, LLE; ◊, p.p.; …, tie line; —, eq. (2.35).

Table (A_0.5): Experimental solubility for water (1) + ethanol (2) + cyclohexane (3) at 298.15 K and 0.1 MPa

x_1	x_2	x_3	x_1	x_2	x_3
0.515	0.459	0.027	0.166	0.605	0.229
0.470	0.495	0.034	0.151	0.590	0.260
0.429	0.528	0.043	0.125	0.555	0.321
0.396	0.552	0.052	0.109	0.514	0.377
0.357	0.579	0.064	0.102	0.504	0.394
0.320	0.597	0.083	0.083	0.450	0.467
0.279	0.610	0.112	0.077	0.437	0.486
0.257	0.613	0.130	0.075	0.418	0.508
0.227	0.621	0.151	0.057	0.369	0.574
0.204	0.619	0.177	0.044	0.303	0.653
0.189	0.616	0.195	0.033	0.249	0.718

Binodal eq.: $x_2 = 0.2258 + 2.0098\, x_3^{0.5} - 2.6883\, x_3 + 0.5255\, x_3^2 - 0.0696\, x_3^3$; R^2=0.956

Table (A_0.6): Experimental liquid-liquid equilibrium data for water (1) + ethanol (2) + cyclohexane (3) at 298.15 K and 0.1 MPa

feed mixture		water-rich phase		cyclohexane-rich phase	
x_1	x_2	x_1^{α}	x_2^{α}	x_1^{β}	x_2^{β}
0.258	0.541	0.300	0.600	0.036	0.253
0.282	0.499	0.349	0.575	0.016	0.160
0.305	0.458	0.385	0.563	0.011	0.120
0.357	0.394	0.469	0.505	0.001	0.056
0.363	0.351	0.508	0.477	0.001	0.049
0.399	0.292	0.581	0.418	0.001	0.045
0.408	0.254	0.616	0.378	0.0003	0.012
0.497	0.127	0.799	0.200	0.0003	0.013
x^{cs}		0.149	0.586	0.149	0.586

Hand eq.: $\ln\left(x_2^{\beta} / x_3^{\beta}\right) = A + B \ln\left(x_2^{\alpha} / x_1^{\alpha}\right)$; y = -3.054 + 2.880 x, R^2=0.956

Othmer-Tobias eq.: $\ln\left\{\left(1 - x_3^{\beta}\right)/x_3^{\beta}\right\} = A + B.\ln\left\{\left(1 - x_1^{\alpha}\right)/x_1^{\alpha}\right\}$; y = -3.140 + 2.263 x, R^2=0.985

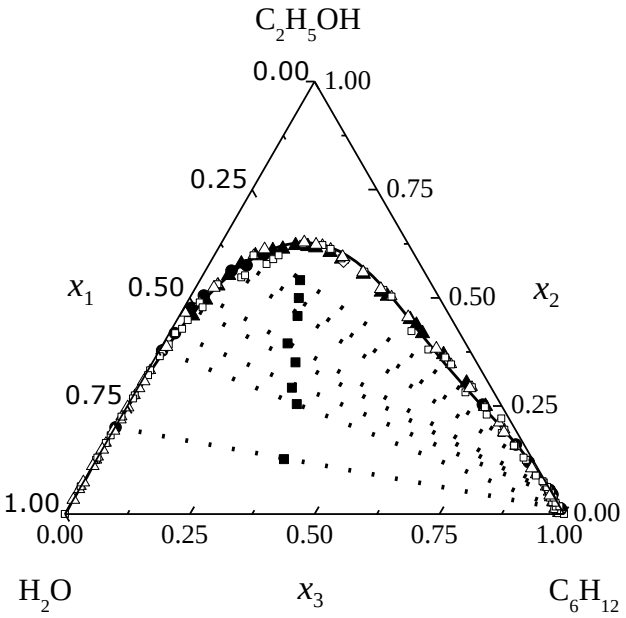

Figure (A_0.5): Solubility and liquid-liquid equilibrium data for water (1) + ethanol (2) + cyclohexane (3) at 298.15 K: ▲, solubility; ▽, from ref. [83]; □, from ref. [84]; ■, feed mixture; ●, LLE; ◊, p.p; ..., tie line; —, NRTL eq.

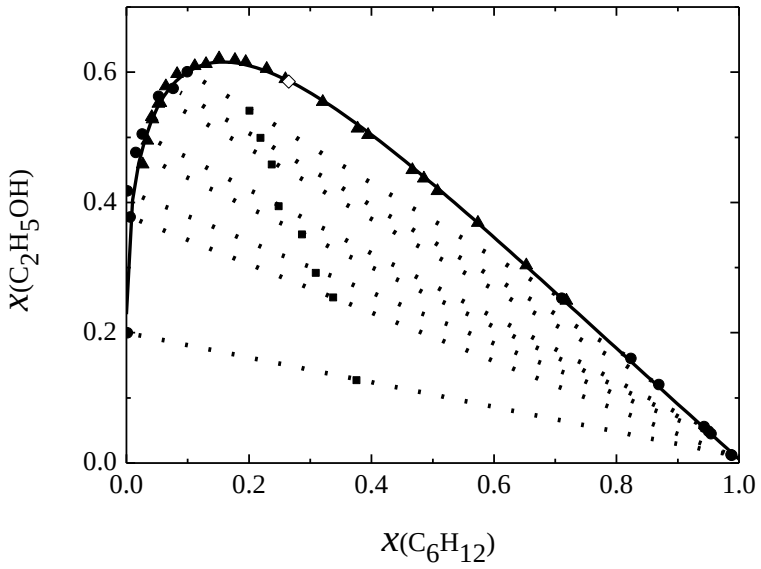

Figure (A_0.6): Solubility and liquid-liquid equilibrium data for water (1) + ethanol (2) + cyclohexane (3) at 298.15 K: ▲, solubility; ■, feed mixture**;** ●, LLE; ◊, p.p.; ..., tie line; —, eq. (2.35).

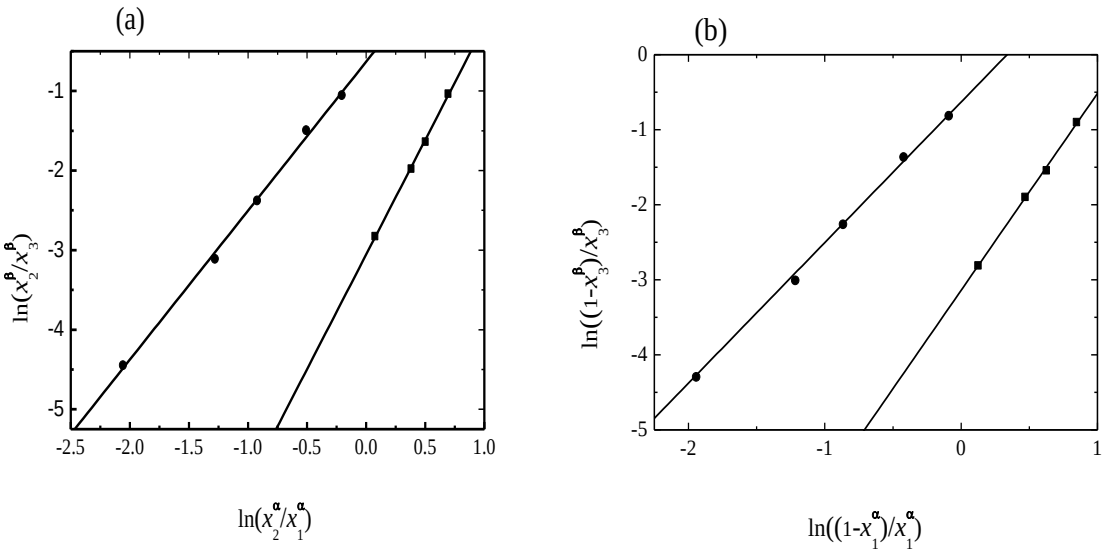

Figure (A_0.7): Correlation of the liquid-liquid equilibrium data for water (1) + ethanol (2) + solvent (3) mixtures at 298.15 K: ●, toluene; ■, cyclohexane; (a), Hand; —, eq. (2.36); (b), Othmer-Tobias; — eq. (2.37).

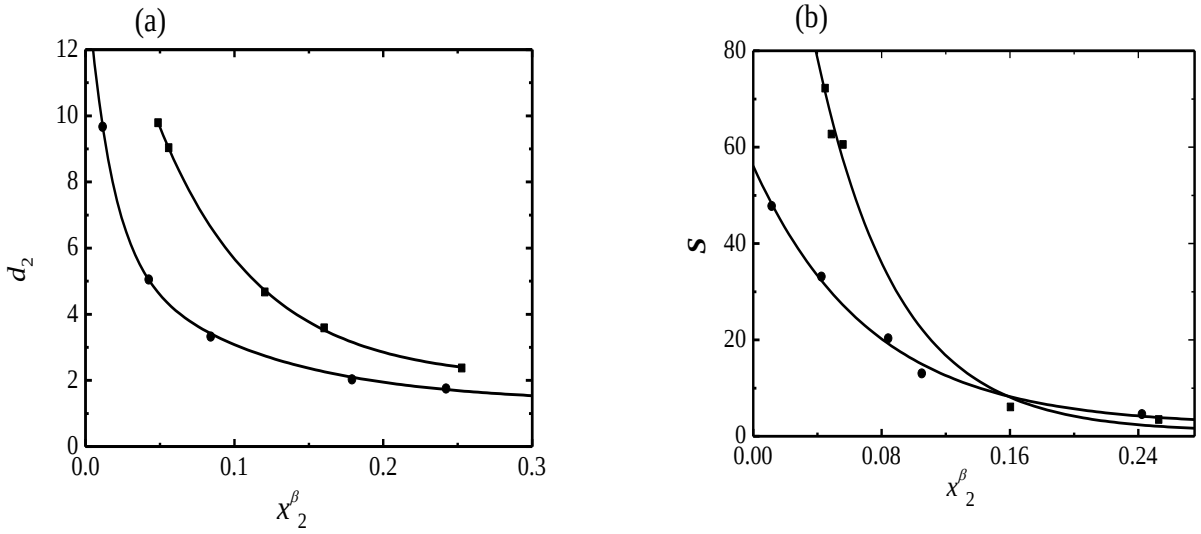

Figure(A_0.8): Distribution coefficient d_2 of methanol and selectivity S for liquid-liquid equilibrium of water (1) + ethanol (2) + solvent (3) at 298.15 K: ; ●, toluene; ■, cyclohexane. (a), distribution coefficient; (b), selectivity.

Table (A_0.7): Experimental liquid-liquid equilibrium data for methanol (1) + hexane (2) + cyclohexane (3) at 293.15 K and 0.1 MPa

feed mixture		methanol-rich phase		(cyclohexane-hexane)-rich phase	
x_1	x_2	x_1^{α}	x_2^{α}	x_1^{β}	x_2^{β}
0.504	0.214	0.829	0.068	0.216	0.343
0.502	0.101	0.833	0.042	0.176	0.155
0.489	0.059	0.835	0.033	0.154	0.087
0.503	0.313	0.793	0.128	0.226	0.482
0.512	0.360	0.807	0.155	0.241	0.540
0.501	0.404	0.808	0.170	0.251	0.579
0.503	0.269	0.820	0.098	0.226	0.424
0.515	0.445	0.844	0.184	0.252	0.672

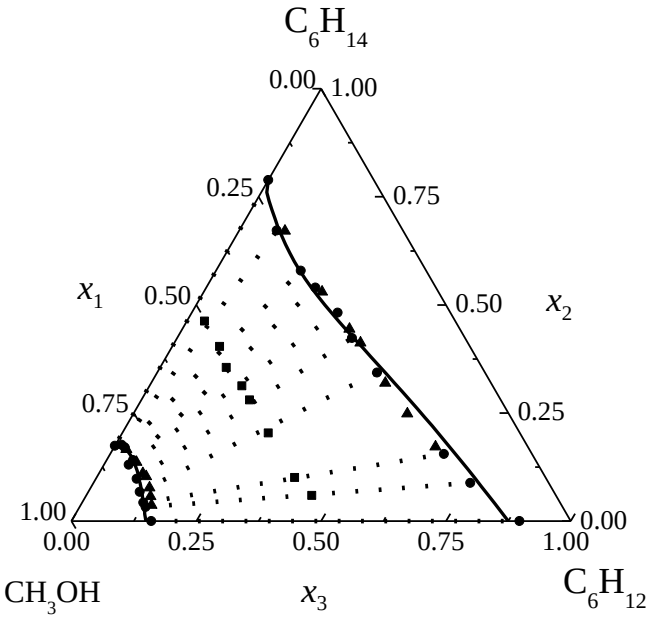

Figure (A_0.9): Liquid-liquid equilibrium for methanol (1) + hexane (2) + cyclohexane (3) at 293.15 K: ■, feed mixture; ●, LLE; ▲, from ref. [85]; ..., tie line; —, UNIQUAC.

Table (A.1.1): Experimental liquid-liquid equilibrium data for hexane (1) + 2,2,2-trifluoroethanol (2) at 0.1 MPa

T/K	feed mixture		hexane-rich phase		trifluoroethanol-rich phase	
	x_1	x_2	x_1^{α}	x_2^{α}	x_1^{β}	x_2^{β}
278.15	0.507	0.493	0.880	0.121	0.075	0.925
283.15	0.513	0.487	0.856	0.144	0.081	0.919
288.15	0.502	0.498	0.829	0.171	0.099	0.901
293.15	0.499	0.501	0.802	0.198	0.122	0.878
298.15	0.499	0.501	0.761	0.239	0.155	0.845
303.15	0.502	0.498	0.726	0.274	0.184	0.816
308.15	0.496	0.504	0.678	0.322	0.226	0.774
310.15	0.492	0.508	0.643	0.357	0.245	0.755
313.15	0.502	0.498	0.574	0.426	0.325	0.675

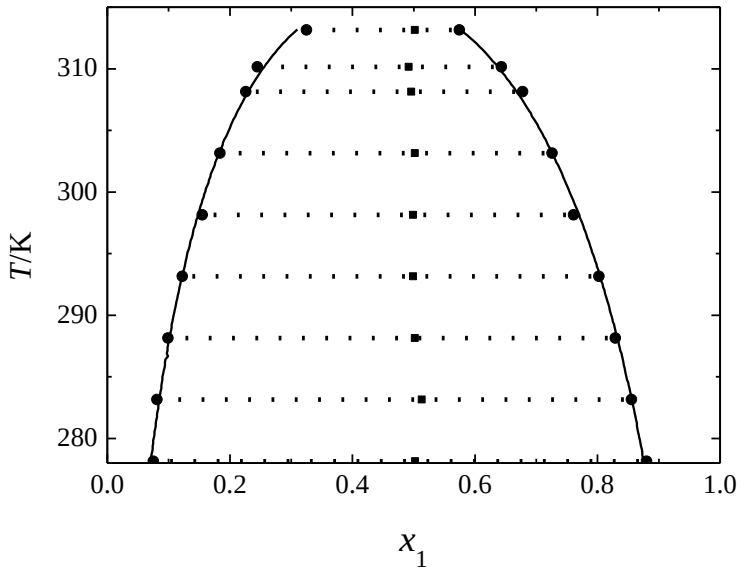

Figure (A.1.1): Liquid-liquid equilibrium for hexane (1) + 2,2,2-trifluoroethanol (2): ■, feed mixture; ●, LLE; ..., tie line; —, NRTL.

Table (A.1.2): Experimental liquid-liquid equilibrium data for cyclohexane (1) + 2,2,2-trifluoroethanol (2) at 0.1 MPa

T/K	feed mixture		cyclohexane-rich phase		trifluoroethanol-rich phase	
	x_1	x_2	x_1^{α}	x_2^{α}	x_1^{β}	x_2^{β}
283.15	0.501	0.499	0.925	0.075	0.045	0.955
288.15	0.500	0.500	0.899	0.101	0.054	0.946
293.15	0.500	0.500	0.880	0.120	0.069	0.931
298.15	0.499	0.502	0.865	0.135	0.088	0.912
303.15	0.496	0.504	0.850	0.150	0.106	0.894
308.15	0.503	0.498	0.837	0.163	0.111	0.889
313.15	0.498	0.502	0.812	0.188	0.119	0.881
316.15	0.502	0.498	0.786	0.214	0.144	0.856
318.15	0.499	0.502	0.767	0.233	0.167	0.833

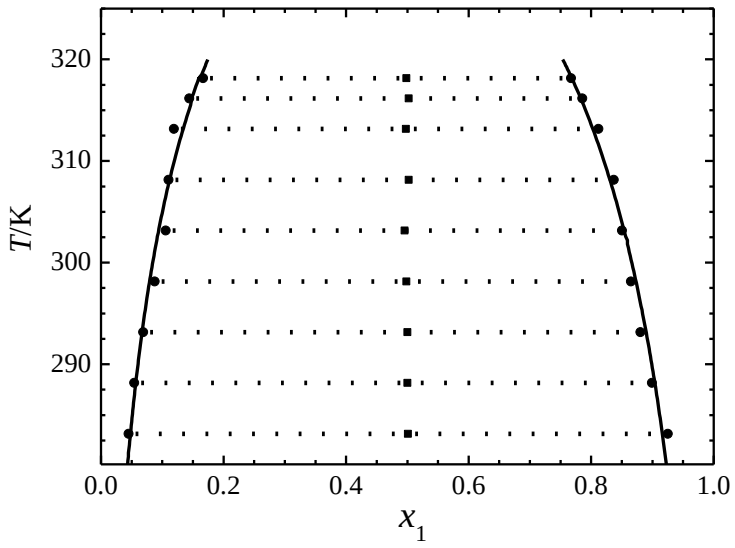

Figure (A.1.2): Liquid-liquid equilibrium for cyclohexane (1) + 2,2,2-trifluoroethanol (2): ■, feed mixture; ●, LLE; ..., tie line; —, NRTL.

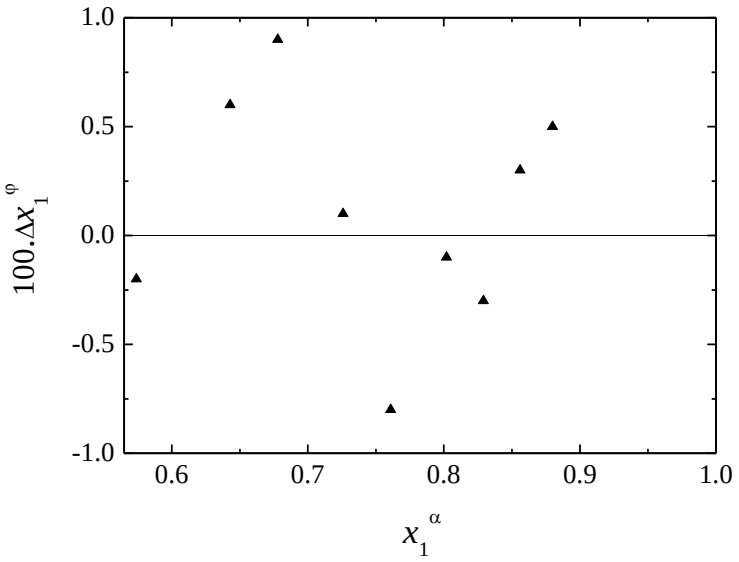

Figure (A.1.3): Deviations in phase mole fractions from the UNIQUAC correlation for hexane (1) + 2,2,2-trifluoroethanol (2).

Table (A.1.3): Interaction parameters, $A_{ij} = a_{ij} + b_{ij}T$, for NRTL and UNIQUAC equations for hydrocarbon (1) + 2,2,2-trifluoroethanol (2) at 0.1 MPa

	NRTL			UNIQUAC	
Components *ij*	α_{ij}	a_{ij}/K	b_{ij}	a_{ij}/K	b_{ij}
hexane (1) + 2,2,2-trifluoroethanol (2)					
1.2	0.2	1073.926	-2.657	337.427	-0.378
2.1		1324.91	-2.634	368.074	-1.078
cyclohexane (1) + 2,2,2-trifluoroethanol (2)					
1.2	0.2	1126.75	-2.538	352.93	-0.514
2.1		1493.01	-2.982	483.02	-1.238

Table (A.2.1): Experimental Solubility for water (1) + methanol (2) + iodoethane (3) at 298.15 K and 0.1 MPa

x_1	x_2	x_3	x_1	x_2	x_3
0.098	0.292	0.609	0.241	0.634	0.125
0.112	0.345	0.542	0.268	0.631	0.101
0.124	0.403	0.473	0.293	0.624	0.082
0.129	0.464	0.406	0.314	0.617	0.069
0.145	0.502	0.353	0.338	0.604	0.057
0.160	0.555	0.284	0.061	0.159	0.780
0.176	0.585	0.239	0.385	0.575	0.040
0.184	0.604	0.212	0.428	0.542	0.030
0.199	0.619	0.183	0.451	0.525	0.024
0.217	0.628	0.154	0.489	0.493	0.018

Binodal eq.: $x_2 = 4.0184\, x_3^{0.5} - 6.6252\, x_3 + 4.1351\, x_3^2 - 1.5338\, x_3^3$; $R^2 = 0.965$

Table (A.2.2): Experimental liquid-liquid equilibrium data for water (1) + methanol (2) + iodoethane (3) at 298.15 K and 0.1 MPa

feed mixture		water-rich phase		iodoethane-rich phase	
x_1	x_2	x_1^{α}	x_2^{α}	x_1^{β}	x_2^{β}
0.258	0.558	0.323	0.615	0.101	0.342
0.308	0.493	0.374	0.581	0.072	0.224
0.354	0.419	0.462	0.515	0.051	0.146
0.394	0.333	0.541	0.447	0.033	0.090
0.430	0.287	0.597	0.392	0.025	0.071
0.489	0.216	0.690	0.299	0.012	0.041
0.533	0.148	0.776	0.215	0.008	0.029
0.558	0.095	0.850	0.139	0.004	0.011
x^{cs}		0.154	0.540	0.154	0.540

Hand eq.: $\ln\left(x_2^{\beta} / x_3^{\beta}\right) = A + B \ln\left(x_2^{\alpha} / x_1^{\alpha}\right)$; y = -1.767 + 1.532 x; $R^2 = 0.982$

Othmer-Tobias eq.: $\ln\left\{\left(1 - x_3^{\beta}\right)/x_3^{\beta}\right\} = A + B.\ln\left\{\left(1 - x_1^{\alpha}\right)/x_1^{\alpha}\right\}$; y = -1.58 + 1.527 x; $R^2 = 0.989$

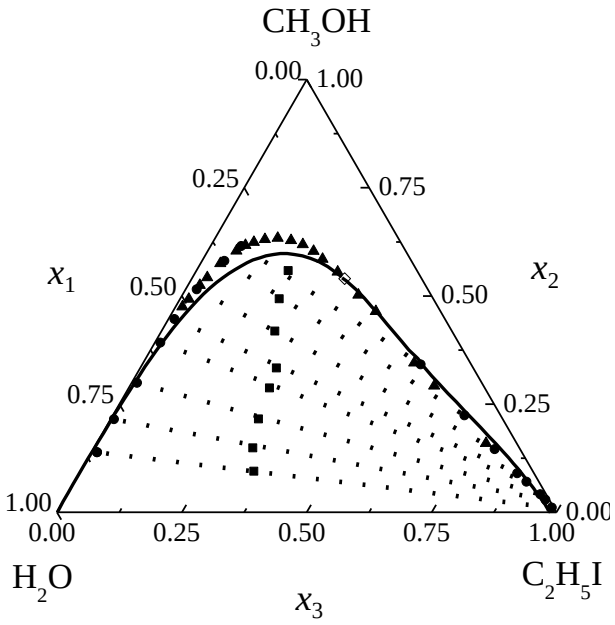

Figure (A.2.1): Solubility and liquid-liquid equilibrium data for water (1) + methanol (2) + iodoethane (3) at 298.15 K: ▲, solubility; ■, feed mixture; ●, LLE; ◊, p.p.; …, tie line; —, NRTL.

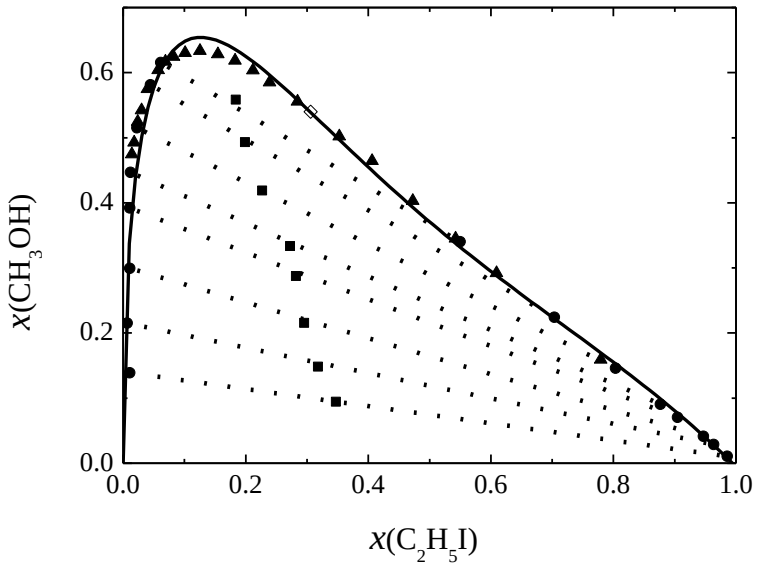

Figure (A.2.2): solubility and liquid-liquid equilibrium data for water (1) + methanol (2) + iodoethane (3) at 298.15 K: ▲, solubility; ■ feed mixture; ●, LLE; ◊ p.p.; …, tie line; —, eq. (2.35).

Table (A.2.3): Experimental Solubility for water (1) + ethanol (2) + iodoethane (3) at 298.15 K and 0.1 MPa

x_1	x_2	x_3	x_1	x_2	x_3
0.039	0.148	0.833	0.402	0.432	0.166
0.080	0.231	0.689	0.447	0.426	0.128
0.120	0.281	0.599	0.483	0.417	0.100
0.146	0.325	0.529	0.529	0.397	0.074
0.166	0.351	0.482	0.569	0.375	0.056
0.239	0.392	0.369	0.596	0.360	0.043
0.270	0.411	0.318	0.636	0.333	0.031
0.306	0.426	0.268	0.662	0.315	0.023
0.345	0.435	0.221	0.671	0.311	0.019
0.393	0.432	0.175	0.697	0.291	0.012

Binodal eq.: $x_2 = 0.1179 + 1.6326\, x_3^{0.5} - 2.2614\, x_3 + 1.0424\, x_3^2 - 0.5304\, x_3^3$; R^2 = 0.974

Table (A.2.4): Experimental liquid-liquid equilibrium data for water (1) + ethanol (2) + iodoethane (3) at 298.15 K and 0.1 MPa

feed mixture		water-rich phase		iodoethane-rich phase	
x_1	x_2	x_1^{α}	x_2^{α}	x_1^{β}	x_2^{β}
0.387	0.397	0.443	0.425	0.069	0.236
0.417	0.342	0.528	0.393	0.064	0.187
0.452	0.313	0.582	0.362	0.047	0.162
0.490	0.261	0.661	0.307	0.023	0.130
0.499	0.209	0.747	0.251	0.010	0.099
0.539	0.141	0.817	0.178	0.008	0.073
0.588	0.119	0.843	0.148	0.007	0.066
0.593	0.072	0.901	0.096	0.005	0.032
x^{cs}		0.201	0.378	0.201	0.380

Hand eq.: $\ln\left(x_2^{\beta} / x_3^{\beta}\right) = A + B \ln\left(x_2^{\alpha} / x_1^{\alpha}\right)$; y = -1.086 + 0.987 x; R^2 = 0.987

Othmer-Tobias eq.: $\ln\left\{\left(1 - x_3^{\beta}\right)/x_3^{\beta}\right\} = A + B.\ln\left\{\left(1 - x_1^{\alpha}\right)/x_1^{\alpha}\right\}$; y = -1.028 + 0.974 x; R^2 = 0.991

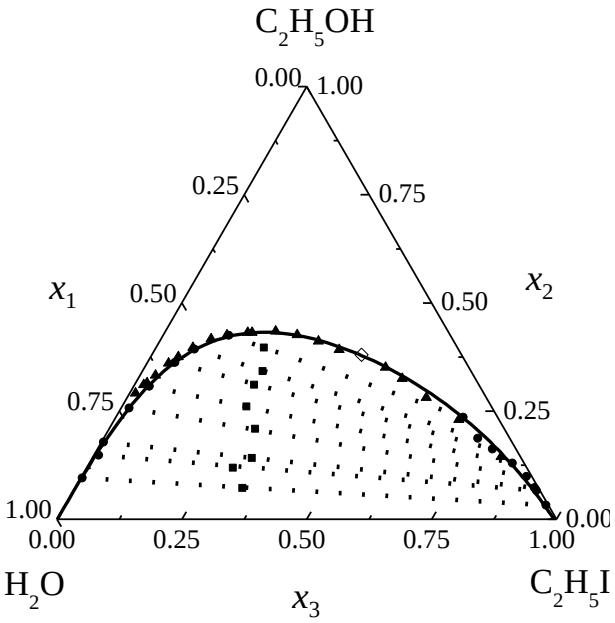

Figure (A.2.3): Solubility and liquid-liquid equilibrium data for water (1) + ethanol (2) + iodoethane (3) at 298.15 K: ▲, solubility; ■, feed mixture; ●, LLE. ◊, p.p.; ..., tie line; —, NRTL.

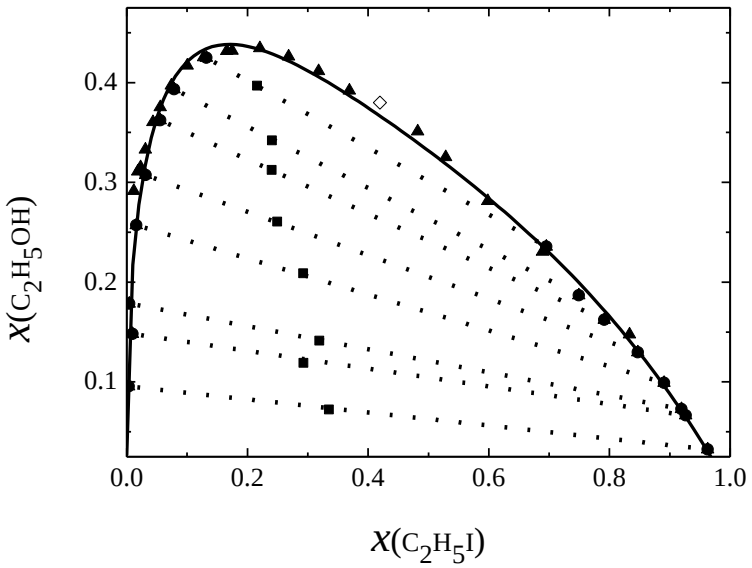

Figure (A.2.4): Solubility and liquid-liquid equilibrium data for water (1) + ethanol (2) + iodoethane (3) at 298.15 K: ▲, solubility; ■, feed mixture; ●, LLE; ◊, p.p.; ..., tie line; —, eq. (2.35).

Table (A.2.5): Experimental Solubility for water (1) + 1-propanol (2) + iodoethane (3) at 298.15 K and 0.1 MPa

x_1	x_2	x_3	x_1	x_2	x_3
0.025	0.125	0.851	0.347	0.407	0.246
0.056	0.191	0.752	0.416	0.406	0.178
0.100	0.251	0.650	0.468	0.393	0.139
0.134	0.309	0.557	0.510	0.378	0.113
0.165	0.343	0.492	0.555	0.355	0.090
0.197	0.372	0.431	0.598	0.331	0.072
0.219	0.383	0.398	0.641	0.303	0.056
0.254	0.396	0.350	0.693	0.265	0.042
0.291	0.403	0.307	0.726	0.241	0.033

Binodal eq.: $x_2 = -0.065 + 2.1577\, x_3^{0.5} - 2.6268\, x_3 + 1.0185\, x_3^2 - 0.5126\, x_3^3$; $R^2 = 0.998$

Table (A.2.6): Experimental liquid-liquid equilibrium data for water (1) + 1-propanol (2) + iodoethane (3) at 298.15 K and 0.1 MPa

feed mixture		water-rich phase		iodoethane-rich phase	
x_1	x_2	x_1^{α}	x_2^{α}	x_1^{β}	x_2^{β}
0.376	0.362	0.684	0.278	0.250	0.401
0.397	0.324	0.737	0.227	0.208	0.374
0.402	0.285	0.775	0.202	0.180	0.351
0.412	0.266	0.807	0.178	0.156	0.328
0.410	0.246	0.848	0.137	0.134	0.316
0.450	0.198	0.892	0.094	0.105	0.281
0.493	0.170	0.909	0.079	0.095	0.264
0.471	0.149	0.938	0.054	0.087	0.238
0.498	0.121	0.964	0.029	0.071	0.206
x^{cs}		0.396	0.410	0.396	0.410

Hand eq.: $\ln\left(x_2^{\beta} / x_3^{\beta}\right) = A + B \ln\left(x_2^{\alpha} / x_1^{\alpha}\right)$; y = 0.446 + 0.519 x; $R^2 = 0.959$

Othmer-Tobias eq.: $\ln\left\{\left(1 - x_3^{\beta}\right)/x_3^{\beta}\right\} = A + B.\ln\left\{\left(1 - x_1^{\alpha}\right)/x_1^{\alpha}\right\}$; y = 0.918 + 0.613 x; $R^2 = 0.961$

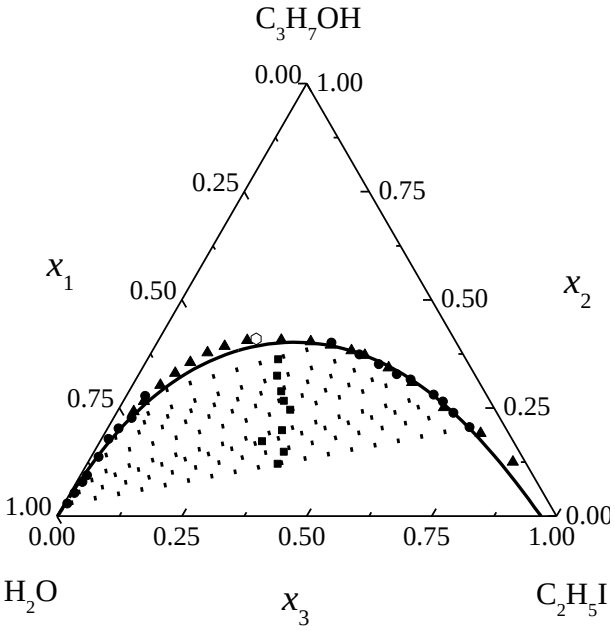

Figure (A.2.5): Solubility and liquid-liquid equilibrium data for water (1) + 1-propanol (2) + iodoethane (3) at 298.15 K: ▲, solubility; ■, feed mixture; ●, LLE; ◊, p.p.; …, tie line; —, NRTL.

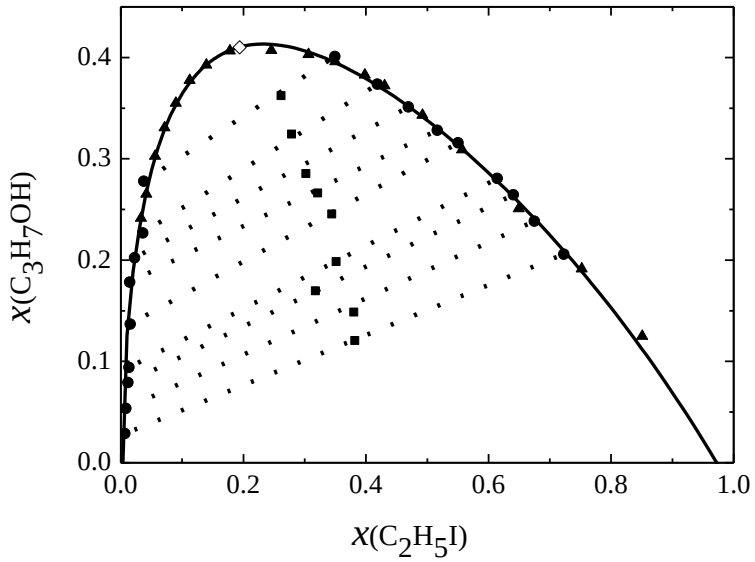

Figure (A.2.6): solubility and liquid-liquid equilibrium data for water (1) + 1-propanol (2) + iodoethane (3) at 298.15 K: ▲, solubility; ■, feed mixture; ●, LLE; ◊ p.p.; …, tie line; —, eq. (2.35).

Table (A.2.7): Distribution coefficient d_1, d_2 and selectivity S for liquid-liquid equilibrium for water (1) + alcohol (2) + iodoethane (3) at 298.15 K and 0.1 MPa

d_1	d_2	S
water (1) + methanol (2) + iodoethane (3)		
3.2	1.8	1.8
5.2	2.6	2.0
9.1	3.5	2.6
16.3	4.9	3.3
24.2	5.6	4.3
58.7	7.3	8.1
100.0	7.4	13.4
223.8	13.2	17.0
water (1) + ethanol (2) + iodoethane (3)		
6.4	1.8	3.6
8.3	2.1	3.9
12.3	2.2	5.5
28.3	2.4	11.9
71.8	2.5	28.4
105.9	2.4	43.2
120.3	2.2	54.0
176.7	3.0	59.7
water (1) + 1-propanol (2) + iodoethane (3)		
2.7	0.7	3.9
3.5	0.6	5.8
4.3	0.6	7.5
5.2	0.5	9.5
6.3	0.4	14.6
8.5	0.3	25.4
9.6	0.3	32.0
10.8	0.2	47.5
13.6	0.1	96.4

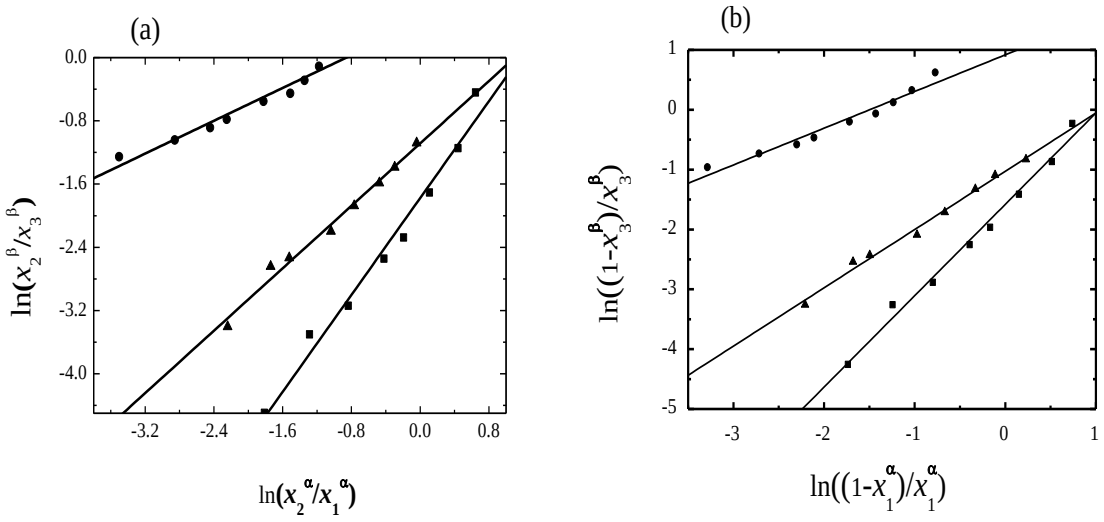

Figure (A.2.7): Liquid-liquid equilibrium data correlation for water (1) + alcohol (2) + iodoethane (3) at 298.15 K: ■, methanol; ▲, ethanol; ●, 1-propanol; (a), Hand; ── , eq. (2.36); (b), Othmer-Tobias; ── , eq. (2.37).

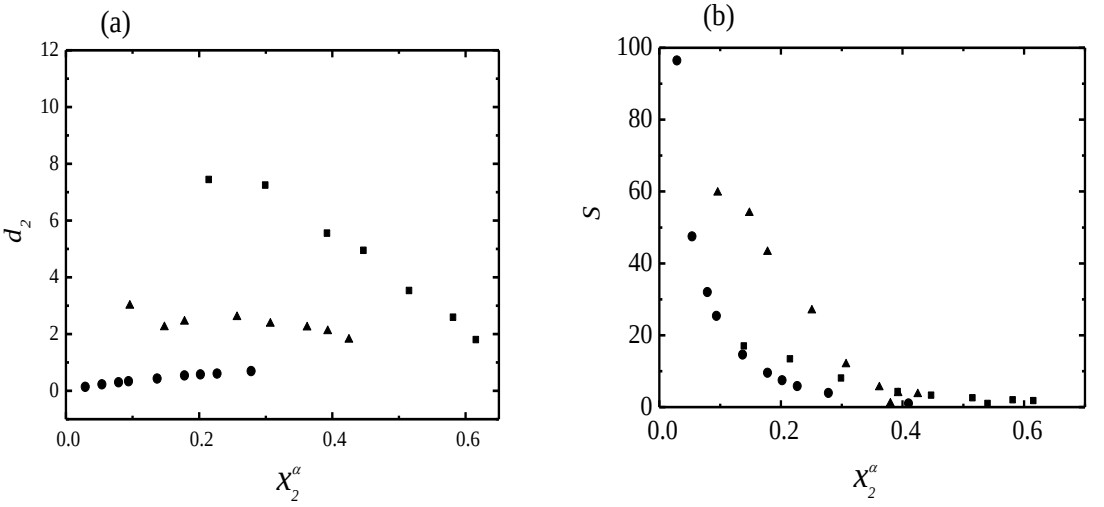

Figure (A.2.8): Experimental distribution coefficient d_2 of alcohol and selectivity S for liquid-liquid equilibrium for water (1) + alcohol (2) + iodoethane (3) at 298.15 K: ■, methanol; ▲, ethanol; ●, 1-propanol. (a), distribution coefficient; (b), selectivity.

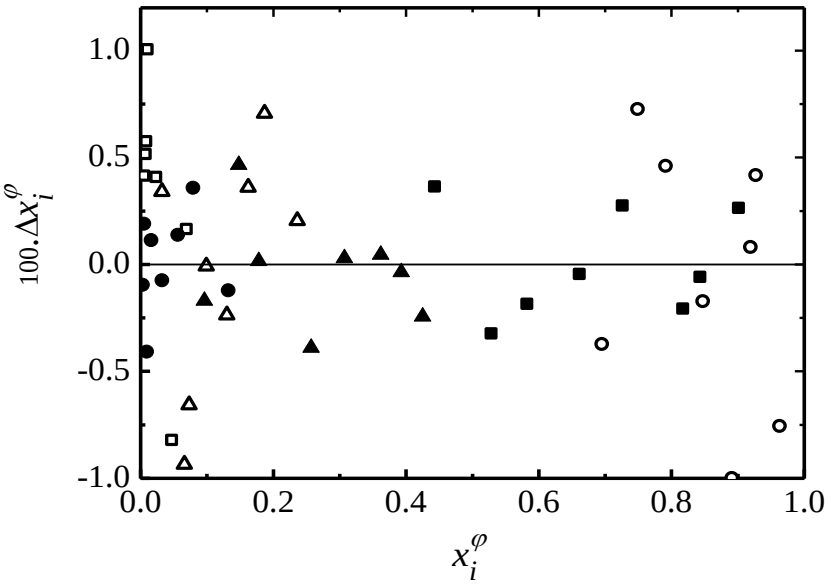

Figure (A.2.9): Deviations for predicting the liquid-liquid equilibrium data for water (1) + ethanol (2) + iodoethane (3) at 298.15 K using NRTL eq. solid symbols, water-rich phase; open symbols, iodoethane-rich phase: ■, □, water; ▲, Δ, ethanol; ●, ○, iodoethane.

Table (A.2.8): RMSD of correlation for the liquid-liquid equilibrium data for water (1) + alcohol (2) + iodoethane (3) at 0.1 MPa

	water-rich phase			iodoethane-rich phase			
equation	$\sigma(x_1^{\alpha})$	$\sigma(x_2^{\alpha})$	$\sigma(x_3^{\alpha})$	$\sigma(x_1^{\beta})$	$\sigma(x_2^{\beta})$	$\sigma(x_3^{\beta})$	correlation
			water (1) + methanol (2) + iodoethane (3)				
NRTL	0.009	0.019	0.023	0.008	0.012	0.011	0.015
UNIQUAC	0.011	0.011	0.063	0.014	0.013	0.012	0.011
			water (1) + ethanol (2) + iodoethane (3)				
NRTL	0.002	0.004	0.005	0.007	0.005	0.005	0.485
UNIQUAC	0.002	0.004	0.005	0.007	0.005	0.004	0.005
			water (1) + propanol (2) + iodoethane (3)				
NRTL	0.006	0.008	0.006	0.002	0.006	0.006	0.006
UNIQUAC	0.016	0.014	0.092	0.005	0.007	0.010	0.108

Table (A.2.9): Parameters values of NRTL and UNIQUAQ for water (1) + alcohol (2) iodoethane (3) at 298.15 K and 0.1 MPa

	NRTL (α = 0.2)		UNIQUAC	
Component *i* -*j*	$\Delta\lambda_{ij}$ /K	$\Delta\lambda_{ji}$ /*K*	Δu_{ij} /K	Δu_{ji} /*K*
water (1) + methanol (2) + iodoethane (3)				
1, 2	642.6	-1092.6	152.9	-976.8
1, 3	3121.7	782.1	825.2	171.8
2, 3	606.6	-33.6	17.8	252.0
water (1) + ethanol (2) + iodoethane (3)				
1, 2	1023.8	-654.0	481.2	-286.7
1, 3	2051.4	1081.0	806.8	1111.5
2, 3	255.8	75.1	-84.9	357.7
water (1) + 1-propanol (2) + iodoethane (3)				
1, 2	-810.7	61.1	48.9	64.3
1, 3	1551.4	547.0	229.1	823.4
2, 3	-436.2	-1058.8	304.5	-130.4

Table (A.3.1): Experimental Solubility for cyclohexane (1) + 1-butanol (2) + 2,2,2-trifluoroethanol (3) at 288.15 K and 0.1 MPa

x_1	x_2	x_3	x_1	x_2	x_3
0.055	0.085	0.860	0.352	0.302	0.346
0.065	0.115	0.820	0.424	0.295	0.281
0.073	0.145	0.781	0.536	0.254	0.211
0.090	0.185	0.725	0.492	0.274	0.234
0.112	0.222	0.666	0.600	0.223	0.177
0.152	0.252	0.595	0.643	0.203	0.154
0.213	0.287	0.501	0.697	0.162	0.141
0.254	0.294	0.451	0.722	0.145	0.133
0.276	0.303	0.422	0.784	0.102	0.114

Binodal eq.: $x_2 = -1.785 + 9.147\,x_3^{0.5} - 11.533\,x_3 + 6.805\,x_3^2 - 2.7143\,x_3^3$; $R^2 = 0.986$

Table (A.3.2): Experimental Solubility for cyclohexane (1) + 1-butanol (2) + 2,2,2-trifluoroethanol (3) at 288.15 K and 0.1 MPa

feed mixture		cyclohexane-rich phase		trifluoroethanol-rich phase	
x_1	x_2	x_1^{α}	x_2^{α}	x_1^{β}	x_2^{β}
0.485	0.250	0.602	0.222	0.252	0.292
0.475	0.211	0.674	0.174	0.193	0.270
0.462	0.194	0.717	0.146	0.167	0.258
0.495	0.158	0.765	0.102	0.143	0.225
0.499	0.126	0.818	0.066	0.104	0.193
0.486	0.099	0.856	0.042	0.074	0.166
0.500	0.058	0.873	0.024	0.055	0.102
x^{cs}		0.415	0.297	0.415	0.297

Hand eq.: $\ln\left(x_2^{\beta} / x_3^{\beta}\right) = A + B\ln\left(x_2^{\alpha} / x_1^{\alpha}\right)$; y = 0.047 + 0.528 x; $R^2 = 0.996$

Othmer-Tobias eq.: $\ln\left\{\left(1 - x_3^{\beta}\right)/x_3^{\beta}\right\} = A + B.\ln\left\{\left(1 - x_1^{\alpha}\right)/x_1^{\alpha}\right\}$; y = 0.574 + 0.960 x; $R^2 = 0.99$

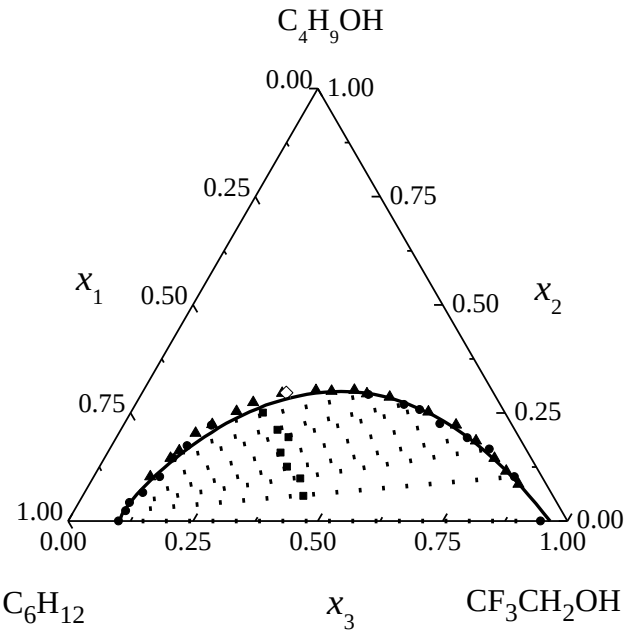

Figure (A.3.1): Solubility and liquid-liquid equilibrium data for cyclohexane (1) + 1-butanol (2) + 2,2,2-trifluoroethanol (3) at 288.15 K: ▲, solubility; ■ feed mixture; ●, LLE; ◊, p.p.; ..., tie line; —, NRTL.

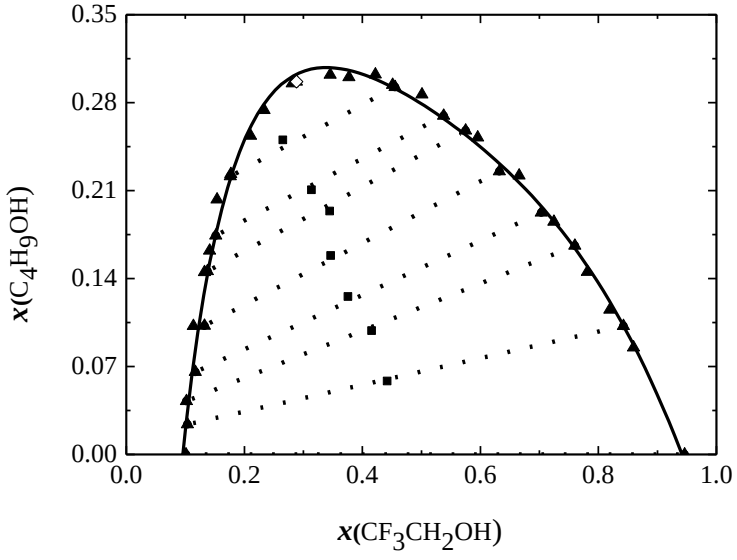

Figure (A.3.2): Solubility and liquid-liquid equilibrium data for cyclohexane (1) + 1-butanol (2) + 2,2,2-trifluoroethanol (3) at 288.15 K: ▲, solubility; ■, feed mixture; ●, LLE; ◊, p.p.; ..., tie line; —, eq. (2.35).

Table (A.3.3): Experimental solubility for cyclohexane (1) + 1-butanol (2) + 2,2,2-trifluoroethanol (3) at 298.15 K and 0.1 MPa

x_1	x_2	x_3	x_1	x_2	x_3
0.091	0.070	0.839	0.396	0.252	0.352
0.098	0.098	0.804	0.462	0.241	0.307
0.103	0.114	0.783	0.562	0.200	0.247
0.125	0.159	0.716	0.492	0.224	0.284
0.162	0.188	0.650	0.600	0.180	0.220
0.200	0.219	0.581	0.634	0.160	0.205
0.253	0.238	0.508	0.662	0.142	0.196
0.272	0.246	0.483	0.679	0.125	0.186
0.303	0.249	0.448	0.750	0.085	0.165
0.356	0.254	0.394	0.792	0.055	0.153

Binodal eq.: $x_2 = -2.043 + 9.399\,x_3^{0.5} - 11.185\,x_3 + 6.123\,x_3^2 - 2.409\,x_3^3$; $R^2 = 0.999$

Table (A.3.4): Experimental liquid-liquid equilibrium data for cyclohexane (1) + 1-butanol (2) + 2,2,2-trifluoroethanol (3) at 298.15 K and 0.1 MPa

feed mixture		cyclohexane-rich phase		TFE-rich phase	
x_1	x_2	x_1^{α}	x_2^{α}	x_1^{β}	x_2^{β}
0.472	0.197	0.650	0.151	0.328	0.251
0.461	0.185	0.693	0.122	0.267	0.239
0.462	0.163	0.727	0.095	0.227	0.220
0.494	0.121	0.773	0.064	0.179	0.182
0.497	0.095	0.812	0.041	0.122	0.156
0.501	0.074	0.832	0.026	0.110	0.130
0.523	0.036	0.847	0.014	0.088	0.064
x^{cs}		0.534	0.205	0.534	0.205

Hand eq.: $\ln\left(x_2^{\beta} / x_3^{\beta}\right) = A + B\ln\left(x_2^{\alpha} / x_1^{\alpha}\right)$; y = 0.361 + 0.626 x; $R^2 = 0.994$

Othmer-Tobias eq.: $\ln\left\{\left(1 - x_3^{\beta}\right)/x_3^{\beta}\right\} = A + B.\ln\left\{\left(1 - x_1^{\alpha}\right)/x_1^{\alpha}\right\}$; y = 1.247 + 1.496 x; $R^2 = 0.998$

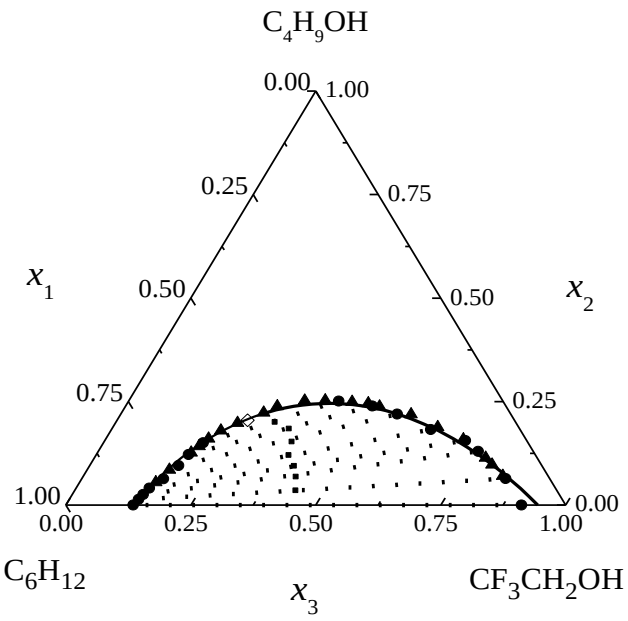

Figure (A.3.3): Solubility and liquid-liquid equilibrium data for cyclohexane (1) + 1-butanol (2) + 2,2,2-trifluoroethanol (3) at 298.15 K: ▲, solubility; ■, feed mixture; ●,LLE; ◊, p.p.; ..., tie line; —, NRTL.

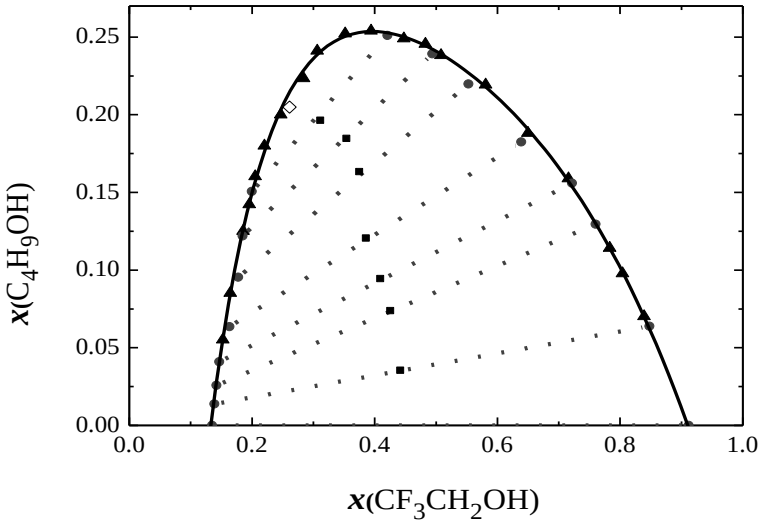

Figure (A.3.4): Solubility and liquid-liquid equilibrium data for cyclohexane (1) + 1-butanol (2) + 2,2,2-trifluoroethanol (3) at 298.15 K: ▲, solubility; ■, feed mixture; ●, LLE; ◊, p.p.; ..., tie line; —, eq. (2.35).

Table (A.3.5): Experimental Solubility for cyclohexane (1) + 1-butanol (2) + 2,2,2-trifluoroethanol (3) at 308.15 K and 0.1 MPa

x_1	x_2	x_3	x_1	x_2	x_3
0.145	0.102	0.752	0.386	0.192	0.422
0.158	0.127	0.715	0.420	0.189	0.391
0.165	0.147	0.687	0.452	0.180	0.367
0.181	0.165	0.654	0.493	0.171	0.335
0.208	0.180	0.612	0.523	0.161	0.316
0.253	0.193	0.554	0.552	0.149	0.298
0.293	0.195	0.512	0.586	0.139	0.275
0.325	0.195	0.480	0.636	0.116	0.248
0.356	0.195	0.449	0.692	0.084	0.223

Binodal eq.: $x_2 = -2.631 + 12.046\ x_3^{0.5} - 15.432\ x_3 + 10.533\ x_3^2 - 4.857\ x_3^3$; $R^2 = 0.986$

Table (A.3.6): Experimental liquid-liquid equilibrium data for cyclohexane (1) + 1-butanol (2) + 2,2,2-trifluoroethanol (3) at 308.15 K and 0.1 MPa

feed mixture		cyclohexane-rich phase		TFE-rich phase	
x_1	x_2	x_1^{α}	x_2^{α}	x_1^{β}	x_2^{β}
0.502	0.023	0.642	0.106	0.226	0.185
0.500	0.041	0.701	0.085	0.185	0.169
0.495	0.062	0.752	0.051	0.158	0.141
0.531	0.069	0.775	0.037	0.158	0.119
0.498	0.090	0.796	0.025	0.152	0.099
0.501	0.112	0.812	0.015	0.153	0.081
0.495	0.134	0.819	0.009	0.140	0.051
x^{cs}		0.431	0.183	0.431	0.183

Hand eq.: $\ln\left(x_2^{\beta} / x_3^{\beta}\right) = A + B\ln\left(x_2^{\alpha} / x_1^{\alpha}\right)$; y = -0.266 + 0.503 x; $R^2 = 0.994$

Othmer-Tobias eq.: $\ln\left\{\left(1 - x_3^{\beta}\right)/x_3^{\beta}\right\} = A + B.\ln\left\{\left(1 - x_1^{\alpha}\right)/x_1^{\alpha}\right\}$; y = 0.198 + 0.943 x; $R^2 = 0.998$

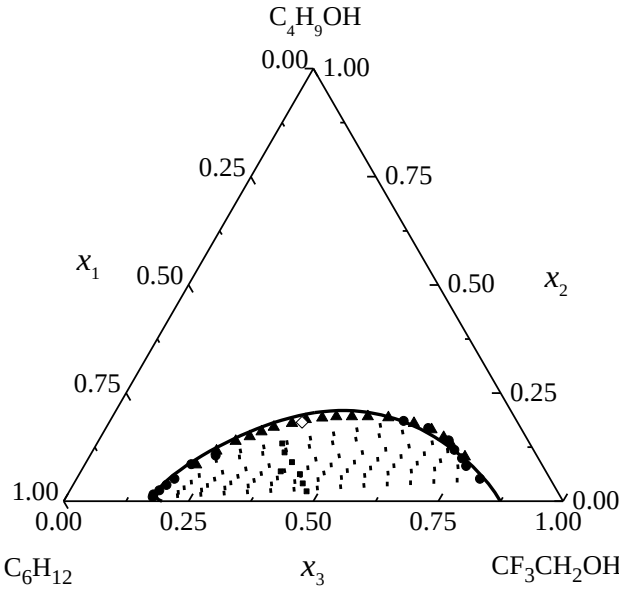

Figure (A.3.5): Solubility and liquid-liquid equilibrium data for cyclohexane (1) + 1-butanol (2) + 2,2,2-trifluoroethanol (3) at 308.15 K: ▲, solubility; ■, feed mixture; ●, LLE; ◊, p.p.; ..., tie line, —, NRTL.

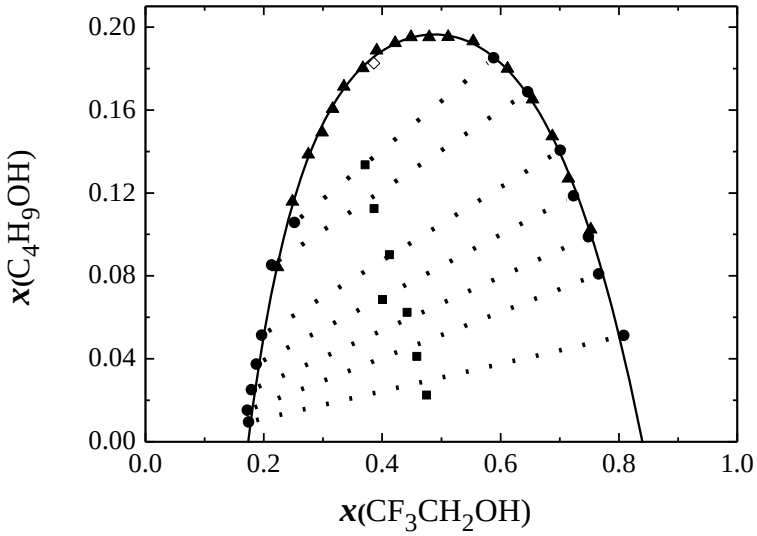

Figure (A.3.6): Solubility and liquid-liquid equilibrium data for cyclohexane (1) + 1-butanol (2) + 2,2,2-trifluoroethanol (3) at 308.15 K: ▲, solubility; ■, feed mixture; ●,LLE; ◊, p.p.; ..., tie line; —, eq. (2.35).

Table (A.3.7): Distribution coefficient d_1, d_2 and selectivity S for liquid-liquid equilibrium for cyclohexane (1) + 1-butanol (2) + 2,2,2-trifluoroethanol (3) at 0.1 MPa

d_1	d_2	S
	T = 288.15 K	
2.39	0.79	3.01
3.49	0.64	5.42
4.29	0.57	7.59
5.35	0.45	11.80
7.87	0.34	23.00
11.57	0.25	45.72
15.87	0.24	67.46
	T = 298.15 K	
1.98	0.60	3.30
2.60	0.51	5.09
3.20	0.43	7.37
4.33	0.35	12.41
6.63	0.26	25.29
7.55	0.20	38.00
9.61	0.22	44.22
	T = 308.15 K	
2.84	0.57	4.97
3.79	0.51	7.49
4.75	0.37	13.02
4.91	0.32	15.53
5.22	0.25	20.64
5.30	0.19	28.14
5.84	0.18	31.62

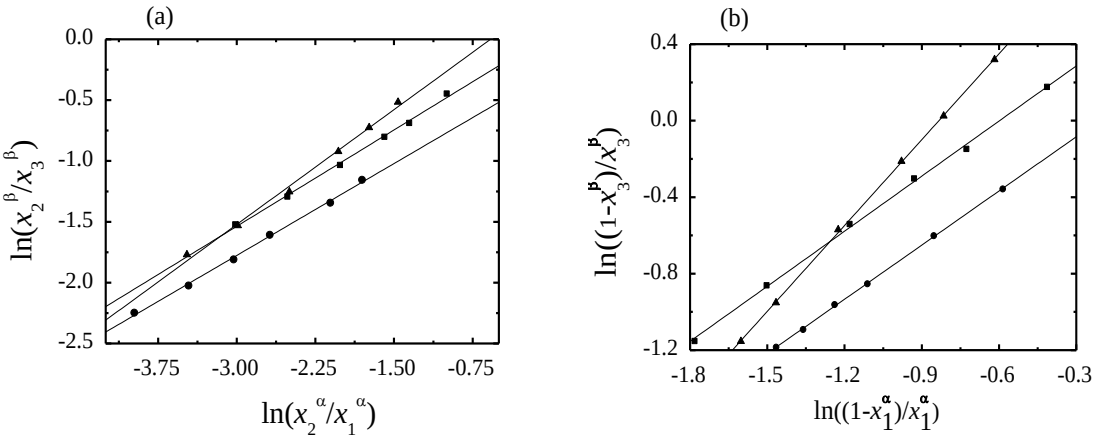

Figure (A.3.7): Liquid-liquid equilibrium data correlation for cyclohexane (1) + 1-butanol (2) + 2,2,2-trifluoroethanol (3): ■, 288.15 K; ▲, 298.15 K; ●; 308.15 K: (a), Hand; ─, eq. (2.36); (b), Othmer-Tobias; ─, eq. (2.37).

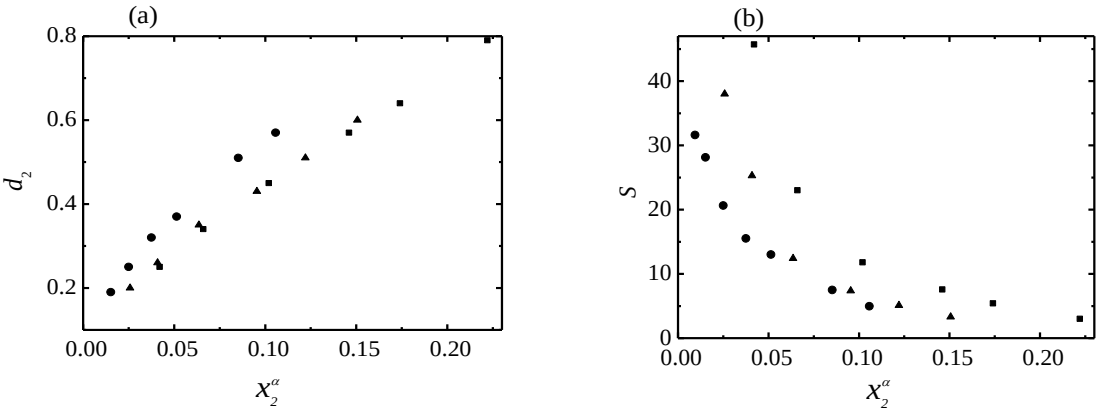

Figure (A.3.8): Experimental distribution coefficient d_2 of alcohol and selectivity S for liquid-liquid equilibrium of cyclohexane (1) + 1-butanol (2) + 2,2,2-trifluoroethanol (3): ■, 288.15 K; ▲, 298.15 K; ●, 308.15 K; (a), distribution coefficient; (b), selectivity.

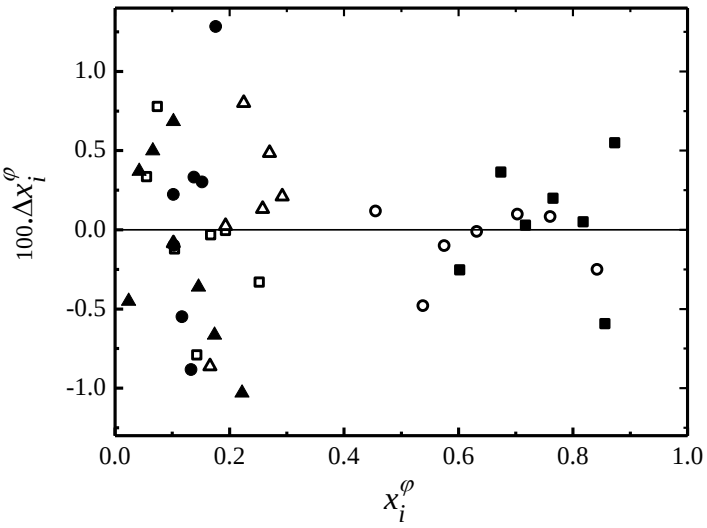

Figure (A.3.9): Deviations for predicting the liquid-liquid equilibrium data for cyclohexane (1) + 1-butanol (2) + 2,2,2-trifluoroethanol (3) at 288.15 K using UNIQUAC eq. solid symbols, cyclohexane-rich phase; open symbols, 1-butanol-rich phase: ■, □, cyclohexane; ▲, Δ, 1-butanol; ●, ○, 2,2,2-trifluoroethanol.

Table (A.3.8): RMSD of correlation for the liquid-liquid equilibrium data for cyclohexane (1) + 1-butanol (2) + 2,2,2-trifluoroethanol (3) at 0.1 MPa

	cyclohexane-rich phase			TFE-rich phase			
equation	$\sigma(x_1^{\alpha})$	$\sigma(x_2^{\alpha})$	$\sigma(x_3^{\alpha})$	$\sigma(x_1^{\beta})$	$\sigma(x_2^{\beta})$	$\sigma(x_3^{\beta})$	correlation
			T = 288.15 K				
NRTL	0.004	0.007	0.007	0.005	0.005	0.002	0.005
UNIQUAC	0.004	0.005	0.006	0.005	0.007	0.002	0.005
			T = 298.15 K				
NRTL	0.009	0.005	0.007	0.018	0.009	0.011	0.011
UNIQUAC	0.005	0.004	0.005	0.005	0.006	0.003	0.005
			T = 308.15 K				
NRTL	0.064	0.007	0.008	0.008	0.005	0.003	0.006
UNIQUAC	0.008	0.009	0.009	0.010	0.007	0.004	0.008

Table (A.3.9): Parameters values of NRTL and UNIQUAQ for cyclohexane (1) + 1-butanol (2) + 2,2,2-trifluoroethanol (3) at 0.1 MPa

	NRTL (α_{ij} = 0.2)		UNIQUAC	
Component *i-j*	$\Delta\lambda_{ij}$ /K	$\Delta\lambda_{ji}$ /K	Δu_{ij} /K	Δu_{ji} /K
		T = 288.15 K		
1, 2	-376.2	-52.2	-230.8	-79.2
1, 3	316.0	794.3	144.5	199.8
2, 3	-436.2	-641.1	-130.0	-455.0
		T = 298.15 K		
1, 2	417.3	-124.6	202.0	-32.6
1, 3	286.2	736.9	141.6	138.4
2, 3	-182.6	-185.2	254.0	-203.1
		T = 308.15 K		
1, 2	-945.0	2317.8	-733.2	134.4
1, 3	314.3	572.3	149.1	93.7
2, 3	-789.1	-204.4	-201.0	-695.7

Table (A.4.1): Experimental liquid-liquid equilibrium data for cyclohexane (1) + methanol (2) + 2,2,2-trifluoroethanol (3) at 283.15 K and 0.1 MPa

feed mixture		cyclohexane-rich phase		(TFE-MeOH)-rich phase	
x_1	x_2	x_1^{α}	x_2^{α}	x_1^{β}	x_2^{β}
0.482	0.043	0.914	0.020	0.037	0.079
0.491	0.085	0.911	0.036	0.041	0.157
0.489	0.121	0.911	0.040	0.041	0.230
0.491	0.187	0.910	0.046	0.033	0.321
0.490	0.243	0.909	0.049	0.040	0.406
0.476	0.295	0.908	0.052	0.050	0.509
0.497	0.309	0.907	0.055	0.053	0.581
0.491	0.344	0.906	0.060	0.063	0.621
0.494	0.383	0.907	0.058	0.063	0.716
0.490	0.424	0.908	0.061	0.079	0.762
0.499	0.459	0.922	0.066	0.092	0.836

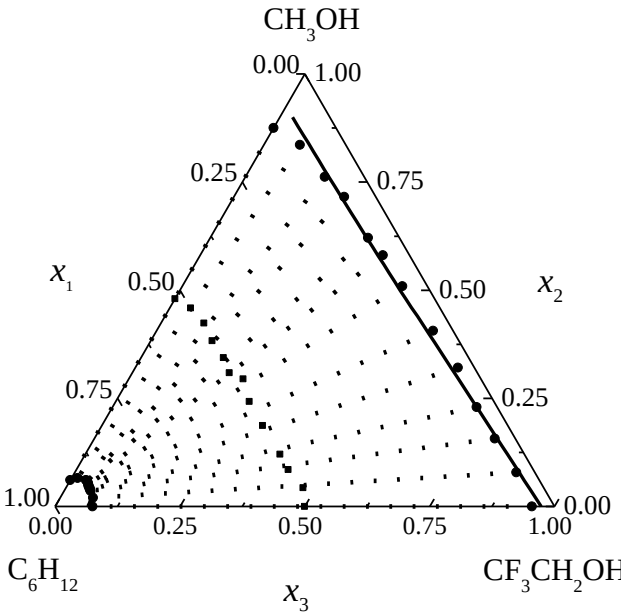

Figure (A.4.1): Liquid-liquid equilibrium for cyclohexane (1) + methanol (2) + 2,2,2-trifluoroethanol (3) at 283.15 K: ■, feed mixture; ●, LLE; ..., tie line; —, NRTL.

Table (A.4.2): Experimental liquid-liquid equilibrium data for cyclohexane (1) + methanol (2) + 2,2,2-trifluoroethanol (3) at 293.15 K and 0.1 MPa

feed mixture		cyclohexane-rich phase		(TFE-MeOH)-rich phase	
x_1	x_2	x_1^{α}	x_2^{α}	x_1^{β}	x_2^{β}
0.493	0.036	0.864	0.009	0.099	0.157
0.490	0.433	0.865	0.010	0.098	0.052
0.495	0.070	0.860	0.011	0.101	0.202
0.498	0.102	0.861	0.019	0.104	0.253
0.491	0.132	0.860	0.033	0.117	0.337
0.489	0.177	0.858	0.045	0.103	0.432
0.488	0.230	0.857	0.057	0.104	0.461
0.485	0.260	0.856	0.079	0.107	0.578
0.474	0.322	0.854	0.095	0.103	0.636
0.482	0.362	0.860	0.106	0.104	0.698
0.492	0.396	0.851	0.119	0.106	0.744

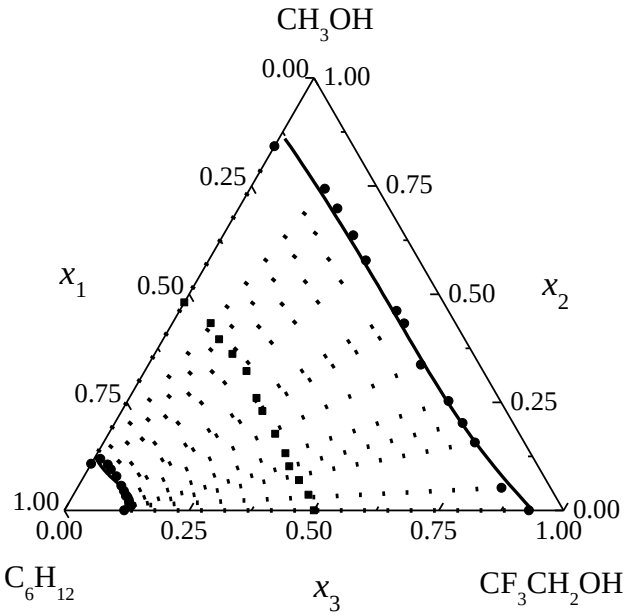

Figure (A.4.2): Liquid-liquid equilibrium for cyclohexane (1) + methanol (2) + 2,2,2-trifluoroethanol (3) at 293.15 K: ■, feed mixture; ●, LLE; ..., tie line**;** **—,** NRTL.

Table (A .4.3): Experimental liquid-liquid equilibrium data for cyclohexane (1) + methanol (2) + 2,2,2-trifluoroethanol (3) at 303.15 K and 0.1 MPa

feed mixture		cyclohexane-rich phase		(TFE-MeOH)-rich phase	
x_1	x_2	x_1^{α}	x_2^{α}	x_1^{β}	x_2^{β}
0.500	0.025	0.827	0.012	0.114	0.031
0.493	0.052	0.827	0.013	0.116	0.085
0.491	0.105	0.818	0.024	0.126	0.176
0.493	0.139	0.811	0.036	0.127	0.263
0.482	0.223	0.803	0.059	0.125	0.358
0.474	0.278	0.802	0.070	0.128	0.446
0.474	0.322	0.793	0.095	0.138	0.547
0.502	0.343	0.783	0.121	0.161	0.601
0.499	0.388	0.790	0.146	0.160	0.658
0.495	0.421	0.791	0.160	0.178	0.744
0.502	0.442	0.782	0.167	0.174	0.715

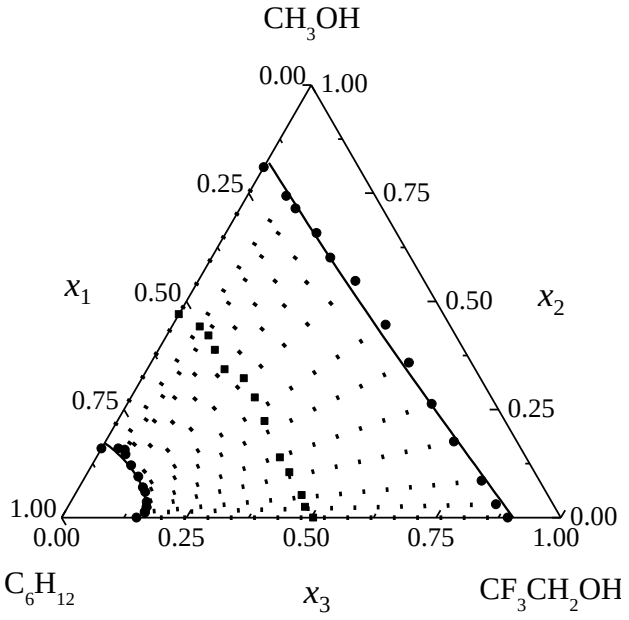

Figure (A.4.3): Liquid-liquid equilibrium for cyclohexane (1) + methanol (2) + 2,2,2-trifluoroethanol (3) at 303.15 K: ■, feed mixture; ●, LLE; ..., tie line; —, NRTL.

Table (A.4.4): Experimental liquid-liquid equilibrium data for cyclohexane (1) + methanol (2) + 2,2,2-trifluoroethanol (3) at 313.15 K and 0.1 MPa

feed mixture		cyclohexane-rich phase		(TFE-MeOH)-rich phase	
x_1	x_2	x_1^{α}	x_2^{α}	x_1^{β}	x_2^{β}
0.491	0.034	0.791	0.012	0.121	0.082
0.506	0.086	0.771	0.052	0.131	0.148
0.490	0.123	0.770	0.066	0.139	0.207
0.489	0.174	0.762	0.076	0.143	0.300
0.495	0.203	0.754	0.083	0.149	0.373
0.490	0.276	0.748	0.108	0.163	0.483
0.492	0.302	0.743	0.126	0.183	0.556
0.504	0.346	0.738	0.160	0.205	0.594
0.502	0.391	0.737	0.188	0.202	0.631
0.492	0.425	0.736	0.212	0.216	0.667
0.490	0.454	0.734	0.231	0.220	0.697

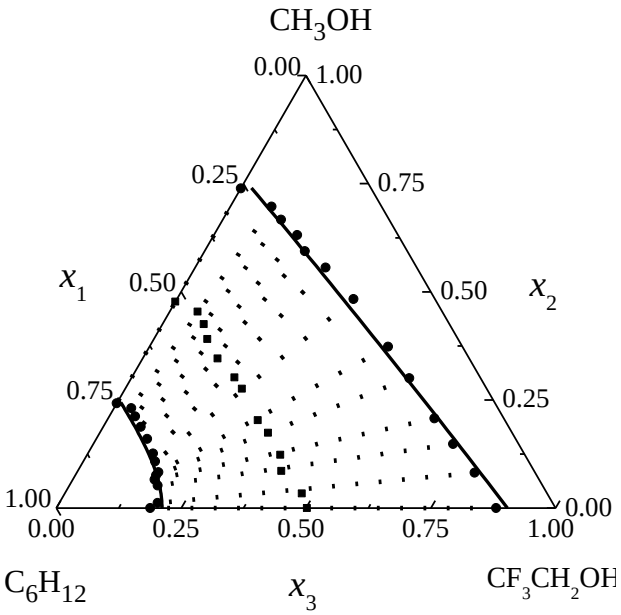

Figure (A.4.4): Liquid-liquid equilibrium for cyclohexane (1) + methanol (2) + 2,2,2-trifluoroethanol (3) at 313.15 K: ■, feed mixture; ●, LLE; ..., tie line; —, NRTL.

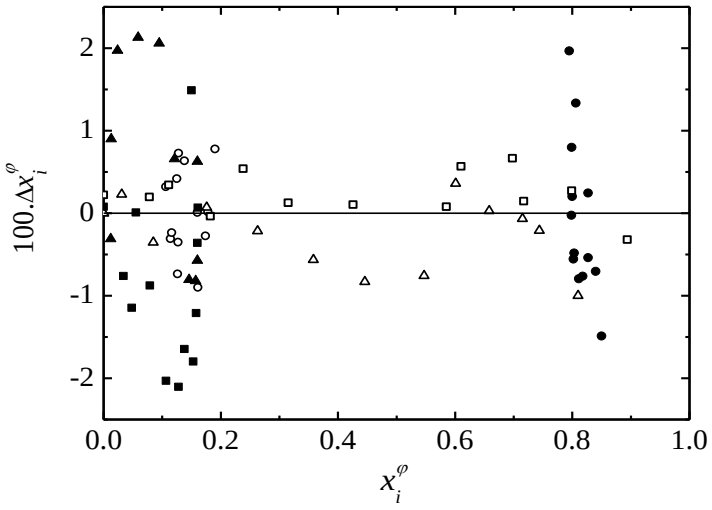

Figure (A.4.5): Deviations for predicting liquid-liquid equilibrium data for cyclohexane (1) + methanol (2) + 2,2,2-trifluoroethanol (3) at 303.15 K using UNIQUAC eq. solid symbols, (methanol + trifluoroethanol)-rich phase; open symbols, cyclohexane-rich phase: ■, □, cyclohexane; ▲, Δ, methanol; ●,○, 2,2,2-trifluoroethanol.

Table (A.4.5): RMSD of correlation for the liquid-liquid equilibrium data for cyclohexane (1) + methanol (2) + 2,2,2-trifluoroethanol (3) at 0.1 MPa

	cyclohexane-rich phase			(TFE + MeOH)-rich phase			
equation	$\sigma(x_1^{\alpha})$	$\sigma(x_2^{\alpha})$	$\sigma(x_3^{\alpha})$	$\sigma(x_1^{\beta})$	$\sigma(x_2^{\beta})$	$\sigma(x_3^{\beta})$	correlation
			T = 283.15 K				
NRTL	0.005	0.007	0.007	0.014	0.008	0.006	0.009
UNIQUAC	0.005	0.006	0.008	0.008	0.004	0.003	0.006
			T = 293.15 K				
NRTL	0.010	0.013	0.009	0.012	0.007	0.006	0.010
UNIQUAC	0.006	0.012	0.012	0.013	0.006	0.008	0.010
			T = 303.15 K				
NRTL	0.011	0.015	0.017	0.011	0.008	0.005	0.012
UNIQUAC	0.009	0.015	0.013	0.005	0.005	0.003	0.009
			T = 313.15 K				
NRTL	0.011	0.019	0.023	0.012	0.011	0.008	0.015
UNIQUAC	0.008	0.020	0.019	0.005	0.005	0.006	0.012

Table (A.4.6): binary interaction parameters from NRTL and UNIQUAC for cyclohexane (1) + methanol (2) + 2,2,2-trifluoroethanol (3) at 0.1 MPa

	NRTL (α_{ij} = 0,2)		UNIQUAC	
Component *i* -*j*	$\Delta\lambda_{ij}$ /K	$\Delta\lambda_{ji}$ /K	Δu_{ij} /K	Δu_{ji} /K
	T = 283.15 K			
1, 2	401.7	-55.3	470.3	-75.3
1, 3	878.2	398.3	215.0	166.4
2, 3	424.4	548.8	670.2	21.8
	T = 293.15 K			
1, 2	1082.2	-573.6	91.3	-36.5
1, 3	671.0	327.2	194.5	105.7
2, 3	435.0	327.2	21.1	623.2
	T = 303.15 K			
1, 2	89.07	46.38	293.01	-81.69
1, 3	509.56	298.25	100.26	193.24
2, 3	379.91	515.25	6.92	613.42
	T = 313.15 K			
1, 2	371.8	-256.7	208.5	-74.2
1, 3	692.8	244.3	117.5	168.0
2, 3	408.8	387.1	0.8	595.1

Table (A.5.1): Experimental liquid-liquid equilibrium data for hexane (1) + methanol (2) + 2,2,2-trifluoroethanol (3) at 288.15 K and 0.1 MPa

feed mixture		hexane-rich phase		(TFE-MeOH)-rich phase	
x_1	x_2	x_1^{α}	x_2^{α}	x_1^{β}	x_2^{β}
0.511	0.489	0.676	0.324	0.276	0.724
0.502	0.000	0.726	0.000	0.184	0.000
0.495	0.057	0.710	0.040	0.210	0.086
0.487	0.082	0.697	0.057	0.218	0.125
0.476	0.134	0.691	0.088	0.217	0.192
0.491	0.186	0.679	0.121	0.207	0.238
0.493	0.226	0.668	0.155	0.213	0.327
0.499	0.253	0.667	0.182	0.222	0.371
0.498	0.295	0.661	0.220	0.230	0.431
0.506	0.328	0.661	0.233	0.231	0.486
0.494	0.381	0.658	0.263	0.240	0.541
0.485	0.439	0.657	0.293	0.257	0.634

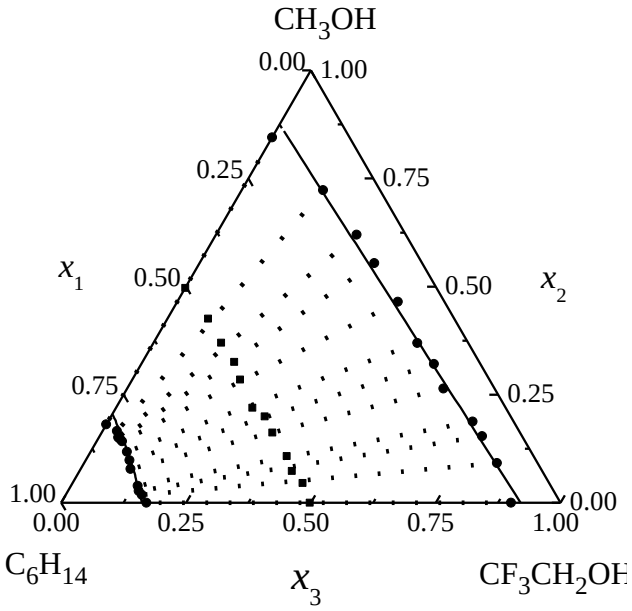

Figure (A.5.1): Liquid-liquid equilibrium for hexane (1) + methanol (2) + 2,2,2-trifluoroethanol (3) at 288.15 K: ■, feed mixture; ●, LLE; ..., tie line**;** — NRTL.

Table (A.5.2): Experimental liquid-liquid equilibrium data for hexane (1) + methanol (2) + 2,2,2-trifluoroethanol (3) at 298.15 K and 0.1 MPa

feed mixture		hexane-rich phase		(TFE-MeOH)-rich phase	
x_1	x_2	x_1^{α}	x_2^{α}	x_1^{β}	x_2^{β}
0.505	0.495	0.741	0.259	0.214	0.786
0.726	0.000	0.761	0.000	0.155	0.000
0.500	0.058	0.757	0.032	0.146	0.084
0.497	0.115	0.755	0.066	0.151	0.160
0.499	0.163	0.751	0.111	0.162	0.231
0.499	0.203	0.742	0.130	0.160	0.302
0.487	0.235	0.741	0.142	0.154	0.358
0.501	0.268	0.751	0.155	0.165	0.417
0.501	0.328	0.746	0.183	0.164	0.501
0.499	0.384	0.742	0.220	0.161	0.596
0.498	0.430	0.744	0.226	0.174	0.696
0.499	0.463	0.742	0.241	0.190	0.742

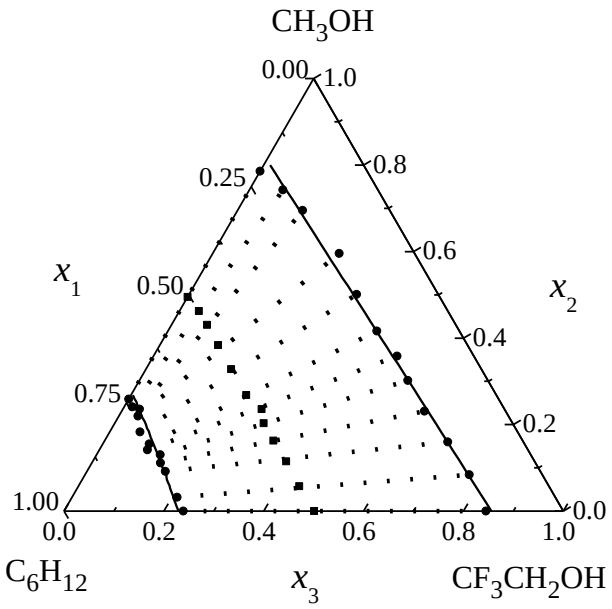

Figure (A.5.2): Liquid-liquid equilibrium for hexane (1) + methanol (2) + 2,2,2-trifluoroethanol (3) at 298.15 K: ■, feed mixture; ●, LLE; ..., tie line**;** **—** , NRTL.

Table (A.5.3): Experimental liquid-liquid equilibrium data for hexane (1) + methanol (2) + 2,2,2-trifluoroethanol (3) at 303.15 K and 0.1 MPa

feed mixture		hexane-rich phase		(TFE-MeOH)-rich phase	
x_1	x_2	x_1^{α}	x_2^{α}	x_1^{β}	x_2^{β}
0.511	0.489	0.676	0.324	0.276	0.724
0.502	0.000	0.726	0.000	0.184	0.000
0.495	0.057	0.710	0.040	0.210	0.086
0.487	0.082	0.697	0.057	0.218	0.125
0.476	0.134	0.691	0.088	0.217	0.192
0.491	0.186	0.679	0.121	0.207	0.238
0.493	0.226	0.668	0.155	0.213	0.327
0.499	0.253	0.667	0.182	0.222	0.371
0.498	0.295	0.661	0.220	0.230	0.431
0.506	0.328	0.661	0.233	0.231	0.486
0.494	0.381	0.658	0.263	0.240	0.541
0.485	0.439	0.657	0.293	0.257	0.634

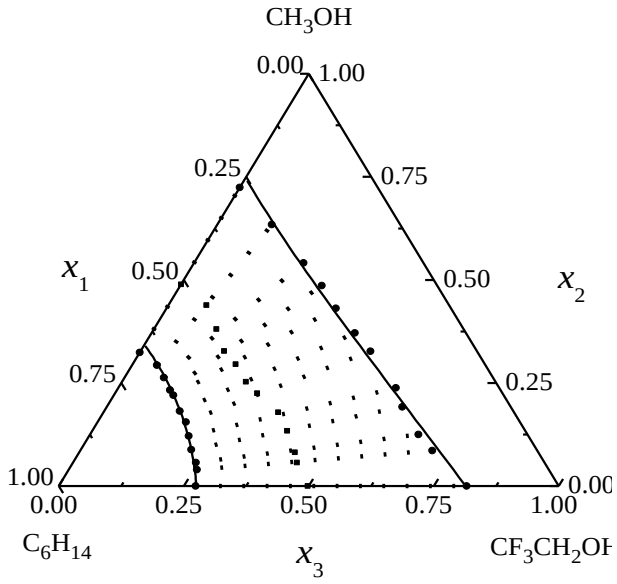

Figure (A.5.3): Liquid-liquid equilibrium for hexane (1) + methanol (2) + 2,2,2-trifluoroethanol (3) at 303.15 K: ■, feed mixture; ●, LLE; ..., tie line; —, NRTL.

Table (A.5.4): Experimental liquid-liquid equilibrium data for hexane (1) + methanol (2) + 2,2,2-trifluoroethanol (3) at 308.15 K and 0.1 MPa

feed mixture		hexane-rich phase		(TFE-MeOH)-rich phase	
x_1	x_2	x_1^{α}	x_2^{α}	x_1^{β}	x_2^{β}
0.494	0.059	0.693	0.065	0.300	0.038
0.496	0.092	0.627	0.125	0.279	0.076
0.477	0.141	0.551	0.192	0.257	0.111
0.490	0.191	0.495	0.248	0.227	0.157
0.480	0.243	0.408	0.327	0.195	0.201
0.475	0.281	0.357	0.371	0.169	0.239
0.498	0.317	0.299	0.421	0.139	0.281
0.500	0.373	0.242	0.462	0.126	0.303
0.482	0.436	0.188	0.499	0.106	0.326
0.499	0.472	0.113	0.522	0.080	0.370

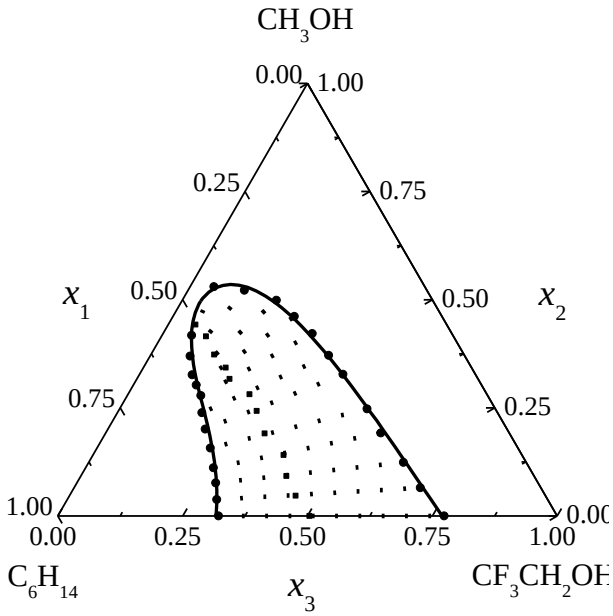

Figure (A.5.4): Liquid-liquid equilibrium for hexane (1) + methanol (2) + 2,2,2-trifluoroethanol (3) at 308.15 K: ■, feed mixture; ●, LLE; ..., tie line; —, NRTL.

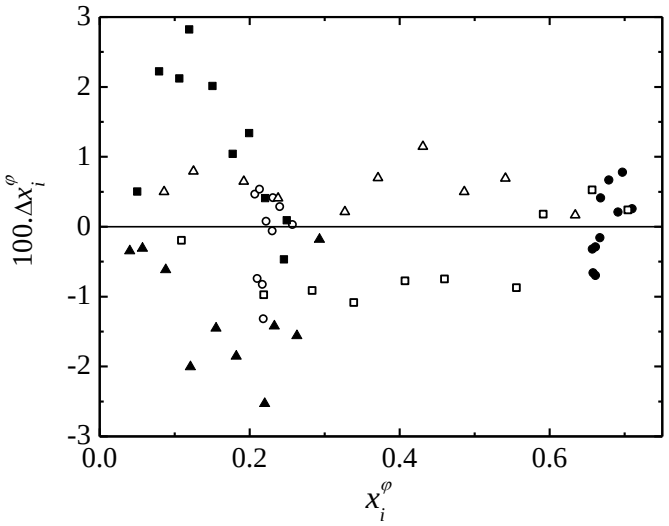

Figure (A.5.5): Deviations for predicting liquid-liquid equilibrium data for hexane (1) + methanol (2) + 2,2,2-trifluoroethanol (3) at 303.15 K using UNIQUAC eq.: solid symbols, (methanol + trifluoroethanol)-rich phase; open symbols, hexane-rich phase: ■, □, hexane; ▲, Δ, methanol; ●,○, 2,2,2-trifluoroethanol.

Table (A.5.5): RMSD of correlation for the liquid-liquid equilibrium data for hexane (1) + methanol (2) + 2,2,2-trifluoroethanol (3) at 0.1 MPa

	hexane-rich phase			(TFE + MeOH)-rich phase			
equation	$\sigma(x_1^{\alpha})$	$\sigma(x_2^{\alpha})$	$\sigma(x_3^{\alpha})$	$\sigma(x_1^{\beta})$	$\sigma(x_2^{\beta})$	$\sigma(x_3^{\beta})$	correlation
			T = 288.15 K				
NRTL	0.009	0.013	0.019	0.013	0.006	0.008	0.014
UNIQUAC	0.009	0.009	0.022	0.009	0.006	0.006	0.014
			T = 298.15 K				
NRTL	0.009	0.022	0.019	0.010	0.007	0.009	0.014
UNIQUAC	0.010	0.023	0.023	0.006	0.007	0.008	0.015
			T = 303.15 K				
NRTL	0.007	0.014	0.011	0.011	0.006	0.009	0.010
UNIQUAC	0.005	0.013	0.015	0.007	0.006	0.008	0.010
			T = 308.15 K				
NRTL	0.011	0.018	0.010	0.060	0.008	0.013	0.013
UNIQUAC	0.004	0.017	0.015	0.008	0.007	0.011	0.011

Table (A.5.6): Binary interaction parameters from NRTL and UNIQUAC for hexane + methanol (2) + 2,2,2-trifluoroethanol (3)

	NRTL (α_{ij} = 0,2)		UNIQUAC	
Component *i-j*	$\Delta\lambda_{ij}$ /K	$\Delta\lambda_{ji}$ /K	Δu_{ij} /K	Δu_{ji} /K
	T = 288.15 K			
1, 2	279.04	546.97	560.78	16.94
1, 3	248.78	629.71	223.36	68.15
2, 3	50.86	-25.34	-46.98	122.2
	T = 298.15 K			
1, 2	272.55	506.07	563.94	2.52
1, 3	279.59	545.93	235.9	39.03
2, 3	16.66	-8.01	-81.82	183.8
	T = 303.15 K			
1, 2	256.46	479.1	565.91	-6.25
1, 3	271.67	520.53	235.9	30.84
2, 3	35.65	16.07	54.98	165.31
	T = 308.15 K			
1, 2	236.96	467.8	566.14	-18.375
1, 3	246.24	527.29	212.13	20.561
2, 3	12.197	-20.948	-110.89	258.11

قياس وحساب خواص التوازنات سائل ــ سائل للمحاليل المحتوية على الماء، الكحولات، الإيثيرات، والمركبات الفلوروهيدروكربونية

الملخص:

إن للمعطيات الجديدة للانحلالية والتوازنات سائل ــ سائل فوائد علمية جمة في الوحدات الصناعية، وكذا في المعالجة المثلى لعمليات الفصل الكيميائية وذلك لتقدير وحساب خواص المزج لبعض التحويلات الصناعية الهامة تقنيا وتطبيقيا .

نعطي في هذا العمل قياسات جديدة للانحلالية والتوازنات سائل ــ سائل مرفقة بمعطيات ترموديناميكية فيما يخص التأثير الطاقي مابين الجزيئات لجمل ثنائية وثلاثية مكونة من الماء ومحلات عضوية أكسجينية ومركبات هالوجينية بدرجات حرارة مختلفة وضغط 0.1MPa .

اجريت قياسات عيارية لمزج ثنائية وثلاثية واعطت قياسات متوافقة جدا مع المنشورات العلمية.

استعملت القياسات الجديدة المحصل عليها لتقدير معاملات الفصل وكذا انتقائية المحلات (الكحولات) للجمل التي لها مخطط أطوار سائل ــ سائل من النموذج I .

اعطت التحاليل الترموديناميكية لقياسات الانحلالية والتوازن سائل–سائل باستعمال معادلات تجريبية لــHand و-Othmer Tobias قيما ذات نوعية جيدة. كما تمت معالجة القيم التجريبية للتوازن سائل ــ سائل باستعمال معادلات ترموديناميكية NRTL و UNIQUAC والتي اعطت معاملات انحراف قياسية في المجال 1.2%

كما حللت النتائج المحصل عليها للتوازنات سائل ــ سائل ذات النموذج I للحصول على النقطة الحرجة للمحاليل التي بدورها حسبت من النموذجين NRTL و UNIQUAC

وأخيرا تم تقدير تأثير درجة الحرارة وكذا البنية الجزيئية للمركبات المكونة للمزج على فجوة الامتزاج.

قياس وحساب خواص التوازنات سائل ــ سائل للمحاليل المحتوية على الماء، الكحولات، الإيثيرات، والمركبات الفلوروهيدروكربونية

مذكرة ماجستير

جامعة العلوم والتكنولوجيا هواري بومدين

وهيبة كربوب

كلية الكيمياء

مخبر علم البلورات–الترموديناميك

الجمهورية الجزائرية الديمقراطية الشعبية

وزارة التعليم العالي و البحث العلمي

جامعة العلوم والتكنولوجيا هواري بومدين

مذكرة ماجستير

قياس وحساب خواص التوازنات سائل ــ سائل للمحاليل المحتوية على الماء، الكحولات، الإثيرات، والمركبات الفلوروهيدروكربونية

وهيبة كربوب

كلية الكيمياء

مخبر علم البلورات–الترموديناميك